2018

Condensation - warming up to mitotic DNA architecture

Donglai Shen
Lehigh University, nebulachina@hotmail.com

Condensation - warming up to mitotic DNA architecture

by

Donglai Shen

A Dissertation

Presented to the Graduate and Research Committee

of Lehigh University

in Candidacy for the Degree of

Doctor of Philosophy

in

Biological Sciences

Lehigh University

11/19/2018

Approved and recommended for acceptance as a dissertation in partial fulfillment of the requirements for the degree of Doctor of Philosophy

Donglai Shen
Condensation - warming up to mitotic DNA architecture

_____

Defense Date

_____

Dissertation Director
Robert V. Skibbens Ph.D.

_____

Approved Date

Committee Members:

_____

Lynne Cassimeris Ph.D.

_____

Gregory I. Lang Ph.D.

_____

Matthew L. Bochman Ph.D.

ACKNOWLEDGMENTS

I thank the Skibbens lab members for helpful discussion throughout this process and especially my advisor Dr. Skibbens for great support and guidance throughout my doctoral study. I also thank the rest of my Graduate Committee - Dr. Lynne Cassimeris, Dr. Gregory Lang and Dr. Matthew Bochman for their precious advice and support.

I thank the Dr. Gregory Lang lab, Dr. Maria Ocampo-Hafalla, Dr. Frank Uhlmann, Dr. Vincent Guacci and Dr. Doug Koshland for kindly sharing yeast strains and reagents.

My studies are supported by an award from the National Institutes of General Medicine (GM11031 to RVS), the Marjorie Nemes Fellowships, and the College of Arts & Sciences Graduate Fellowship from Lehigh University. Thank you for the funding resources that support my studies.

I thank my Mom and Dad for their support and love throughout my life.

TABLE OF CONTENTS

LIST OF FIGURES

LIST OF TABLES

ABSTRACT

During interphase, chromatin is in a state of least condensation and most accessible to transcription factors. When cells enter mitosis, replicated chromosomes are compacted, and sister chromatids are cohered to form specific mitotic architectures, which are essential for appropriate chromosome segregation. Disruption of the formation, regulation and maintenance of mitotic chromosome structure results in aneuploidy, which is tightly correlated with severe developmental maladies, aging and tumorigenesis. To understand how cells achieve mitotic condensed DNA architectures, we focus on the regulation of helicase activity and also the impact of site-specific condensation events. We report that helicase the Chl1 acts a novel regulator of mitotic chromosome condensation through cohesin-based mechanisms, revealing an exciting interface between native DNA structure that relies on helicase activity and higher-ordered chromosome compaction that requires cohesin complex. We also report for the first time that the condensed rDNA locus retains great plasticity during mitosis and responds to elevated temperature through a novel hypercondensation activity. This hyperthermic-induced rDNA hypercondensation is based on heat shock chaperone Hsp82, revealing a new role for chaperones in regulating mitotic DNA architecture.

Chapter 1

Introduction

Structural changes to the genome during the cell cycle are important yet mysterious processes that impact many cellular events. DNA undergoes replication during S phase that results in duplication of the whole genome. Replication products, also known as sister chromatids, are held together until anaphase onset through the mechanism termed cohesion [1-3]. When cells enter mitosis, chromatids start to compact into a more condensed state known as chromosome condensation. Condensation ensures that during telophase, chromosomes are positioned far from the spindle equator so that subsequent cytokinesis does not cleave the DNA. Condensation also promotes sister chromatid resolution by removing DNA catenations [4]. Disruption of mitotic condensation results in chromosome segregation defects, which are highly related to T cell lymphomas, colon cancer, microcephaly and severe developmental maladies [5-9]. Thus, cells utilize multi-level compaction mechanisms require several different factors such as histones, cohesins and condensins to promote mitotic condensation (Figure 1).

1.1 Histones and histone modifiers function in chromosome condensation.

Histones provide the first level of DNA compaction. Two copies each of histone protein H2A, H2B, H3, and H4 form a nucleosome octamer that is the basic unit of DNA packaging in eukaryotes [10]. DNA wrapped around nucleosomes is compacted about 5- to 10-fold in length [11]. Beyond that, histone post-translational modifications drive additional levels of chromosome condensation. For instance, histone H3 phosphorylation leads to the recruitment of the histone deacetylase Hst2. In turn, Hst2 deacetylates histone H4, setting the H4 tail free to interact with histone H2A. This histone-histone interaction contributes to chromosome condensation by generating interactions between neighboring

nucleosomes to condense the DNA fiber [12]. Additionally, overexpression of the histone H3 lysine 4 demethylase Jhd2 causes rDNA decondensation [13], indicating that histone methylation promotes chromosome condensation in budding yeast. Histone H1 associates with the linker DNA between two nucleosomes to further promote compaction from a 10-nm nucleosomal fiber into a 30-nm solenoid fiber [14]. Thus, Histone H1 phosphorylation also plays a role in chromosome condensation - providing for one of many additional points of regulation [15-17]. To achieve complete compaction, however, histone-independent forms of mitotic condensation, such as those involving cohesins and condensins, are required.

1.2 Cohesin and cohesion factors function in chromosome condensation.

The cohesin complex contains five subunits: Smc1, Smc3, Mcd1, Scc3 and Pds5 (yeast names provided for this evolutionarily conserved complex) [1, 2, 18-21]. Cohesins promote the tethering together of chromosome replication products, termed sister chromatid cohesion. Although how cohesins affect condensation is not fully understood, numerous lines of evidence confirm that cohesins function in condensation. For instance, Mcd1, Scc3 and Pds5 are all key cohesin structural components whose temperature-sensitive mutants exhibit both significant cohesion and condensation defects [1, 22-27]. In addition to structural cohesin components, many cohesion regulators function in condensation. For instance, the Scc2, 4 heterodimer loads cohesins onto DNA and is essential during S phase. Mutation in either Scc2 or Scc4 causes severe cohesion defects but also produces condensation defects, at least at the rDNA locus [2, 28]. Recent evidence suggests that Scc2 also promotes condensin deposition onto DNA [28].

Another cohesion regulator, Eco1, also functions in condensation. Eco1 is a Smc3 acetyltransferase that is required to convert chromatin-bound cohesins to a tethering-competent state specifically during DNA replication [29-32]. *eco1* mutant cells exhibit both cohesion and condensation defects [29, 30]. Rad61, also named Wapl1, is another cohesion regulator that functions in condensation [33]. Rad61, however, appears to negatively regulate condensation pathways because *rad61* mutant cells exhibit hypercondensed chromosomes [34]. Thus, cohesin components Mcd1 and Pds5 and cohesion regulators Scc2, 4, Eco1 and Rad61 all impact chromosome condensation. Beyond histones and cohesins, condensation requires additional factors to compact DNA, *i.e.*, condensins.

1.3 Condensin and condensation factors function in chromosome condensation.

The budding yeast condensin complex consists of five subunits: Smc2, Smc4, Brn1, Ycg1 and Ycs4 [35] (yeast names provided for this evolutionarily conserved complex). Condensin promotes mitotic condensation in multiple ways. Condensin promotes the introduction of positive supercoils into chromatin, helps complementary single-stranded DNA reannealing into double-stranded DNA and facilitates DNA catenation resolution [35]. Condensin DNA association and activation also generates intra-chromosome linkages to shorten the chromosome [36]. Condensin is thought to loop the chromatin in both axial and lateral directions to produce highly condensed mitotic chromosomes [37, 38]. In *S. cerevisiae*, the condensin subunits deposit onto DNA throughout the cell cycle, unlike cohesins whose DNA deposition peaks during S phase [28]. The total level of chromatin-bound condensin remains constant between G1 and metaphase. However,

functional condensation requires a multi-step condensin activation process that occurs during mitosis [39].

Condensin activity is strictly regulated. Previous studies provided evidence that mitotic kinases regulate condensation in budding yeast. In early mitosis, cyclin-dependent kinase 1 (Cdk1) phosphorylates condensin subunits Brn1, Ycs4 and Ycg1 to trigger mitotic condensation [39]. Later, Brn1, Ycg1 and Ycs4 are phosphorylated by Polo-like kinase Cdc5 to further promote condensin activity from anaphase until the end of mitosis [39, 40]. In addition, the aurora B kinase Ipl1 indirectly maintains condensation phosphorylation through an unknown mechanism [39, 41]. In contrast, condensin's role in condensation is actively inhibited through opposing post-translational modifications. For instance, human casein kinase II phosphorylates almost all condensin I subunits except the Smc2 homolog Cap-E during interphase and blocks chromatin compaction during this time period [42]. These condensation-inhibiting phosphorylations are removed by phosphatases that become activated at the start of mitosis [43]. Thus, condensin activity is regulated by phosphorylation/dephosphorylation modifications to generate condensation with appropriate timing.

1.4 Helicase activity in regulating mitotic chromosome architecture.

To achieve appropriate mitotic condensation, histones, cohesins and condensins are all required to function on the common substrate: DNA. However, it remains elusive whether DNA itself is modified to facilitate accessibility and activity of different compaction components. To address this question, we are now using the Chl1

(Chromosome loss 1) DNA helicase as a tool to provide a direct linkage between native DNA structure and higher-ordered mitotic chromosome structure formation.

Chl1 promotes sister chromatids cohesion and ensures appropriate chromosome segregation. Chl1 was first identified in a chromosome loss mutation screen in 1978 and then a chromosome transmission fidelity screen in 1990 [44, 45]. *chl1* mutation causes more severe mis-segregation of smaller chromosomes than larger chromosomes. This effect was attributed to a role in cohesion because shorter chromosomes are posited to contain less cohesins [46]. Chl1's function in cohesion was later demonstrated directly in that *chl1* deletion strains exhibit increased premature sister separation compared to wildtype [47-49]. It is now well documented that Chl1 is a cohesion regulator [47-49, 50, 51]. Chl1 physically interacts with Eco1, an acetyltransferase that converts chromatin-bound cohesin to a tethering-competent state [29-32, 47]. The interaction between Chl1 and Eco1 appears physiologically relevant in that *eco1* mutant cells deleted for *chl1* are inviable [47]. More recent evidence suggests that Chl1 regulates cohesin enrichment onto chromosomes during S-phase [51]. Cohesin loading onto DNA requires the deposition of the Scc2, 4 complex, while Scc2 loading onto chromatin requires Chl1. Thus, *chl1* deletion causes decreased loading of both Scc2 and cohesin [51].

Chl1 also exhibits various enzymatic activities and is implicated in numerous aspects of chromosome biology in addition to cohesion. Previous *in silico* analysis revealed that Chl1 exhibits the greatest similarity to DNA helicases [52]. Subsequent biochemical studies identified the human Chl1 homolog as ChlR1/DDX11/FANCJ that exhibits helicase activity and that unwinds DNA/DNA duplexes and moves along single-stranded DNA templates *in vitro* [53]. ChlR1 also resolves DNA secondary structure

such as G-quadruplexes generated along guanosine-rich tracts [54-58]. A G-quadruplex (referred to as G4) is a specific DNA secondary structure that is hypothesized to block both transcription and DNA replication, such that unresolved G4s result in DNA damage and hotspots for genomic instability [59]. Whether G4s impact mitotic chromosome condensation remains unknown. ChlR1 is also able to disrupt protein-DNA interactions *in vitro*, revealing a function in stripping off proteins from duplex DNA [55, 57, 58]. These observations lead to a possibility that Chl1 may function in histone positioning, though direct evidence is required to confirm this role.

Recent studies show that Chl1 promotes cohesin loader Scc2, 4 deposition onto chromatin, which in turn appears to maintain nucleosome-free regions [51, 60]. Thus, Chl1 may function in generating nucleosome-free regions. In parallel, the RSC chromatin remodeling complex affects cohesin loader Scc2 deposition, which in turn appears to maintain nucleosome-free regions enriched at transcription start sites [60]. The RSC complex is a defined cohesion regulator, and its function in condensin deposition and mitotic condensation was revealed later [60-63]. These findings suggest that Chl1 might function in nucleosome positioning that impact mitotic condensation.

In summary, Chl1 and its homolog regulate DNA secondary structure, histone positioning, cohesin deposition and cohesion. These observations lead to an untested hypothesis that Chl1 function may extend to mitotic condensation through G4 resolving-, histone modification/positioning- and/or cohesin-based pathways. Some of these possibilities regarding Chl1 function in condensation are addressed in chapter 2.

1.5 Alternative condensation pathways in response to environmental changes.

In *Saccharomyces cerevisiae*, condensation of the rDNA locus is distinct from the rest of the genome. During G1 phase, rDNA is uncondensed and exhibits puff-like morphology. Later during mitosis, rDNA condenses into discrete loop-like structures and segregates later than most other regions [64-66]. Both condensins and cohesins are required for mitotic rDNA condensation. Mutations in any of the cohesin/condensin subunits and cohesion regulators, such as the cohesin loader Scc2, 4 and acetyltransferase Eco1, all produce profound impacts on condensation such that mitotic rDNA fails to compact and appears as diffuse puff-like structures [1, 28, 29, 30, 33, 47, 57].

Interestingly, rDNA condensation status is highly dynamic and sensitive to environmental cues, indicating alternative condensation pathways exist to regulate rDNA structure in response to environmental changes. Interphase rDNA acquires pre-mature condensation in response to nutrient starvation [67, 68]. The volume of the total rDNA mass is significantly contracted upon nutrient depletion. This pre-mature condensation during G1 requires condensin re-localization to rDNA arrays and the function of high mobility group protein Hmo1 [68]. Interestingly, direct inhibition of rDNA transcription activator Tor1 by rapamycin treatment causes similar rDNA contraction with condensin enrichment at rDNA loci. However, transcriptional repression using Pol I mutants cannot recapitulate the pre-mature rDNA condensation. These observations indicate that pre-mature condensation during G1 phase is condensin-dependent and upstream of Pol I transcription machinery. Later during mitosis, rDNA condenses into a discrete loop/line-like structure. It remains elusive whether the mitotic condensed rDNA locus retains its ability to respond to environmental cues. If mitotic rDNA is still a dynamic substrate that is regulated under environmental changes, then what factors are involved in this

alternative condensation pathway? Does it require novel condensation factors? These questions are addressed for rDNA-specific condensation regulation in Chapters 3 and 4.

Figures

Figure 1

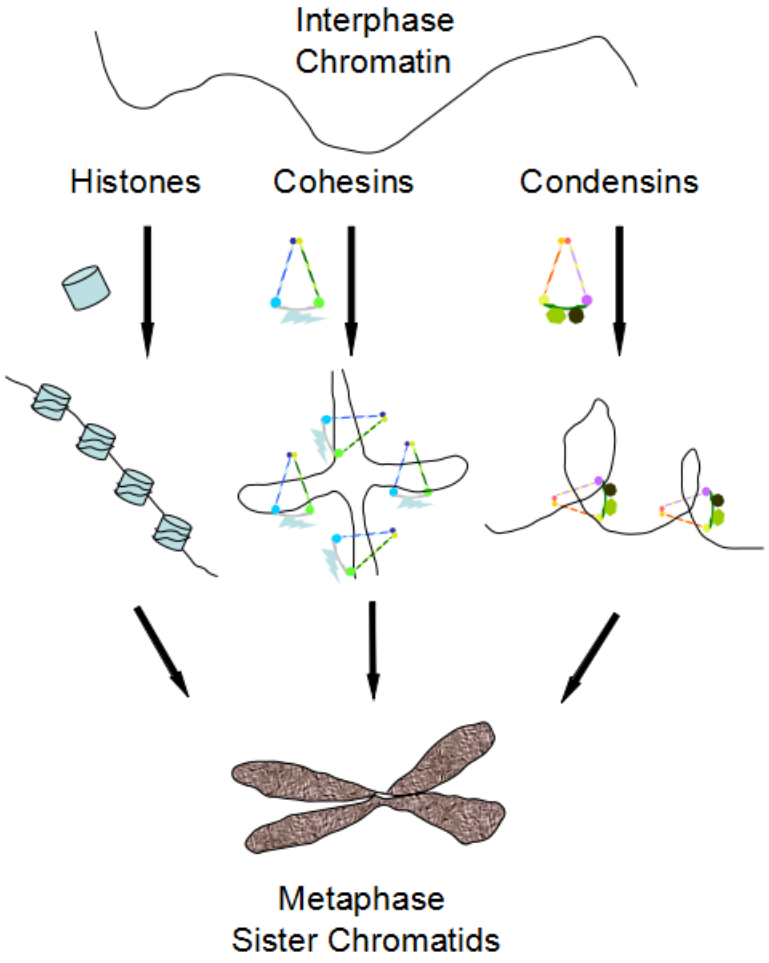

Figure 1. Histones, cohesin and condensin all function in chromatin condensation. Hypothetical model of how cohesin and condensin associate with the chromatin.

References

1. Guacci V, Koshland D, Strunnikov A. A direct link between sister chromatid cohesion and chromosome condensation revealed through the analysis of MCD1 in *S. cerevisiae*. *Cell.* 1997;91(1): 47–57.

2. Ciosk R, Shirayama M, Shevchenko A, Tanaka T, Toth A, Shevchenko A, et al. Cohesin's binding to chromosomes depends on a separate complex consisting of Scc2 and Scc4 proteins. *Mol Cell.* 2000;5(2): 243–254.

3. Jan-Michael P and Nishiyama T. Sister Chromatid Cohesion. *Cold Spring Harb Perspect Biol.* 2012 Nov; 4(11): a011130.

4. Cuylen S, Metz J, Hruby A, Haering CH. Entrapment of chromosomes by condensin rings prevents their breakage during cytokinesis. *Dev Cell.* 2013;25;27(4):469-78.

5. Feng XD, Song Q, Li CW, Chen J, Tang HM, Peng ZH, et al. Structural maintenance of chromosomes 4 is a predictor of survival and a novel therapeutic target in colorectal cancer. *Asian Pac J Cancer Prev.* 2014;15(21): 9459–9465.

6. Yin L, Jiang LP, Shen QS, Xiong QX, Zhuo X; Zhang LL, et al. NCAPH plays important roles in human colon cancer. *Cell Death Dis*. 2017;8(3): e2680.

7. Woodward J, Taylor GC, Soares DC, Boyle S, Sie D, Read D, et al. Condensin II mutation causes T-cell lymphoma through tissue-specific genome instability. *Genes Dev.* 2016;30(19): 2173–2186.

8. Martin CA, Murray JE, Carroll P, Leitch A, Mackenzie KJ, Halachev M, et al. Deciphering Developmental Disorders Study, Wood AJ, Vagnarelli P, Jackson AP. Mutations in genes encoding condensin complex proteins cause microcephaly through

decatenation failure at mitosis. *Genes Dev.* 2016;30(19): 2158–2172.

9. Perche O, Menuet A, Marcos M, Liu L, Pâris A, Utami KH, et al. Combined deletion of two Condensin II system genes (NCAPG2 and MCPH1) in a case of severe microcephaly and mental deficiency. *Eur J Med Genet.* 2013;56(11): 635–641.

10. White CL, Suto RK, Luger K. Structure of the yeast nucleosome core particle reveals fundamental changes in internucleosome interactions. *EMBO J.* 2001; 20(18): 5207–5218.

11. Felsenfeld G and Groudine M. Controlling the double helix. *Nature.* 2003;421(6921):448-53.

12. Wilkins BJ, Rall NA, Ostwal Y, Kruitwagen T, Hiragami-Hamada K, Winkler M, Barral Y, Fischle W, Neumann H. A cascade of histone modifications induces chromatin condensation in mitosis. *Science.* 2014;343(6166):77-80.

13. Hong-Yeoul Ryu and Seong Hoon Ahn. Yeast histone H3 lysine 4 demethylase Jhd2 regulates mitotic ribosomal DNA condensation; *BMC Biol.* 2014;12:75.

14. F. Thoma, TH. Koller, and A. Klug. Involvement of histone H1 in the organization of the nucleosome and of the salt-dependent superstructures of chromatin. *J Cell Biol.* 1979;83(2 Pt 1):403-27.

15. Yoh-ichi Matsumoto, Hideyo Yasuda, Shiro mita, Tohru marunouchi & Masa-atsu Yamada. Evidence for the involvement of H1 histone phosphorylation in chromosome condensation. *Nature.* 1980; 284(5752):181-3.

16. Halmer L, Gruss C. Effects of cell cycle dependent histone H1 phosphorylation on chromatin structure and chromatin replication. *Nucleic Acids Res.* 1996 ;24(8):1420-7.

17. Tamara L. Caterino and Jeffrey J. Hayes. Structure of the H1 C-terminal domain

and function in chromatin condensation. *Biochem Cell Biol.* 2011;89(1):35-44.

18. Haarhuis JH, Elbatsh AM, Rowland BD. Cohesin and its regulation: on the logic of X-shaped chromosomes. *Dev Cell.* 2014;31(1):7-18.

19. Skibbens RV. Of Rings and Rods: Regulating Cohesin Entrapment of DNA to Generate Intra- and Intermolecular Tethers. *PLoS Genet.* 2016;12(10): e1006337.

20. Dorsett D, Merkenschlager M. Cohesin at active genes: a unifying theme for cohesin and gene expression from model organisms to humans. *Curr Opin Cell Biol.* 2013;25(3): 327–333.

21. Jeppsson K, Kanno T, Shirahige K, Sjögren C. The maintenance of chromosome structure: positioning and functioning of SMC complexes. *Nat Rev Mol Cell Biol.* 2014;15(9): 601–614.

22. Hartman T, Stead K, Koshland D, Guacci V. Pds5p is an essential chromosomal protein required for both sister chromatid cohesion and condensation in *Saccharomyces cerevisiae*. *J Cell Biol.* 2000;151(3):613-26.

23. Tong K, Skibbens RV. Pds5 regulators segregate cohesion and condensation pathways in *Saccharomyces cerevisiae*. Proc Natl Acad Sci USA. 2015;112(22): 7021–7026.

24. Eng T, Guacci V, Koshland D. ROCC, a conserved region in cohesin's Mcd1 subunit, is essential for the proper regulation of the maintenance of cohesion and establishment of condensation. *Mol Biol Cell.* 2014;25(16):2351-64.

25. Zhang Z, Ren Q, Yang H, Conrad MN, Guacci V, Kateneva A, Dresser ME. Budding yeast PDS5 plays an important role in meiosis and is required for sister chromatid cohesion. *Mol Microbiol.* 2005;56(3):670-80.

26. Shen D, Skibbens RV. Chl1 DNA helicase and Scc2 function in chromosome condensation through cohesin deposition. *PLoS One.* 2017;12(11):e0188739.

27. Srinivasan M, Scheinost JC, Petela NJ, Gligoris TG, Wissler M, Ogushi S, Collier JE, Voulgaris M, Kurze A, Chan KL, Hu B, Costanzo V, Nasmyth KA. The Cohesin Ring Uses Its Hinge to Organize DNA Using Non-topological as well as Topological Mechanisms. *Cell.* 2018;173(6):1508-1519.e18.

28. D'Ambrosio C, Schmidt CK, Katou Y, Kelly G, Itoh T, Shirahige K, et al. Identification of cis-acting sites for condensin loading onto budding yeast chromosomes. *Genes Dev.* 2008;22(16): 2215–2227.

29. Skibbens RV, Corson BL, Koshland D, Hieter P. Ctf7p is essential for sister chromatid cohesion and links mitotic chromosome structure to the DNA replication machinery. *Genes Dev.* 1999;13(3): 307–319.

30. Tóth A, Ciosk R, Uhlmann F, Galova M, Schleiffer A, Nasmyth K. Yeast Cohesin complex requires a conserved protein, Eco1p(Ctf7), to establish cohesion between sister chromatids during DNA replication. *Genes Dev.* 1999;13(3): 320–333.

31. Ivanov D, Schleiffer A, Eisenhaber F, Mechtler K, Haering CH, Nasmyth K. Eco1 is a novel acetyltransferase that can acetylate proteins involved in cohesion. *Curr Biol.* 2002;12(4):323-8.

32. Rolef Ben-Shahar T1, Heeger S, Lehane C, East P, Flynn H, Skehel M, Uhlmann F. Eco1-dependent cohesin acetylation during establishment of sister chromatid cohesion. *Science.* 2008;321(5888):563-6.

33. Kueng S, Hegemann B, Peters BH, Lipp JJ, Schleiffer A, Mechtler K, Peters JM. Wapl controls the dynamic association of cohesin with chromatin. *Cell.* 2006;127(5):955-

67.

34. Lopez-Serra L, Lengronne A, Borges V, Kelly G, Uhlmann F. Budding yeast Wapl controls sister chromatid cohesion maintenance and chromosome condensation. *Curr Biol.* 2013;23(1):64-9.

35. Hirano T. Condensins: universal organizers of chromosomes with diverse functions. *Genes Dev.* 2012;26(15):1659-78.

36. Frosi Y, Haering CH. Control of chromosome interactions by condensin complexes. *Curr Opin Cell Biol.* 2015;34:94-100.

37. Ganji M, Shaltiel IA, Bisht S, Kim E, Kalichava A, Haering CH, Dekker C. Real-time imaging of DNA loop extrusion by condensin. *Science.* 2018;360(6384):102-105.

38. Schalbetter SA, Goloborodko A, Fudenberg G, Belton JM, Miles C, Yu M, Dekker J, Mirny L, Baxter J. SMC complexes differentially compact mitotic chromosomes according to genomic context. *Nat Cell Biol.* 2017;19(9):1071-1080.

39. Bazile F, St-Pierre J, D'Amours D. Three-step model for condensin activation during mitotic chromosome condensation. *Cell Cycle.* 2010;9(16):3243-55.

40. St-Pierre J, Douziech M, Bazile F, Pascariu M, Bonneil E, Sauvé V, Ratsima H, D'Amours D. Polo kinase regulates mitotic chromosome condensation by hyperactivation of condensin DNA supercoiling activity. *Mol Cell.* 2009;34(4):416-26.

41. Vas AC, Andrews CA, Kirkland Matesky K, Clarke DJ. In vivo analysis of chromosome condensation in *Saccharomyces cerevisiae*. *Mol Biol Cell.* 2007;18(2):557-68.

42. Takemoto A, Kimura K, Yanagisawa J, Yokoyama S, Hanaoka F. Negative regulation of condensin I by CK2-mediated phosphorylation. *EMBO J.*

2006 ;25(22):5339-48.

43. Takemoto A, Maeshima K, Ikehara T, Yamaguchi K, Murayama A, Imamura S, Imamoto N, Yokoyama S, Hirano T, Watanabe Y, et al. The chromosomal association of condensin II is regulated by a noncatalytic function of PP2A. *Nat Struct Mol Biol.* 2009;16(12):1302-8.

44. Liras P, McCusker J, Mascioli S, Haber JE. Characterization of a mutation in yeast causing nonrandom chromosome loss during mitosis. *Genetics.* 1978;88(4 Pt 1):651-71.

45. Gerring SL, Spencer F, Hieter P. The CHL 1 (CTF 1) gene product of *Saccharomyces cerevisiae* is important for chromosome transmission and normal cell cycle progression in G2/M. *EMBO J.* 1990;9(13):4347-58.

46. L Holloway S. CHL1 is a nuclear protein with an essential ATP binding site that exhibits a size-dependent effect on chromosome segregation. *Nucleic Acids Res.* 2000;28(16):3056-64.

47. Skibbens RV. Chl1p, a DNA Helicase-Like Protein in Budding Yeast, Functions in Sister-Chromatid Cohesion. *Genetics.* 2004;166(1): 33–42.

48. Mayer ML, Pot I, Chang M, Xu H, Aneliunas V, Kwok T, et al. Identification of protein complexes required for efficient sister chromatid cohesion. *Mol Biol Cell.* 2004;15(4): 1736–1745.

49. Petronczki M, Chwalla B, Siomos MF, Yokobayashi S, Helmhart W, Deutschbauer AM, et al. Sister-chromatid cohesion mediated by the alternative RF-CCtf18/Dcc1/Ctf8, the helicase Chl1 and the polymerase-alpha-associated protein Ctf4 is essential for chromatid disjunction during meiosis II. *J Cell Sci.* 2004;117(16): 3547–

3559.

50. Rudra S, Skibbens RV. Sister chromatid cohesion establishment occurs in concert with lagging strand synthesis. *Cell Cycle.* 2012;11(11): 2114–2121.

51. Rudra S, Skibbens RV. Chl1 DNA helicase regulates Scc2 deposition specifically during DNA-replication in *Saccharomyces cerevisiae*. *PLoS One.* 2013;8(9): e75435.

52. Amann J, Kidd VJ, Lahti JM. Characterization of putative human homologues of the yeast chromosome transmission fidelity gene, CHL1. *J Biol Chem.* 1997;272(6):3823-32.

53. Hirota Y, Lahti JM. Characterization of the enzymatic activity of hChlR1, a novel human DNA helicase. *Nucleic Acids Res.* 2000;28(4): 917–924.

54. Wu Y, Shin-ya K, Brosh RM Jr. FANCJ Helicase Defective in Fanconia Anemia and Breast Cancer Unwinds G-Quadruplex DNA To Defend Genomic Stability. *Mol Cell Biol.* 2008;28(12): 4116–4128.

55. Wu Y, Sommers JA, Khan I, de Winter JP, Brosh RM Jr. Biochemical characterization of Warsaw breakage syndrome helicase. *J Biol Chem.* 2012;287(2): 1007–1021.

56. Kuryavyi V, Patel DJ. Solution structure of a unique G-quadruplex scaffold adopted by a guanosine-rich human intronic sequence. *Structure.* 2010;18(1): 73–82.

57. Bharti SK, Sommers JA, George F, Kuper J, Hamon F, Shin-Ya K, et al. Specialization among iron-sulfur cluster helicases to resolve G-quadruplex DNA structures that threaten genomic stability. *J Biol Chem.* 2013;288(39): 28217–2829.

58. Bharti SK, Khan I, Banerjee T, Sommers JA, Wu Y, Brosh RM Jr. Molecular functions and cellular roles of the ChlR1 (DDX11) helicase defective in the rare

cohesinopathy Warsaw breakage syndrome. *Cell Mol Life Sci.* 2014;71(14): 2625–2639.

59. Bochman ML, Paeschke K, Zakian VA. DNA secondary structures: stability and function of G-quadruplex structures. *Nat Rev Genet.* 2012;13(11): 770–780.

60. Lopez-Serra L, Kelly G, Patel H, Stewart A, Uhlmann F. The Scc2-Scc4 complex acts in sister chromatid cohesion and transcriptional regulation by maintaining nucleosome-free regions. *Nat Genet.* 2014;46(10): 1147–1151.

61. Baetz KK, Krogan NJ, Emili A, Greenblatt J, Hieter P. The ctf13-30/CTF13 genomic haploinsufficiency modifier screen identifies the yeast chromatin remodeling complex RSC, which is required for the establishment of sister chromatid cohesion. *Mol Cell Biol.* 2004;24(3):1232-44.

62. Huang J, Hsu JM, Laurent BC. The RSC nucleosome-remodeling complex is required for Cohesin's association with chromosome arms. *Mol Cell.* 2004;13(5):739-50.

63. Toselli-Mollereau E, Robellet X, Fauque L, Lemaire S, Schiklenk C, Klein C, Hocquet C, Legros P, N'Guyen L, Mouillard L, et al. Nucleosome eviction in mitosis assists condensin loading and chromosome condensation. *EMBO J.* 2016;35(14):1565-81.

64. Guacci V, Hogan E, Koshland D. Chromosome condensation and sister chromatid pairing in budding yeast. *J Cell Biol.* 1994;125(3): 517–530.

65. Torres-Rosell J, Machín F, Jarmuz A, Aragón L. Nucleolar segregation lags behind the rest of the genome and requires Cdc14p activation by the FEAR network. *Cell Cycle.* 2004;3(4):496-502.

66. de Los Santos-Velázquez AI, de Oya IG, Manzano-López J, Monje-Casas F. Late rDNA Condensation Ensures Timely Cdc14 Release and Coordination of Mitotic Exit Signaling with Nucleolar Segregation. *Curr Biol.* 2017;27(21):3248-3263.e5.

67. Tsang CK, Li H, Zheng XS. Nutrient starvation promotes condensin loading to maintain rDNA stability. *EMBO J.* 2007;26(2):448-58.

68. Wang D, Mansisidor A, Prabhakar G, Hochwagen A. Condensin and Hmo1 Mediate a Starvation-Induced Transcriptional Position Effect within the Ribosomal DNA Array. *Cell Rep.* 2016;17(2):624.

Chapter 2*

Chl1 DNA helicase and Scc2 function in chromosome condensation through cohesin deposition.

*Modified from Shen D, Skibbens RV. *PLoS One*. 2017 Nov 29;12(11):e0188739

Abstract

Chl1 DNA helicase promotes sister chromatid cohesion and associates with both the cohesion establishment acetyltransferase Eco1/Ctf7 and the DNA polymerase processivity factor PCNA that supports Eco1/Ctf7 function. Mutation in CHL1 results in precocious sister chromatid separation and cell aneuploidy, defects that arise through reduced levels of chromatin-bound cohesins which normally tether together sister chromatids (trans tethering). Mutation of Chl1 family members (BACH1/BRIP/FANCJ and DDX11/ChlR1) also exhibit genotoxic sensitivities, consistent with a role for Chl1 in trans tethering which is required for efficient DNA repair. Chl1 promotes the recruitment of Scc2 to DNA which is required for cohesin deposition onto DNA. There is limited evidence, however, that Scc2 also directs the deposition onto DNA of condensins which promote tethering in cis (intramolecular DNA links). Here, we test the ability of Chl1 to promote cis tethering and the role of both Chl1 and Scc2 to promote condensin recruitment to DNA. The results reveal that *chl1* mutant cells exhibit significant condensation defects both within the rDNA locus and genome-wide. Importantly, *chl1* mutant cell condensation defects do not result from reduced chromatin binding of condensin, but instead through reduced chromatin binding of cohesin. We tested *scc2-4* mutant cells and similarly found no evidence of reduced condensin recruitment to chromatin. Consistent with a role for Scc2 specifically in cohesin deposition, *scc2-4* mutant cell condensation defects are irreversible. We thus term Chl1 a novel regulator of both chromatin condensation and sister chromatid cohesion through cohesin-based mechanisms. These results reveal an exciting interface between DNA structure and the highly conserved cohesin complex.

Introduction

Structural changes to the genome that occur over the cell cycle are fundamental yet mysterious features that underlie many cellular events. During G1 phase of the cell cycle, chromatin compaction and higher order DNA assemblies termed TADS (topological associated domains) are largely regional [1, 2]. These cis-based (intramolecular) and trans-based (intermolecular) tetherings of DNA segments must remain dynamic to allow for plasticity and appropriate transcriptional responses to external cues such as changes in temperature, nutrient levels and signaling factors [1, 3–5]. During S phase, trans tethers are established specifically between the products of chromosome replication, termed sister chromatids. These trans tethers remain stable and thus identify chromatids as sisters until anaphase onset. Cis tethers established during prophase also are stable—maintaining fully condensed and disentangled chromosomes through mitosis. These cis tethers are required for high fidelity chromosome segregation and the positioning of chromosomes away from the cytokinetic furrow. In an impressive coopting of function through evolution, each of these tethering activities in combination are mediated by SMC (stability of minichromosomes or structural maintenance of chromosomes) complexes that include cohesins (Smc1, Smc3, Mcd1/Scc1/RAD21, Pds5, Scc3/Irr1/SA1,2 and Sororin in vertebrate cells) and condensins (Smc2/Cut14, Smc4/Cut3, Ycs4/Cnd1/DPY-28, Ycg1/Cdn3/CAP-G1, Brn1/Cdn2/DPY-26) [1, 2, 6, 7].

Divisions between SMC complex functions are not always distinct. For instance, it is well established that cohesins form both cis and trans tethers that function in DNA replication, repair, chromosome segregation, chromatin condensation and transcription regulation [1, 2]. Thus, mutations of cohesin pathways produce aneuploidy, are tightly

correlated with numerous cancers and directly result in severe developmental maladies that include Robert Syndrome, Cornelia de Lange Syndrome and Warsaw Breakage Syndrome [2, 8, 9]. Condensins on the other hand, which primarily tether DNA segments in cis conformations, provide for longitudinal chromatin compaction, removal of DNA catenations, chromosomal disentanglement, and dosage compensation [6, 7]. Mutations of condensation pathways result in T cell lymphomas, colon cancer, microcephaly, and are predictors of cancer survivorship [10–14]. Mechanistically, convincing evidence suggests that both cohesins and condensins entrap individual DNA segments within a topologically closed structure. In turn, DNA segment tethering requires oligomerization of the appropriate SMC complexes, although little is known regarding how these oligomerization steps are directed toward either cis or trans conformations [1, 15–17].

The targeting and deposition of cohesins and condensins onto DNA represents a critical regulatory mechanism that spans a wide range of cellular activities, but remains largely undefined. What is clear is that cohesin deposition onto DNA requires the loader complex comprising Scc2/NIPBL and Scc4/MAU-2 [18–22]. One particular study, however, implicated Scc2,4 in the recruitment of condensin to DNA, a finding largely based on fluorescent intensity levels performed on chromosome spreads [23]. In yeast, Scc2,4 recruitment to DNA is regulated at the level of DNA structure and requires the conserved Chl1 DNA helicase [24–26]. At least during S phase, Scc2 deposition appears coordinated with DNA replication fork progression given that Chl1 physically interacts with numerous DNA replication fork factors (PCNA, Rad27/FEN1, MCMs) and the S phase acetyltransferase Eco1/Ctf7 [24, 25, 27–30]. Thus, Chl1 DNA helicase appears as the earliest regulator identified to date of Scc2 and cohesin recruitment to DNA.

Despite the wealth of evidence that Chl1 is critical for sister chromatid trans-tethering [27, 31–34], a role for Chl1 in cis-tethering remains untested. The issue is a critical one given that mutations in the Chl1 human homologs ChlR1/DDX11 and BACH1/BRIP1/FANCJ collectively result in Warsaw Breakage Syndrome, Fanconi anemia, cell aneuploidy and breast and ovarian cancers [27, 31, 32, 34–40]. Moreover, the extent to which Chl1 DNA helicase regulation of Scc2 translates to both cohesin and condensin recruitment to chromatin is unknown, revealing a significant deficit in our understanding of these clinically relevant processes. Here, we report that Chl1 and Scc2 are indeed regulators of genome-wide condensation, but that these roles occur independent of condensin binding to DNA and instead rely primarily on cohesin function.

Results

2.1 Chl1 DNA helicase promotes rDNA condensation

Chl1 DNA helicase is critical for Scc2 recruitment to DNA [25], but the extent through which SMC-dependent DNA compaction is regulated through Chl1 remains untested. Here, we exploit the structural changes that rDNA undergoes across the cell cycle. In yeast, rDNA comprises up to 150 copies of linearly arrayed 9 kb sequence that form a diffuse and amorphous puff-like structure during G1 and condense into a discrete line and loop-like structure during mitosis [43, 44, 47, 48]. Fluorescence in situ Hybridization (FISH) is a well-established methodology for detecting structural changes of rDNA loci, but is both time intensive and involves sequential application of three different antibodies and labeled probe [43, 44]. Previously, we developed and validated a streamlined condensation assay based on FISH but one that produces exquisite imaging of rDNA in the absence of antibodies and hybridization of labeled probe (Fig 1A) [45]. To assess the impact of Chl1 helicase on rDNA structure, wildtype and *chl1* deletion cells were synchronized in G1 using medium supplemented with alpha factor, washed and released into fresh medium supplemented with nocodazole for 3 hours. The resulting synchronized pre-anaphase cells were then processed to quantify the status of rDNA condensation (Fig 1B). The results confirm that wildtype cells exhibit high levels (78%) of tightly condensed (loop/line-like) rDNA loci while *chl1* mutant cells exhibit significantly lower levels (58%) of condensed rDNA loci. In fact, *chl1* mutant cells exhibited nearly twice the frequency of decondensed rDNA than wildtype cells (Fig 1C and 1D).

Chl1 DNA helicase is not essential for DNA replication, but we were nonetheless concerned that loss of Chl1 might produce a minor cell cycle delay that could be misinterpreted as a condensation defect. We assessed this possibility in three ways. First, we assessed cells after only 2.5 hours of preanaphase synchronization in medium supplemented with nocodazole. The results obtained by flow cytometry clearly reveal that both wildtype and *chl1* mutant cells are synchronized at this early step in the arrest protocol (S1 Fig). Thus, any imperceptible cell cycle delays will be fully compensated for by the additional 30 minutes of synchronization in the procedure described above. Second, we exploited the well-established changes in yeast cell morphology in which G1 cells are unbudded, S phase entry typically correlates with bud emergence, and subsequent G2 and M phases denoted by increased bud growth [49]. Our results reveal nearly identical large budded populations of wildtype and *chl1* mutant cells after 3 hours arrest in nocodazole (S1 Fig). Third, we quantified the minor 1N DNA peak in the preanaphase arrested cultures. The results reveal that 9.6% of wildtype cells exhibit a 1N DNA content while only 6.2% *chl1* mutant cells exhibit a 1N DNA content. Thus, *chl1* mutant cells arrest in preanaphase as efficiently as wildtype cells, negating the model that the two-fold increase in decondensed rDNA is due to cell cycle progression defects (S1 Fig).

Net1 is an rDNA binding protein such that Net1-GFP is another established method from which to monitor for architectural changes within the rDNA locus [23, 26, 42, 45, 50]. To independently assess for rDNA condensation defects in *chl1* mutant cells, Net1-GFP transformants of wildtype and *chl1* deletion cells were synchronized in pre-anaphase (S1 Fig), and the status of rDNA condensation (loops/lines versus puffs) quantified as

previously described [23, 42–44]. As expected, wildtype cells exhibited high levels (77%) of condensed (loop/line-like) rDNA loci. In contrast, *chl1* mutant cells exhibited significantly lower levels (65%) of condensed rDNA loci and over a 50% increase in the number of rDNA puff structures, compared to wildtype cells (Fig 1E and 1F). Importantly, the impact of *chl1* mutation on rDNA structure occurs in the absence of shifting to elevated temperatures (37°C), a procedure that significantly impacts rDNA structure even in wildtype cells [45]. These combined results therefore reveal that Chl1 promotes condensation of the rDNA locus.

2.2 Chl1 helicase promotes arm condensation

rDNA is unique in architecture, associated factors, transcription regulation, and recombination frequency compared to the remainder of the genome [51]. Thus, it became important to assess if Chl1 is an rDNA-specific regulator of condensation or instead impacts condensation genome-wide. We obtained from the lab of Dr. Frank Uhlmann a chromosome arm condensation assay strain that contains two lacO repeats, one integrated telomere-proximal on the left arm and another integrated centromere-proximal on the right arm of chromosome XII [23]. Each LacO cassette is detectable through lacI-GFP binding such that the inter-GFP distance allows for quantification of chromosome arm condensation (Fig 2A). Isogenic chromosome arm condensation assay strains, except for deletion of *CHL1*, were synchronized in G1 using alpha factor, washed and released into fresh medium supplemented with nocodazole (Fig 2B). The resulting pre-anaphase synchronized cells were then fixed in paraformaldehyde and the disposition of arm condensation quantified by measuring the distance between GFP loci. As expected, *chl1*

mutant cells exhibit cohesion defects [27, 32] and we therefore encountered a range of detectable GFP loci. We thus limited our analysis to wildtype and *chl1* mutant cells that contained only 2 GFP dots and in which both were resolvable within a single focal plane (Fig 2A). We found a wide range of inter-GFP distances both in wildtype and *chl1* mutant cells. Regardless, the results reveal that 70% of wildtype cells exhibited inter-GFP distances under 0.52 μm. In contrast, only 53% of *chl1* mutant cells exhibited inter-GFP distances under 0.52 μm. In fact, *chl1* mutant cells exhibited inter-GFP distances above 0.65 μm at roughly 3 times the frequencies of wildtype cells (Fig 2C and 2D). These results reveal for the first time that Chl1 plays a genome-wide role in chromosome condensation.

2.3 Chl1 and Scc2 function in condensation independent of condensin deposition

What is the mechanism through which Chl1 and Scc2 function in condensation? Chl1 is well-documented as a cohesion regulator that is critical for Scc2 recruitment to chromatin [25]. In turn, Scc2 is essential for cohesin deposition onto chromatin, but a role for Scc2 in condensin deposition remains controversial [19, 23]. Thus, it became critical to differentiate between models that Chl1 promotes chromatin compaction through either Scc2-dependent regulation of condensins, cohesins, or both. We first tested whether the condensation defect produced in *chl1* mutant cells occurs through the reduction of condensin deposition onto DNA. Condensin subunit Smc2 was epitope-tagged as the sole source of Smc2 function in both wildtype and *chl1* mutant cells. We included *scc2-4* cells in our analyses so that we could directly compare the roles of Chl1 and Scc2 on condensin deposition. We then exploited Triton X-100 cell fractionation assays

previously used to demonstrate chromatin-association of a spectrum of factors that include Ctf7/Eco1, cohesin subunits, DNA replication initiators and fork stabilization proteins [25, 52–57]. Wildtype, *chl1* and *scc2-4* single mutant strains each expressing Smc2-HA were synchronized in G1 (alpha factor), washed and released at 37°C (non-permissive for *scc2-4*) into fresh medium supplemented with nocodazole (Fig 3A). We validated the cell fractionation procedure using Phosphoglycerokinase (PGK) and Histone 2B (H2B) as cytosolic and chromatin fiduciary markers, respectively. The results show efficient enrichment of H2B, and undetectable levels of PGK, in Triton-X-100 insoluble chromatin bound fractions (Fig 3B). Smc2 titration demonstrates that protein loading is within the linear range of detection (Fig 3B). We first compared the total levels of Smc2-HA, normalized to H2B levels, in whole cell extractions obtained from wildtype, *chl1* and *scc2-4* single mutant cells. The results from whole cell extracts document that Smc2-HA levels are unaffected in either *chl1* or *scc2-4* mutations, compared to wildtype cells (Fig 3C). We then compared the levels of chromatin-bound Smc2-HA. The result revealed that chromatin-bound Smc2-HA levels in both *chl1* and *scc2-4* mutant cells are not reduced, compared to wildtype cells (Fig 3D). Thus, *chl1* and *scc2-4* single mutant cells exhibit significant condensation defects despite full retention of chromatin-bound condensin. These results document that the condensation defects exhibited by *chl1* and *scc2-4* single mutant cells occur largely independent of changes in condensin deposition onto DNA.

2.4 Chl1 and Scc2 function in condensation through cohesins

Having eliminated reduced condensin deposition as a central mechanism through which *chl1* and *scc2-4* mutants produce condensation defects, we turned to cohesin deposition. Wildtype, *chl1* and *scc2-4* single mutant strains were released from G1 into 37°C medium supplemented with nocodazole and the resulting preanaphase cells assayed for cohesin deposition. As before, we confirmed the Triton X-100 cell fractionation assay using PGK and H2B as cytosolic and chromatin fiduciary markers, respectively (Fig 3B). We and others previously ascertained that Mcd1 levels in whole cell lysates are unaffected in either *chl1* or *scc2-4* mutant cells [19, 25]. Thus, we compared the levels of chromatin bound Mcd1, normalized to H2B levels, in wildtype and *chl1* and *scc2-4* single mutant cells using a previously validated Mcd1/Scc1-directed antibody generously provided by Dr. Vincent Guacci of the Koshland Lab [44]. As expected from prior studies, Mcd1 binding to DNA was significantly reduced in *chl1* (38%) and *scc2-4* (82%) single mutant cells (Fig 3E). Notably, the reductions in Mcd1 binding mirrored the severity of the condensation defect, strongly indicative of a dose-dependent cohesin mechanism (Fig 3E). Independently, we repeated the assessment of Smc2-HA in these chromatin fractions now validated for *scc2-4* inactivation through reduced cohesin levels. Our results confirm that Scc2 inactivation has negligible effects on condensin deposition.

While rDNA condensation defects are completely reversible in condensin mutant cells, condensation defects are irreversible in cohesin mutants [58]. If Scc2 promotes condensation only through cohesin deposition, then condensation should be irreversible in *scc2-4* mutant cells. To test this prediction, wildtype and *scc2-4* mutant strains were released from G1 into 37°C medium supplemented with nocodazole for 3 hours and the resulting preanaphase cultures then shifted back to 23°C for 1 hour (Fig 4A). Cell

samples harvested both during the preanaphase arrest at 37°C and after the shift down to 23°C were then assessed for the disposition of rDNA condensation as previously described [45]. As expected, preanaphase wildtype cells arrested at 37°C exhibited high levels (69%) of condensed (loop-like) rDNA loci while *scc2-4* mutant cells instead exhibited significantly low levels (8%) of condensed rDNA loci (Fig 4B). Upon shifting down to 23°C, preanaphase wildtype cells continued to exhibit high levels (71%) of condensed (loop-like) rDNA loci. Importantly, *scc2-4* mutant cells also exhibited significantly low levels (14%) of condensed rDNA loci (Fig 4C). The predominantly irreversible condensation defect in *scc2-4* mutant cells mirrors that of cohesin mutants and is distinct from the complete rescue of condensation defects exhibited in condensin mutant cells following the same regimen [58]. The combination of these results strongly suggest that the condensation defects exhibited by *chl1* and *scc2-4* mutant cells occur predominantly through a reduction in cohesin, but not condensin, chromatin association.

2.5 Scc2 plays a mitotic role in arm condensation but not rDNA condensation

Scc2 inactivation during S phase causes severe chromosome condensation defects and cell lethality [19]. Intriguingly, there is limited evidence that Scc2 inactivation specifically during M phase also produces chromosome arm condensation defects, even while cells retain high viability [23]. We were intrigued by the possibility that *scc2-4* cell viability, during M phase inactivation, might be explained if rDNA remains condensed even while chromosome arms decondense. To test this possibility, wildtype and *scc2-4* mutant strains were synchronized in G1 in medium supplemented with alpha factor, released into 23°C medium supplemented with nocodazole for 3 hours, and the resulting

preanaphase cultures then shifted to 37°C for 1 hour to inactivate *scc2-4* specific during M phase (Fig 5A). Cell samples were processed to determine the status of rDNA condensation as previously described [45]. As expected, preanaphase wildtype cells maintained at 23°C exhibited high levels (77%) of condensed (loop-like) rDNA loci. Even at this temperature permissive for cell viability, *scc2-4* mutant cells exhibited surprisingly modest levels (45%) of condensed rDNA loci (Fig 5B and 5C). Preanaphase wildtype cells shifted to 37°C retained high levels (60%) of condensed rDNA, albeit with shorter rDNA loops as previously described [45]. Importantly, preanaphase *scc2-4* mutant cells shifted to 37°C similarly retained its modest level of condensed rDNA (48%) loci (Fig 5B and 5C). These results reveal that Scc2 is not required for condensation maintenance of rDNA during M phase, in contrast to the role played by Scc2 in condensation along chromosome arms [23]. Thus, Scc2-dependent cohesin roles in condensation differentially effects rDNA and chromosome arm loci during mitosis.

Discussion

Analyses of Chl1 helicase family members are of immediate clinical relevance. Mutations in CHL1 human homologs BACH1/BRIP/FANCJ and ChlR1/DDX11 helicases collectively result in Warsaw Breakage Syndrome, Fanconi anemia, breast and ovarian cancers [27, 35–37, 40, 59–61]. A link between the Chl1 helicase family and global changes in chromatin structure, however, remained untested. The first major revelation of the current study is that Chl1 is an important factor in promoting genome-wide chromosome condensation. Intriguingly, we found that chl1 mutants exhibit both chromosome arm and rDNA condensation defects, but at relatively moderate levels. This suggests that additional factors may support Chl1 in condensation reactions (including Scc2 and cohesin deposition onto DNA) and that cohesin-dependent condensation is taking place in S phase. Regardless, our findings extend the role of Chl1 beyond trans tethering (required for sister chromatid cohesion and DNA repair) to now include cis tethering [27, 31–34]. This distinction is critical in that cis tethering during G1 is thought to stabilize intramolecular DNA loops through which regulatory elements (enhancers, promoters, insulators) are brought into registration and thus deploy developmental transcription programs [1, 2]. Moreover, cis tethering also mediates both regional and genome-wide compaction reactions throughout the cell cycle—the latter of which is required for chromosome segregation. While the current study is unique in identifying a role for Chl1 DNA helicase in chromatin condensation, we note that mutation of other helicases (MCM7, MCM10, FBH1) in C. elegans or Drosophila models produced chromosome condensation defects, but effects attributed to incomplete replication and

often with minimal effects on chromosome segregation [62–66]. Our findings suggest a reevaluation of current models may be warranted.

How does Chl1 DNA helicase promote DNA condensation? A second revelation of the current study is that Chl1, and its downstream target Scc2, function predominantly through cohesin-based condensation. In the current study, we simultaneously monitored both cohesin and condensin chromatin binding levels and found that only cohesins are adversely affected in *chl1* and *scc2-4* mutant strains. Intriguingly, a prior study found that *scc2-4* inactivation during a mitotic-arrest produced a modest condensin binding defect, but an effect predicated on perceived changes in fluorescent intensity levels obtained from chromosome spreads. Notably, that study provided inconsistent data regarding reductions in condensin recruitment to loci assessed by chromatin immunoprecipitations [23]. While our current findings diminish the role of Scc2 (and Chl1) in condensin recruitment, we note that mutation of the RNA helicase Vasa, which produce condensation defects in mitotic germ-line Drosophila cells, exhibit reduced recruitment of the condensin SMC capping factor Barren to DNA [67]. Thus, it will be critical to elucidate the extent through which different model cell systems prioritize the use of SMC complexes to drive chromatin compaction. Assessing these possibilities is complicated, however, due to evidence that condensin recruitment may be mediated indirectly through reduced cohesin recruitment [58].

Elucidating the mechanism through which Chl1 promotes both Scc2 and cohesin recruitment to DNA to mediate cohesion (trans tethering) and condensation (cis tethering) remains an important issue in cell biology. Elegant biochemical findings reveal that Chl1 family members resolve secondary DNA structures such as G4s, triple helices, and 5’

forked/flapped duplexes thought to arise either immediately behind the DNA replication fork or occur within specific loci throughout the genome [28, 34, 68–74]. That these secondary DNA structures can be resolved in a post-fork context is strongly supported by findings that both Chl1 expression and chromatin binding peak during S phase and that Chl1 binds to numerous replication factors (such as Ctf4, Eco1, Fen1, Ctf18 and PCNA) that act in in conjunction with or immediately behind DNA polymerase [24, 27, 28, 30, 52, 54]. More recent findings posit that Scc2,4 binds DNA to maintain nucleosome-free domains onto which cohesins are later deposited [75]. Based on evidence that Chl1 family members disrupt streptavidin binding to biotinylated single-strand DNA oligonucleotides in vitro and resolve DNA secondary structures such as G quadruplexes (G4s) and triple DNA helices [70, 73, 76], we posit that Chl1 helicase actively promotes nucleosome-free domains that promote Scc2 and subsequent cohesin deposition (Fig 6). This helicase-based model in which DNA structure modulates Scc2 recruitment may equally apply to protein-based adaptors of Scc2,4 that include the elongation factor Paf1, Mediator transcription scaffold complex, the pre-Replication Complex (pre-RC), Ctf19/COMA kinetochore complex [77–89].

Materials and methods

Yeast strains and strain construction

Saccharomyces cerevisiae strains used in this study are listed in Table 1. GFP-tagging and deletion of genes were performed following a published protocol [41].

rDNA condensation assays

rDNA condensation assays were performed using Net1-GFP as previously described with the following modifications [23, 42]. Briefly, cells were cultured to log phase (OD600 between 0.2 to 0.4), then incubated for 2.5 hours at 23°C in rich YPD medium supplemented with alpha-factor. The resulting synchronized G1 cells were collected, washed, resuspended in fresh YPD supplemented with nocodazole, and incubated for 3 hours at 23°C. The resulting preanaphase cells were fixed by incubation in 3.7% paraformaldehyde for 10 min at 30°C. GFP signals were then assayed microscopically. Cell cycle progression was confirmed by detection of DNA content using flow cytometry as described [42].

rDNA condensation was independently assessed using a streamlined condensation assay adapted from a published FISH protocol [43–45]. Briefly, log phase cells (OD600 between 0.2 to 0.4) were incubated for 2.5 hours at 23°C in rich YPD medium supplemented with alpha-factor. The resulting synchronized G1 cells were collected, washed, resuspended in fresh YPD supplemented with nocodazole, and incubated for 3 hours at 23°C (where appropriate, additional temperature shifts are described within each experimental design). The resulting preanaphase cells were fixed by incubation in 37%

formaldehyde for 2 hours at 23°C. Cells were washed with distilled water and resuspended in buffer (1 M sorbitol, 20 mM KPO4, pH 7.4), then spheroplasted by the addition of beta-mercaptoethanol and Zymolyase 100T and incubation for 1 hour at 23°C. The resulting spheroplasted cells were placed onto poly-L-lysine coated slides prior to addition of 0.5% Triton X-100 and 0.5% SDS solution. The slides were then incubated in 3:1 methanol:acetic acid solution and stored at 4°C until completely dry. Slides were then treated with RNase in 2X SSC buffer (0.3 M NaCl, 30 mM Sodium Citrate, pH 7.0) followed by washes in 2X SSC and then by a series of cold ethanol washes. Slides were then incubated at 72°C in 70% formamide with 2X SSC followed by a series of cold ethanol washes. DNA masses were detected by DAPI staining and assayed microscopically. Cell cycle progression was confirmed by detection of DNA content using flow cytometry as described [42].

Chromosome arm condensation assay

Chromosome arm condensation assays were performed in yeast cells that contained two lacO repeats, one integrated telomere-proximal on the left arm and another integrated centromere-proximal on the right arm of chromosome XII. Each LacO cassette was monitored microscopically through detection of lacI-GFP [23]. Condensation assays and quantification were performed as previously described with the following modifications [23]. Briefly, log phase cells (OD600 between 0.2 to 0.4) were incubated for 2.5 hours at 23°C in rich YPD medium supplemented with alpha-factor. The resulting synchronized G1 cells were collected, washed, resuspended in fresh YPD supplemented with nocodazole and incubated for 3 hours at 23°C. The resulting preanaphase cells were fixed

by incubation in 3.7% paraformaldehyde for 10 min at 30°C. Wildtype and *chl1* mutant cells that contained a single GFP dot reflected sister chromatids positioned vertical to the z-axial focal plane and were thus excluded from analysis. We also excluded cells that contained three or four GFP loci, since the cohesion defect at one or both loci made it difficult to determine which GFP dot represented an intra- or inter-sister chromatid locus. Distances between two GFP dots were quantified microscopically with images captured using iVision. Cell cycle progression was confirmed by detection of DNA content using flow cytometry as described [42].

Chromatin binding assay

Nocodazole arrested cells were harvested and processed for chromatin binding assay [25]. Briefly, the densities of 50 ml cultures were normalized to an OD600 between 0.4–0.6. Cells were spun down and washed with 25 ml cold sterile water, followed by a wash in 1.2 M sorbitol. Pellets were resuspended in 1 ml CB1 buffer (50 mM Sodium citrate, 40 mM EDTA, 1.2 M sorbitol, pH 7.4) prior to the addition of 125 μl of spheroplast solution (125 μl CB1, 50 μl zymolase, 5 μl BME) and incubation with gentle shaking for 1 hour at 23°C. The spheroplast suspensions were supplemented with protease inhibitor cocktail, washed 2X with 1.2 M cold sorbitol, resuspended in 425 μl of 1.2 M cold sorbitol and snap frozen in liquid Nitrogen. Frozen samples were thawed on ice prior to the addition of 50 μl lysis buffer (500 mM Lithium acetate, 20 mM MgSO4, 200 mM HEPES, pH 7.9) and 20 μl of 25% Triton-X-100. Whole cell extract (WCE) fractions were collected and denatured by the addition of an equal volume of 2X Laemmli buffer, boiled for 5 minutes and then snap frozen. The remaining lysates were centrifuged at

12,000 g for 15 minutes. Supernatants consisting of soluble fractions were collected and denatured by the addition of an equal volume of 2X Laemmli buffer. Pellets were resuspended in Lysis buffer with 150 mM NaCl and centrifuged at 15,000 g for 15 minutes. Chromatin bound fractions were obtained by suspending the resulting pellets 1.2 M sorbitol and then denatured by the addition of an equal volume of 2X Laemmli buffer. Whole cell extract, soluble and chromatin bound fractions were resolved by SDS-PAGE electrophoresis and analyzed by Western blot using anti-HA (1:2000) (Santa Cruz), anti-PGK (1:20000) (Invitrogen) with goat anti mouse HRP (1:50000) (Bio-Rad) or by anti-H2B (1:2000) (Santa Cruz) or 1:60000 (Abcam), anti-Mcd1 [46] in combination with goat anti rabbit HRP (1:50000) (Bio-Rad) and ECL prime (GE Healthcare) for visualization.

Figures

Figure 1

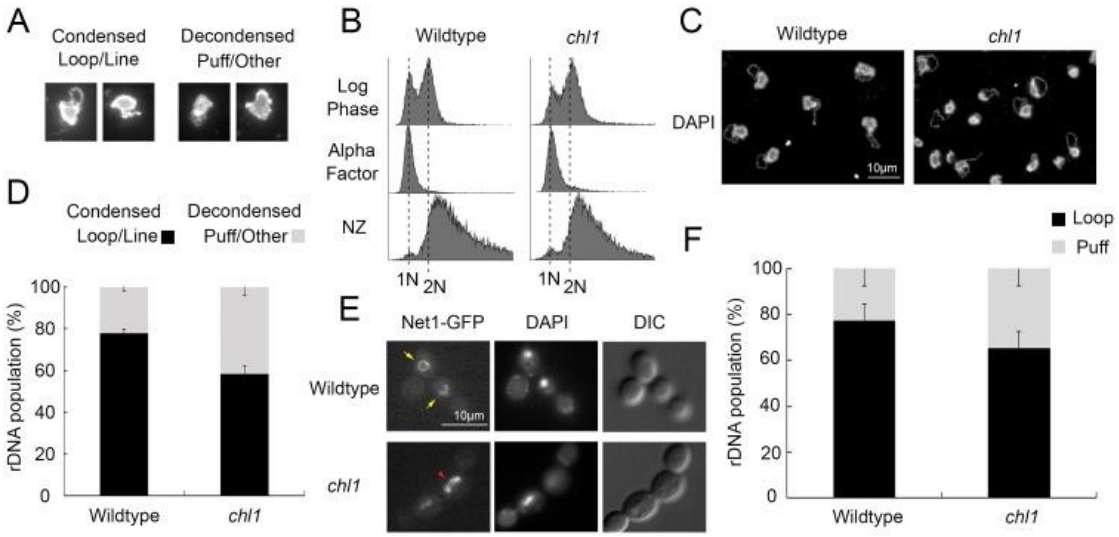

Figure 1. Chl1 helicase promotes rDNA condensation.

A) Representative examples of micrographs that highlight condensed (loop and line) and decondensed (amorphous puff-like and other non-discrete configuration) rDNA structures. B) Flow cytometer of DNA content at times indicated throughout the experimental procedure. Cells were maintained in nocodazole for 3 hours at 23°C post-alpha factor arrest. C) Chromosome mass and rDNA detected using DAPI in wildtype (YBS1019) and *chl1* mutant (YBS1041) strains. D) Quantification of condensed (loop/line) and decondensed (puff/other) rDNA populations in wildtype and *chl1* mutant cells. Data quantified from 3 biological replicates, 100 cells for each strain analyzed per replicate and statistical analysis performed using Student's T-test ($p = 0.005$). E) rDNA structures visualized using Net1-GFP, genome DNA detected using DAPI, and cell morphology images obtained using Differential Interference Contrast (DIC) microscopy.

Yellow arrows indicate condensed rDNA loop/line and red arrowhead indicates decondensed rDNA puff. F) Quantification of condensed (loop) and decondensed (puff) rDNA populations in wildtype (YBS2020) and *chl1* mutant (YBS2080) cells. Data quantified from 3 biological replicates, 100 cells for each strain analyzed per replicate and statistical analysis performed using Student's T-test ($p = 0.006$). Statistical significant differences (*) are based on $p < 0.05$.

Figure 2

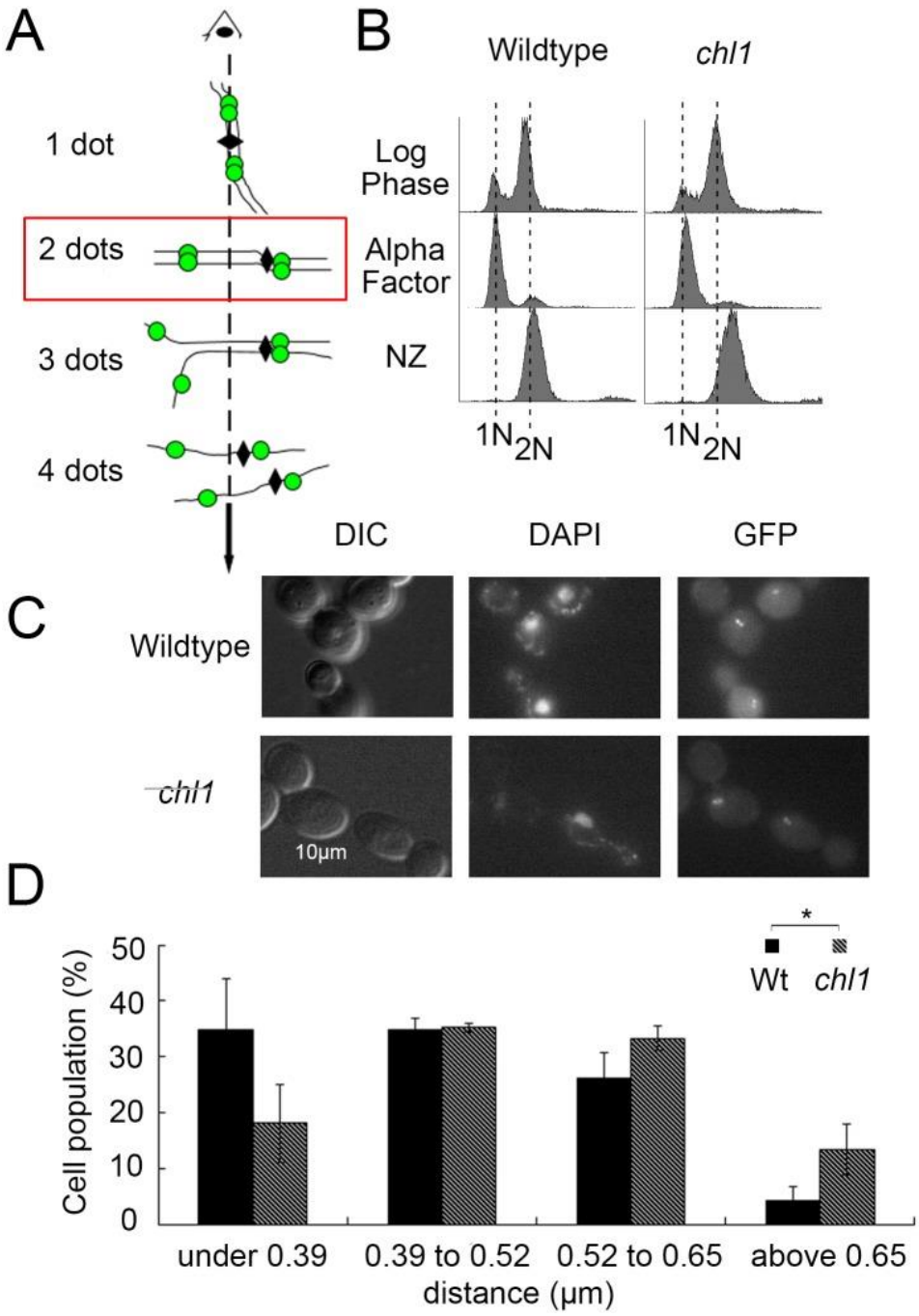

Figure 2. Chl1 helicase promotes chromosome arm condensation.

A) Schematic of chromosome conformations and GFP-labeled loci (dashed line indicates Z-axial microscope orientation, solid line indicates sister chromatid, diamond indicates centromere, green dot indicates GFP locus). Red box indicates cells analyzed. B) Flow cytometer data of DNA content throughout the experiment. Cells were maintained in nocodazole for 3 hours at 23°C post-alpha factor arrest. C) Micrographs of representative fields of view that include GFP loci, genomic mass (DAPI) and cell morphology (DIC). D) Distribution of distances measured between GFP dots in wildtype (YBS2078) and *chl1* mutant (YBS2079) cells. Data obtained from 3 biological replicates, 100 cells for each strain analyzed per replicate and statistical analysis performed using Student's T-test. $p = 3.862E-6$ indicates the significant differences between the average distance (0.44 μm) in wildtype cells versus the average distance (0.50 μm) in *chl1* mutant cells. Statistical significant differences (*) are based on $p < 0.05$.

Figure 3

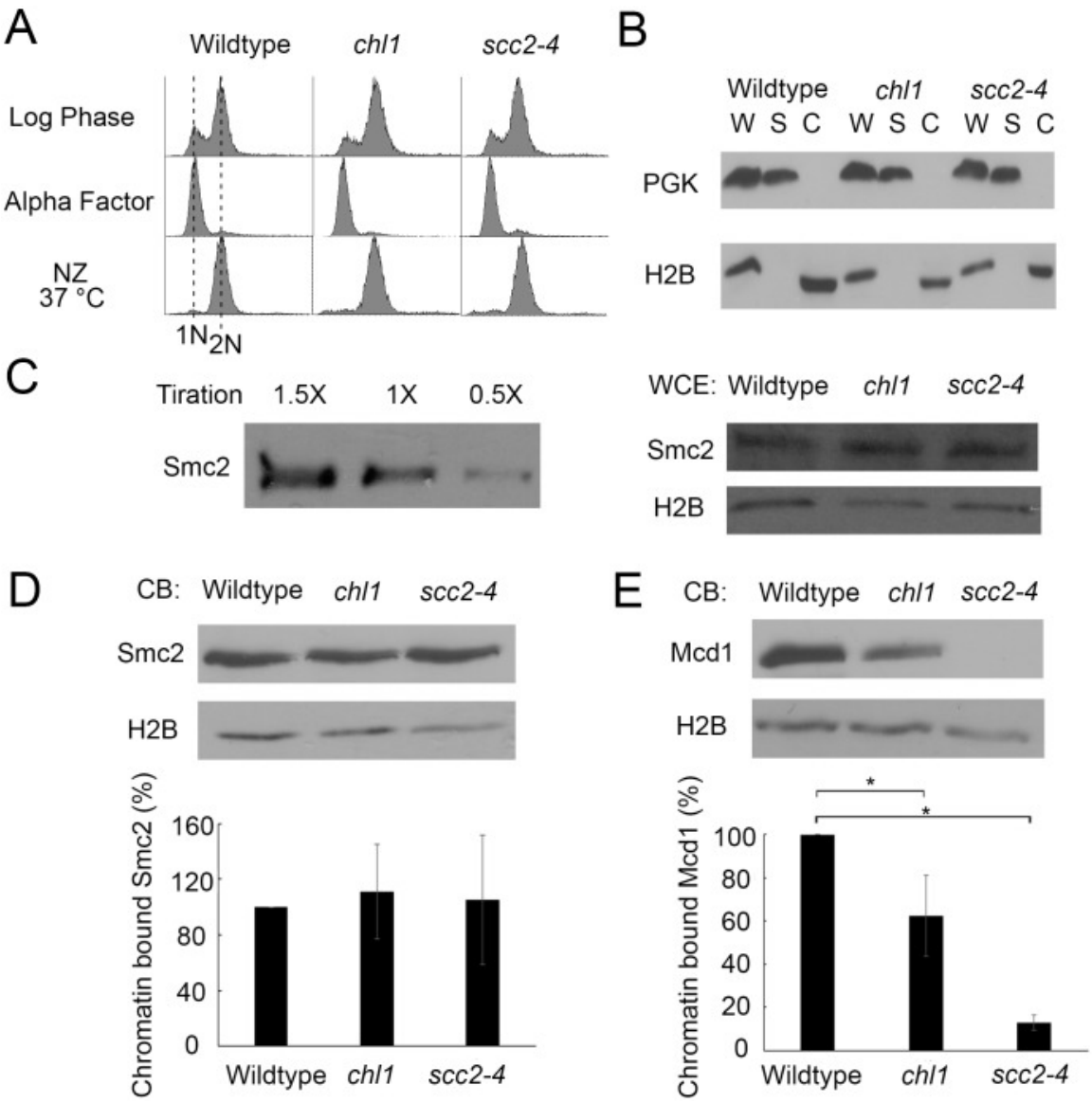

Figure 3. Chl1 helicase promotes chromosome condensation through cohesin, but not condensin, regulation.

A) Flow cytometer data of DNA content throughout the experiment. Cells were maintained in nocodazole for 3 hours at 37°C post-alpha factor arrest. B) Fractionation of preanaphase-arrested wildtype (YDS101), *chl1* (YDS104) and *scc2-4* (YDS108) cells.

Phosphoglycerate kinase (PGK) and Histone 2B (H2B) indicate levels of cytoplasmic and chromatin-bound proteins, respectively, in whole cell extracts (W), cytoplasmic soluble fractions (S) and chromatin bound fractions (C). C) Left: Titration of Smc2-HA indicates 1X sample concentration is in the linear range of detection. Right: Whole cell extracts of Smc2-HA in wildtype, *chl1* and *scc2-4* cells. H2B is shown as internal loading control. All samples reflect 1X concentration levels. D) Top: Chromatin-bound (CB) fraction of Smc2-HA in wildtype, *chl1* and *scc2-4* cells. Chromatin-bound H2B levels are shown as internal loading control. Bottom: Quantification of Smc2-HA binding to chromatin in *chl1* and *scc2-4* mutant cells, based on the ratio of Smc2-HA to H2B levels and normalized to wildtype levels of Smc2-HA obtained from 3 biological replicates. E) Top: Chromatin-bound fraction of Mcd1 in wildtype, *chl1* and *scc2-4* cells. Chromatin-bound H2B levels are shown as loading controls. Bottom: Quantification of Mcd1 binding to chromatin in *chl1* and *scc2-4* mutant cells, based on the ratio of Mcd1 to H2B levels and normalized to wildtype levels obtained from 3 biological replicates. Statistical analysis was performed using one-way ANOVA followed by post-hoc Tukey HSD Test. ($p = 0.024$ for chromatin bound Mcd1 in wildtype versus *chl1* mutant cells. $p = 0.001$ for chromatin bound Mcd1 in wildtype cells versus *scc2-4* mutant cells). Statistical significant differences (*) are based on $p < 0.05$.

Figure 4

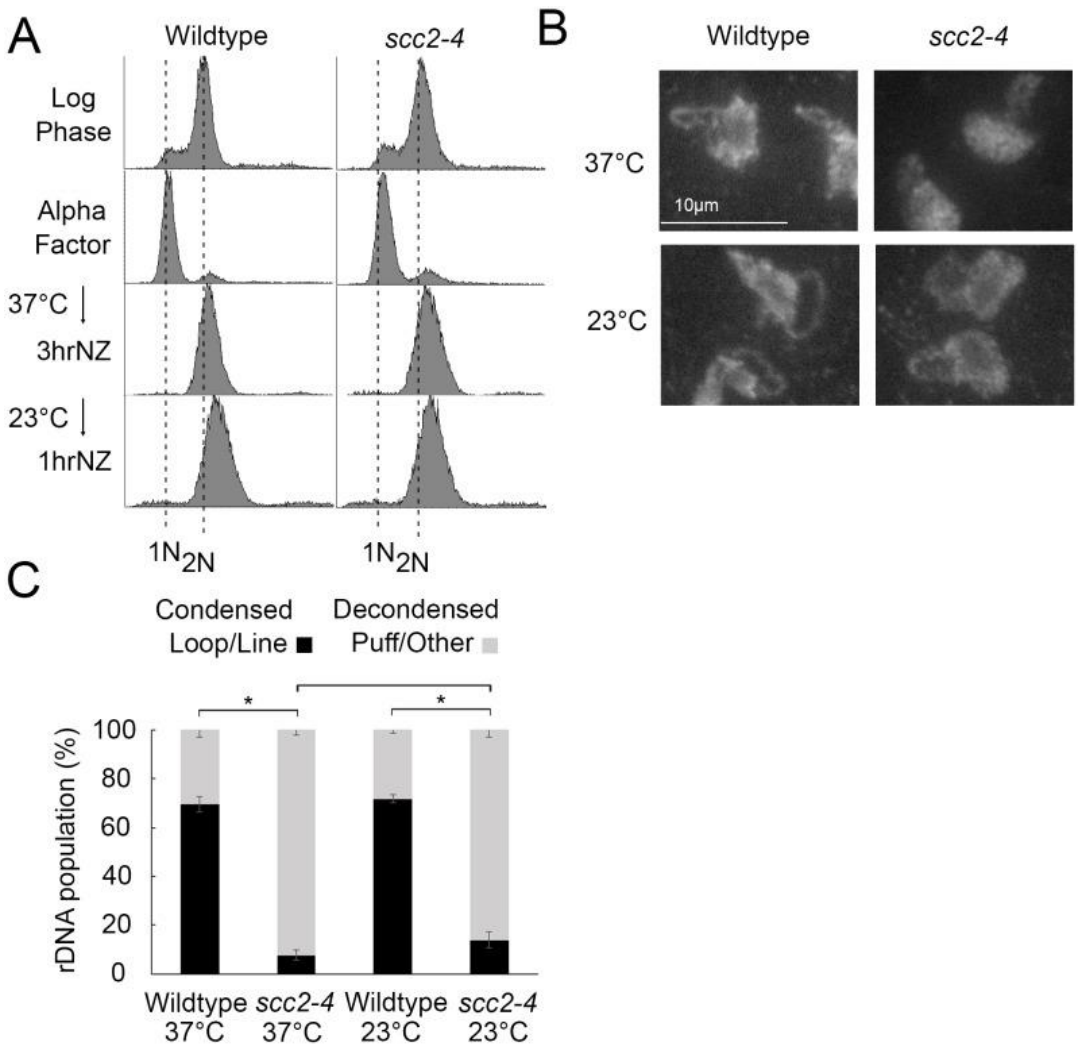

Figure 4. Condensation is irreversible in *scc2-4* mutants.

A) Flow cytometer data reveals DNA content throughout the experimental analyses. Cells were maintained in nocodazole, post-alpha factor release, for 3 hours at 37°C followed by an additional 1 hour at 23°C. B) Chromosome mass and rDNA structures detected using DAPI in wildtype and *scc2-4* mutant strains. C) Quantification of condensed (loop/line) and decondensed (puff/other) rDNA populations in wildtype

(YBS1019) and *scc2-4* mutant (YMM551) cells. Quantifications and statistical analyses of rDNA condensation were obtained from 3 biological replicates for each strain (wildtype and *scc2-4* mutant cells) in which each replicate included 100 cells for each strain. Statistical analyses of condensed populations were performed using one-way ANOVA followed by post-hoc Tukey HSD Test ($p = 0.001$ for wildtype versus *scc2-4* mutant cell rDNA condensation at 37°C; $p = 0.001$ for wildtype versus *scc2-4* mutant cell rDNA condensation at 23°C; $p = 0.890$ for wildtype cell rDNA condensation at 37°C versus 23°C; $p = 0.301$ for *scc2-4* mutant cell rDNA condensation at 37°C versus 23°C). Statistical significant differences (*) are based on $p < 0.05$.

Figure 5

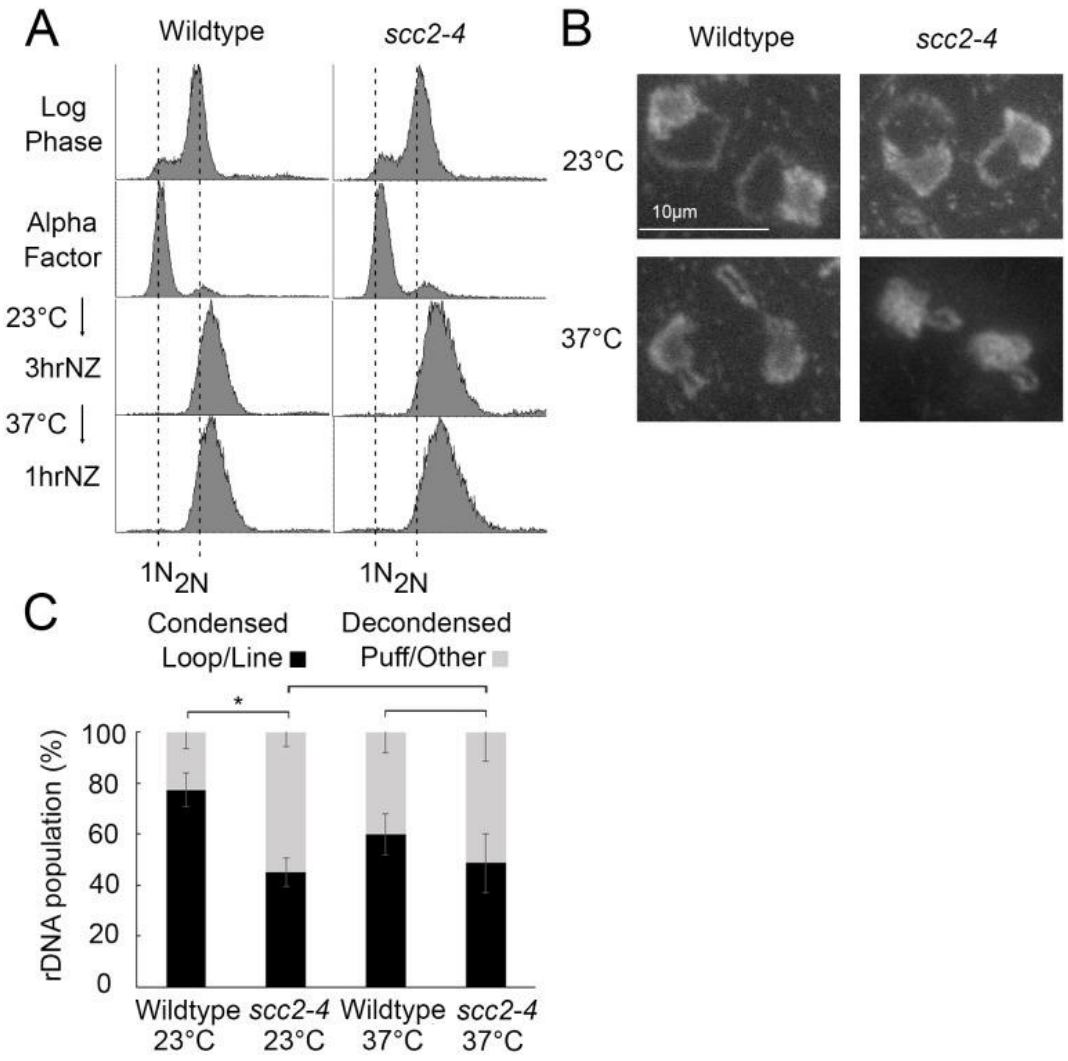

Figure 5. Scc2 is dispensable for condensation maintenance during M phase.

A) Flow cytometer data reveals DNA content throughout the experimental analyses. Cells were maintained in nocodazole, post-alpha factor release, for 3 hours at 23°C followed by an additional 1 hour at 37°C. B) Chromosome mass and rDNA structures detected using DAPI in wildtype and *scc2-4* mutant strains. C) Quantification of condensed (loop/line) and decondensed (puff/other) rDNA populations in wildtype

(YBS1019) and *scc2-4* mutant (YMM551) cells. Quantifications and statistical analyses of rDNA condensation were obtained from 3 biological replicates for each strain (wildtype and *scc2-4* mutant cells) in which each replicate included 100 cells for each strain. Statistical analyses of condensed populations were performed using one-way ANOVA followed by post-hoc Tukey HSD Test ($p = 0.014$ for wildtype cell versus *scc2-4* mutant cell rDNA condensation at 23°C; $p = 0.804$ for wildtype cell versus *scc2-4* mutant cell rDNA condensation at 37°C; $p = 0.133$ for wildtype cell rDNA condensation at 23°C versus 37°C; $p = 0.878$ for *scc2-4* mutant cell rDNA condensation at 23°C versus 37°C). Statistical significant differences (*) are based on $p < 0.05$.

Figure 6

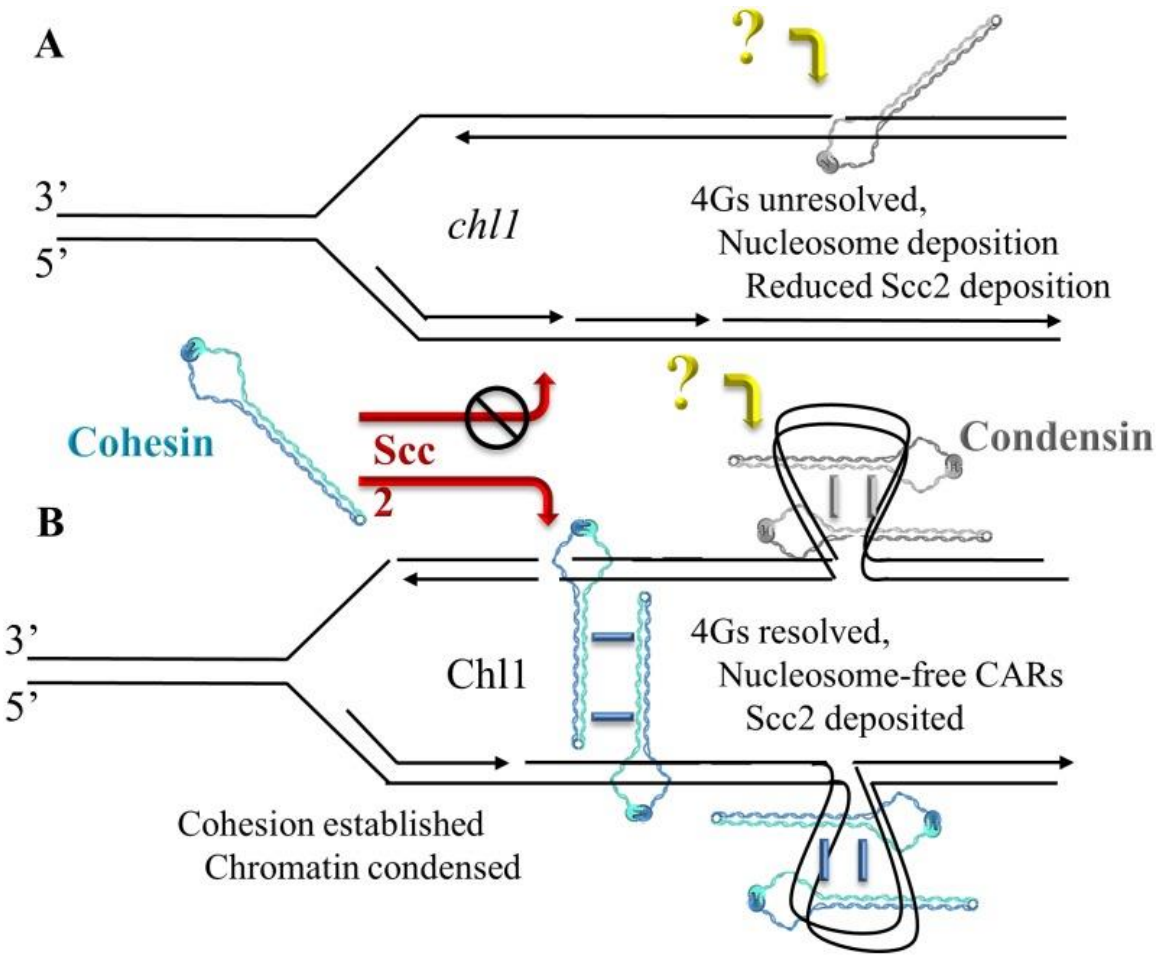

Figure 6. Chl1 DNA helicase functions in condensation.

A) In the absence of Chl1, condensation defects occur despite normal recruitment of condensin ('?' reflects that condensin deposition, but not cohesin deposition, occurs despite Scc2 inactivation). We hypothesize that secondary DNA structures (such as G4s and nucleosomes) reduce both Scc2 and cohesin recruitment, resulting in cohesion and condensation defects. B) Chl1 activities (resolution of DNA secondary structures, histone displacement, etc) provides for both Scc2 and cohesin recruitment, resulting in sister chromatid cohesion (trans tethering) and chromatin condensation (cis tethering). Cohesin

and condensin oligomerization are shown as one of several possible mechanisms of cohesion and condensation [1], [90].

Figure S1

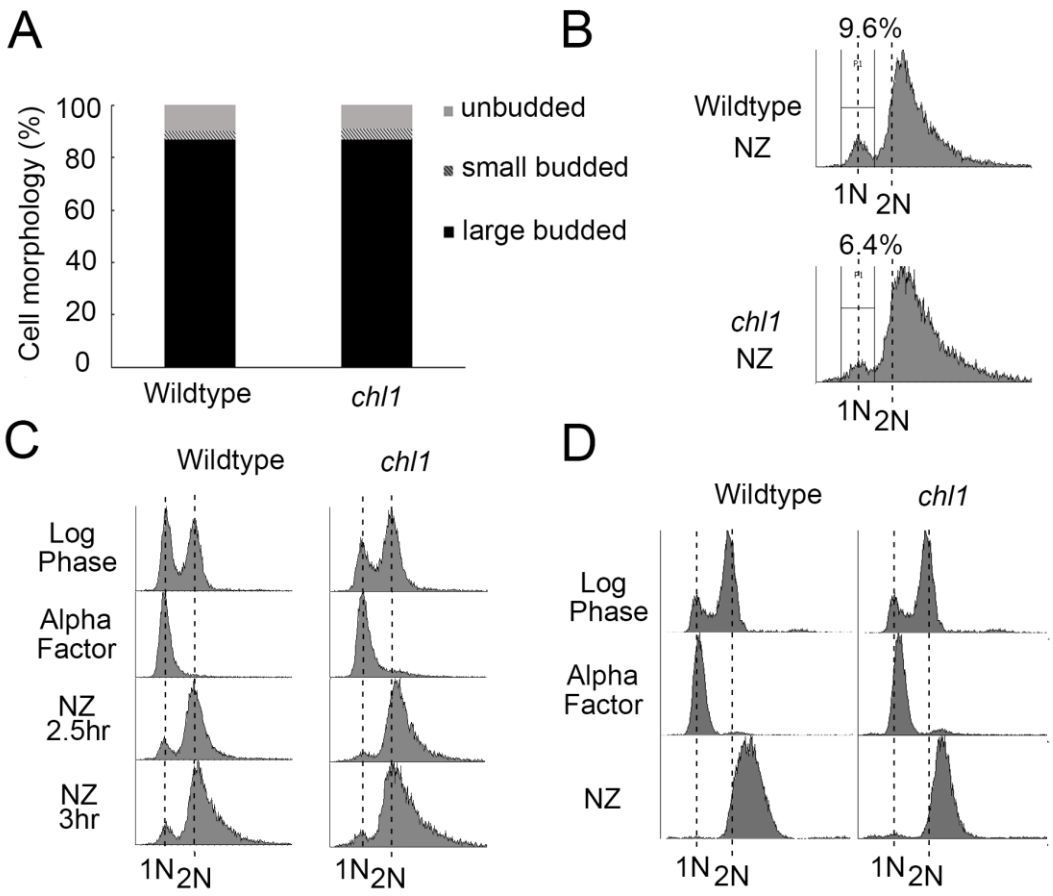

Figure S1. Cell cycle progression in wildtype and *chl1* mutant.

A) Morphology quantification for both nocodazole-arrested wildtype and *chl1* mutant cells (N = 100 cells for each strain). B) 1N peak quantification for both wildtype and *chl1* mutant cells arrested in nocodazole for 3 hours at 23°C. C) Flow cytometer data reveals DNA contents in wildtype and *chl1* mutant cells after nocodazole arrest at 23°C for 2.5 hours and 3 hours. D) Flow cytometer data reveals DNA content in wildtype and *chl1* mutant cells analyzed in Fig 1E and 1F.

Table 1

Yeast strains used in this study.

Strain name	**Genotype**	**Reference**
YBS1019	*MATa; S288C*	24
YBS1041	*MATa; chl1::KAN; S288C*	27
YBS2020	*MATa; NET1:GFP:HIS3; w303*	For this study
YBS2078	*MATa; lacOs::YLR003c-1; lacOs::MMP1; LacI-GFP; w303*	Y2869, 23
YBS2079	*MATa; chl1::TRP; lacOs::YLR003c-1; lacOs::MMP1; LacI-GFP; w303*	For this study
YBS2080	*MATa; NET1:GFP:HIS3; chl1::TRP; w303*	For this study
YDS101	*MATa; SMC2:3HA:KanMX6; w303*	For this study
YDS104	*MATa; SMC2:3HA:KanMX6; chl1::TRP; w303*	For this study
YDS108	*MATa; SMC2:3HA:KanMX6; scc2-4; w303*	For this study
YMM551	*MATa; scc2-4; can1-100; w303*	91

References

1. Skibbens RV. Of Rings and Rods: Regulating Cohesin Entrapment of DNA to Generate Intra- and Intermolecular Tethers. *PLoS Genet.* 2016;12(10): e1006337.

2. Dorsett D, Merkenschlager M. Cohesin at active genes: a unifying theme for cohesin and gene expression from model organisms to humans. *Curr Opin Cell Biol.* 2013;25(3): 327–333.

3. Martin RM, Cardoso MC. Chromatin condensation modulates access and binding of nuclear proteins. *FASEB J.* 2010;24(4): 1066–1072.

4. Piskadlo E, Oliveira RA. Novel insights into mitotic chromosome condensation. *F1000Res.* 2016;5: 1807.

5. Tsang CK, Li H, Zheng XS. Nutrient starvation promotes condensin loading to maintain rDNA stability. *EMBO J.* 2007;26(2): 448–458.

6. Hirano T. Condensins: universal organizers of chromosomes with diverse functions. *Genes Dev.* 2012;26(15): 1659–1678.

7. Jeppsson K, Kanno T, Shirahige K, Sjögren C. The maintenance of chromosome structure: positioning and functioning of SMC complexes. *Nat Rev Mol Cell Biol.* 2014;15(9): 601–614.

8. Mannini L, Musio A. The dark side of cohesin: the carcinogenic point of view. *Mutat Res.* 2011;728(3): 81–87.

9. Mehta GD, Kumar R, Srivastava S, Ghosh SK. Cohesin: functions beyond sister chromatid cohesion. *FEBS Lett.* 2013;587(15): 2299–2312.

10. Feng XD, Song Q, Li CW, Chen J, Tang HM, Peng ZH, et al. Structural maintenance of chromosomes 4 is a predictor of survival and a novel therapeutic target in

colorectal cancer. *Asian Pac J Cancer Prev.* 2014;15(21): 9459–9465.

11. Yin L, Jiang LP, Shen QS, Xiong QX, Zhuo X; Zhang LL, et al. NCAPH plays important roles in human colon cancer. *Cell Death Dis.* 2017;8(3): e2680.

12. Woodward J, Taylor GC, Soares DC, Boyle S, Sie D, Read D, et al. Condensin II mutation causes T-cell lymphoma through tissue-specific genome instability. *Genes Dev.* 2016;30(19): 2173–2186.

13. Perche O, Menuet A, Marcos M, Liu L, Pâris A, Utami KH, et al. Combined deletion of two Condensin II system genes (NCAPG2 and MCPH1) in a case of severe microcephaly and mental deficiency. *Eur J Med Genet.* 2013;56(11): 635–641.

14. Martin CA, Murray JE, Carroll P, Leitch A, Mackenzie KJ, Halachev M, et al. Deciphering Developmental Disorders Study, Wood AJ, Vagnarelli P, Jackson AP. Mutations in genes encoding condensin complex proteins cause microcephaly through decatenation failure at mitosis. *Genes Dev.* 2016;30(19): 2158–2172.

15. Gruber S, Haering CH, Nasmyth K. Chromosomal cohesin forms a ring. *Cell.* 2003;112: 765–777.

16. Cuylen S, Metz J, Haering CH. Condensin structures chromosomal DNA through topological links. *Nat Struct Mol Biol.* 2011;18(8): 894–901.

17. Kalitsis P, Zhang T, Marshall KM, Nielsen CF, Hudson DF. Condensin, master organizer of the genome. *Chromosome Res.* 2017;25(1): 61–76.

18. Rollins RA, Morcillo P, Dorsett D. Nipped-B, a Drosophila homologue of chromosomal adherins, participates in activation by remote enhancers in the cut and Ultrabithorax genes. *Genetics.* 1999;152(2): 577–593.

19. Ciosk R, Shirayama M, Shevchenko A, Tanaka T, Toth A, Shevchenko A, et al.

Cohesin's binding to chromosomes depends on a separate complex consisting of Scc2 and Scc4 proteins. *Mol Cell.* 2000;5(2): 243–254.

20. Tonkin ET, Wang TJ, Lisgo S, Bamshad MJ, Strachan T. NIPBL, encoding a homolog of fungal Scc2-type sister chromatid cohesion proteins and fly Nipped-B, is mutated in Cornelia de Lange syndrome. *Nat Genet.* 2004;36(6): 636–641.

21. Krantz ID, McCallum J, DeScipio C, Kaur M, Gillis LA, Yaeger D, et al. Cornelia de Lange syndrome is caused by mutations in NIPBL, the human homolog of Drosophila melanogaster Nipped-B. *Nat Genet.* 2004;36(6): 631–635.

22. Seitan VC, Banks P, Laval S, Majid NA, Dorsett D, Rana A, et al. Metazoan Scc4 homologs link sister chromatid cohesion to cell and axon migration guidance. *PLoS Biol.* 2006;4(8): e242.

23. D'Ambrosio C, Schmidt CK, Katou Y, Kelly G, Itoh T, Shirahige K, et al. Identification of cis-acting sites for condensin loading onto budding yeast chromosomes. *Genes Dev.* 2008;22(16): 2215–2227.

24. Rudra S, Skibbens RV. Sister chromatid cohesion establishment occurs in concert with lagging strand synthesis. *Cell Cycle.* 2012;11(11): 2114–2121.

25. Rudra S, Skibbens RV. Chl1 DNA helicase regulates Scc2 deposition specifically during DNA-replication in *Saccharomyces cerevisiae*. *PLoS One.* 2013;8(9): e75435.

26. Lopez-Serra L, Lengronne A, Borges V, Kelly G, Uhlmann F. Budding yeast Wapl controls sister chromatid cohesion maintenance and chromosome condensation. *Curr Biol.* 2013;23(1): 64–69.

27. Skibbens RV. Chl1p, a DNA Helicase-Like Protein in Budding Yeast, Functions in Sister-Chromatid Cohesion. *Genetics.* 2004;166(1): 33–42.

28. Farina A, Shin JH, Kim DH, Bermudez VP, Kelman Z, Seo YS, et al. Studies with the Human Cohesin Establishment Factor, ChlR1 association of ChlR1 with CTF18-RFC and Fen1. *J Biol Chem.* 2008;283(30): 20925–20936.

29. Borges V, Smith DJ, Whitehouse I, Uhlmann F. An Eco1-independent sister chromatid cohesion establishment pathway in *S. cerevisiae*. *Chromosoma* (2013; 122(1–2): 121–134.

30. Samora CP, Saksouk J, Goswami P, Wade BO, Singleton MR, Bates PA, et al. Ctf4 Links DNA Replication with Sister Chromatid Cohesion Establishment by Recruiting the Chl1 Helicase to the Replisome. *Mol Cell.* 2016;63(3): 371–384.

31. Petronczki M, Chwalla B, Siomos MF, Yokobayashi S, Helmhart W, Deutschbauer AM, et al. Sister-chromatid cohesion mediated by the alternative RF-CCtf18/Dcc1/Ctf8, the helicase Chl1 and the polymerase-alpha-associated protein Ctf4 is essential for chromatid disjunction during meiosis II. *J Cell Sci.* 2004;117(16): 3547–3559.

32. Mayer ML, Pot I, Chang M, Xu H, Aneliunas V, Kwok T, et al. Identification of protein complexes required for efficient sister chromatid cohesion. *Mol Biol Cell.* 2004;15(4): 1736–1745.

33. Parish JL, Rosa J, Wang X, Lahti JM, Doxsey SJ, Androphy EJ. The DNA helicase ChlR1 is required for sister chromatid cohesion in mammalian cells. *J Cell Sci.* 2006;119(23): 4857–4865.

34. Inoue A, Li T, Roby SK, Valentine MB, Inoue M, Boyd K, et al. Loss of ChlR1 helicase in mouse causes lethality due to the accumulation of aneuploid cells generated by cohesion defects and placental malformation. *Cell Cycle.* 2007;6(13): 1646–1654.

35. Van der Lelij P, Chrzanowska KH, Godthelp BC, Rooimans MA, Oostra AB, Stumm M, et al. Warsaw breakage syndrome, a cohesinopathy associated with mutations in the XPD helicase family member DDX11/ChlR1. *Am J Hum Genet.* 2010;86(2): 262–266.

36. Litman R, Peng M, Jin Z, Zhang F, Zhang J, Powell S, et al. BACH1 is critical for homologous recombination and appears to be the Fanconi anemia gene product FANCJ. *Cancer Cell.* 2005;8(3): 255–265.

37. Rafnar T, Gudbjartsson DF, Sulem P, Jonasdottir A, Sigurdsson A, Jonasdottir A, et al. Mutations in BRIP1 confer high risk of ovarian cancer. *Nat Genet.* 2011;43(11): 1104–1107.

38. Peng M, Litman R, Jin Z, Fong G, Cantor SB. BACH1 is a DNA repair protein supporting BRCA1 damage response. *Oncogene.* 2006;25(15): 2245–53.

39. Cantor SB, Bell DW, Ganesan S, Kass EM, Drapkin R, Grossman S, et al. BACH1, a novel helicase-like protein, interacts directly with BRCA1 and contributes to its DNA repair function. *Cell.* 2001;105(1): 149–160.

40. Cantor S, Drapkin R, Zhang F, Lin Y, Han J, Pamidi S, et al. The BRCA1-associated protein BACH1 is a DNA helicase targeted by clinically relevant inactivating mutations. *Proc Natl Acad Sci U S A. 2*004;101(8): 2357–2362.

41. Longtine MS, McKenzie A 3rd, Demarini DJ, Shah NG, Wach A, Brachat A, et al. Additional modules for versatile and economical PCR-based gene deletion and modification in *Saccharomyces cerevisiae*. *Yeast.* 1988;14(10): 953–961.

42. Tong K, Skibbens RV. Pds5 regulators segregate cohesion and condensation pathways in *Saccharomyces cerevisiae*. *Proc Natl Acad Sci USA.* 2015;112(22): 7021–

7026.

43. Guacci V, Hogan E, Koshland D. Chromosome condensation and sister chromatid pairing in budding yeast. *J Cell Biol.* 1994;125(3): 517–530.

44. Guacci V, Koshland D, Strunnikov A. A direct link between sister chromatid cohesion and chromosome condensation revealed through the analysis of MCD1 in *S. cerevisiae. Cell.* 1997;91(1): 47–57.

45. Shen D, Skibbens RV. Temperature-dependent regulation of rDNA condensation in *Saccharomyces cerevisiae*. *Cell Cycle.* 2017; 1–10.

46. Noble D, Kenna MA, Dix M, Skibbens RV, Unal E, Guacci V. Intersection between the regulators of sister chromatid cohesion establishment and maintenance in budding yeast indicates a multi-step mechanism. *Cell Cycle.* 2006;5(21): 2528–2536.

47. Lavoie BD, Hogan E and Koshland D. In vivo dissection of the chromosome condensation machinery reversibility of condensation distinguishes contributions of condensin and cohesin. *J Cell Biol.* 2002;156(5): 805–815.

48. Kobayashi T. How does genome instability affect lifespan? *Genes Cells.* 2011. June; 16(6): 617–624.

49. Herskowitz I. Life cycle of the budding yeast *Saccharomyces cerevisiae*. *Microbiol Rev.* 1988;52(4): 536–553.

50. Straight AF, Shou W, Dowd GJ, Turck CW, Deshaies RJ, Johnson AD, et al. Net1, a Sir2-associated nucleolar protein required for rDNA silencing and nucleolar integrity. *Cell.* 1999;97(2): 245–256.

51. Nomura M. Ribosomal RNA genes, RNA polymerases, nucleolar structures, and synthesis of rRNA in the yeast *Saccharomyces cerevisiae*. *Cold Spring Harb Symp Quant*

Biol. 2001;66: 555–565.

52. Skibbens RV, Corson BL, Koshland D, Hieter P. Ctf7p is essential for sister chromatid cohesion and links mitotic chromosome structure to the DNA replication machinery. *Genes Dev.* 1999;13(3): 307–319.

53. Tóth A, Ciosk R, Uhlmann F, Galova M, Schleiffer A, Nasmyth K. Yeast Cohesin complex requires a conserved protein, Eco1p(Ctf7), to establish cohesion between sister chromatids during DNA replication. *Genes Dev.* 1999;13(3): 320–333.

54. Moldovan GL, Pfander B, Jentsch S. PCNA controls establishment of sister chromatid cohesion during S phase. *Mol Cell*. 2006;23: 723–732.

55. Méndez J, Stillman B. Chromatin association of human origin recognition complex, cdc6, and minichromosome maintenance proteins during the cell cycle: assembly of prereplication complexes in late mitosis. *Mol Cell Biol.* 2000;20(22): 8602–8612.

56. Leman AR, Noguchi C, Lee CY, Noguchi E. Human Timeless and Tipin stabilize replication forks and facilitate sister-chromatid cohesion. *J Cell Sci.* 2010;123(5): 660–670.

57. Tong K, Skibbens RV. Cohesin without cohesion: a novel role for Pds5 in *Saccharomyces cerevisiae*. *PLoS One.* 2014;9(6): e100470.

58. Lavoie BD, Hogan E, Koshland D. In vivo requirements for rDNA chromosome condensation reveal two cell-cycle-regulated pathways for mitotic chromosome folding. *Genes Dev*. 2004;18(1): 76–87.

59. Amann J, Kidd VJ, Lahti JM. Characterization of putative human homologues of the yeast chromosome transmission fidelity gene, CHL1. *J Biol Chem.* 1997;272(6):

3823–3832.

60. Levitus M, Waisfisz Q, Godthelp BC, de Vries Y, Hussain S, Wiegant WW, et al. The DNA helicase BRIP1 is defective in Fanconi anemia complementation group J. *Nat Genet.* 2005;37(9): 934–935.

61. Gupta R, Sharma S, Sommers JA, Kenny MK, Cantor SB, Brosh RM Jr. FANCJ (BACH1) helicase forms DNA damage inducible foci with replication protein A and interacts physically and functionally with the single-stranded DNA-binding protein. *Blood.* 2007;110(7): 2390–2398.

62. Sonneville R, Craig G, Labib K, Gartner A, Blow JJ. Both Chromosome Decondensation and Condensation Are Dependent on DNA Replication in C. elegans Embryos. *Cell Rep.* 2015;12(3): 405–417.

63. Christensen TW, Tye BK. Drosophila Mcm10 Interacts with Members of the Prereplication Complex and Is Required for Proper Chromosome Condensation. Mol *Biol Cell.* 2003;14(6): 2206–2215.

64. Chmielewski JP, Henderson L, Smith CM, Christensen TW. Drosophila Psf2 has a role in chromosome condensation. *Chromosoma*. 2012;121(6): 585–596.

65. Petrova B, Dehler S, Kruitwagen T, Hériché JK, Miura K, Haering CH. Quantitative Analysis of Chromosome Condensation in Fission Yeast. *Mol Cell Biol.* 2013;335: 984–998.

66. Tsutsui Y, Kurokawa Y, Ito K, Siddique MS, Kawano Y, Yamao F, et al. Multiple Regulation of Rad51-Mediated Homologous Recombination by Fission Yeast Fbh1. *PLoS Genet.* 2014;10(8): e1004542.

67. Pek JW, Kai T. A role for vasa in regulating mitotic chromosome condensation in

Drosophila. *Curr Biol.* 2011;21(1): 39–44.

68. Hirota Y, Lahti JM. Characterization of the enzymatic activity of hChlR1, a novel human DNA helicase. *Nucleic Acids Res.* 2000;28(4): 917–924.

69. Wu Y, Shin-ya K, Brosh RM Jr. FANCJ Helicase Defective in Fanconia Anemia and Breast Cancer Unwinds G-Quadruplex DNA To Defend Genomic Stability. *Mol Cell Biol.* 2008;28(12): 4116–4128.

70. Wu Y, Sommers JA, Khan I, de Winter JP, Brosh RM Jr. Biochemical characterization of Warsaw breakage syndrome helicase. *J Biol Chem.* 2012;287(2): 1007–1021.

71. Kuryavyi V, Patel DJ. Solution structure of a unique G-quadruplex scaffold adopted by a guanosine-rich human intronic sequence. *Structure.* 2010;18(1): 73–82.

72. Bharti SK, Sommers JA, George F, Kuper J, Hamon F, Shin-Ya K, et al. Specialization among iron-sulfur cluster helicases to resolve G-quadruplex DNA structures that threaten genomic stability. *J Biol Chem.* 2013;288(39): 28217–2829.

73. Bharti SK, Khan I, Banerjee T, Sommers JA, Wu Y, Brosh RM Jr. Molecular functions and cellular roles of the ChlR1 (DDX11) helicase defective in the rare cohesinopathy Warsaw breakage syndrome. *Cell Mol Life Sci.* 2014;71(14): 2625–2639.

74. Guo M, Hundseth K, Ding H, Vidhyasagar V, Inoue A, Nguyen C-H, et al. A distinct triplex DNA unwinding activity of ChlR1 helicase. *J Bio Chem*. 2015;290: 5174–5189.

75. Lopez-Serra L, Kelly G, Patel H, Stewart A, Uhlmann F. The Scc2-Scc4 complex acts in sister chromatid cohesion and transcriptional regulation by maintaining nucleosome-free regions. *Nat Genet.* 2014;46(10): 1147–1151.

76. Bochman ML, Paeschke K, Zakian VA. DNA secondary structures: stability and function of G-quadruplex structures. *Nat Rev Genet.* 2012;13(11): 770–780.

77. Gillespie PJ, Hirano T. Scc2 couples replication licensing to sister chromatid cohesion in Xenopus egg extracts. *Curr Biol.* 2004;14: 1598–1603.

78. Takahashi TS, Yiu P, Chou MF, Gygi S, Walter JC. Recruitment of Xenopus Scc2 and cohesin to chromatin requires the pre-replication complex. *Nat Cell Biol.* 2004;6(10): 991–996.

79. Bermudez VP, Farina A, Higashi TL, Du F, Tappin I, Takahashi TS, et al. In vitro loading of human cohesin on DNA by the human Scc2-Scc4 loader complex. *Proc Natl Acad Sci U S A.* 2012;109(24): 9366–9371.

80. Misulovin Z, Schwartz YB, Li XY, Kahn TG, Gause M, MacArthur S, et al. Association of cohesin and Nipped-B with transcriptionally active regions of the Drosophila melanogaster genome. *Chromosoma.* 2008;117(1): 89–102.

81. Muto A, Ikeda S, Lopez-Burks ME, Kikuchi Y, Calof AL, Lander AD, et al. Nipbl and mediator cooperatively regulate gene expression to control limb development. *PLoS Genet. 2*014;10(9): e1004671.

82. Kagey MH, Newman JJ, Bilodeau S, Zhan Y, Orlando DA, van Berkum NL, et al. Mediator and cohesin connect gene expression and chromatin architecture. *Nature.* 2010;467(7314): 430–435.

83. Zakari M, Trimble Ross R, Peak A, Blanchette M, Seidel C, Gerton JL. The SMC Loader Scc2 Promotes ncRNA Biogenesis and Translational Fidelity. *PLoS Genet.* 2015;11(7): e1005308.

84. Fernius J, Nerusheva OO, Galander S, Alves Fde L, Rappsilber J, Marston AL.

Cohesin-Dependent Association of Scc2/4 with the Centromere Initiates Pericentromeric Cohesion Establishment. *Curr Biol.* 2013;23(7): 599–606.

85. Natsume T, Müller CA, Katou Y, Retkute R, Gierliński M, Araki H, et al. Kinetochores coordinate pericentromeric cohesion and early DNA replication by Cdc7-Dbf4 kinase recruitment. *Mol Cell.* 2013;50(5): 661–674.

86. Unal E, Arbel-Eden A, Sattler U, Shroff R, Lichten M, Haber JE, et al. DNA damage response pathway uses histone modification to assemble a double-strand break-specific cohesin domain. *Mol Cell.* 2004;16(6): 991–1002.

87. Unal E, Heidinger-Pauli JM, Kim W, Guacci V, Onn I, Gygi SP, et al. A molecular determinant for the establishment of sister chromatid cohesion. *Science.* 2008;321(5888): 566–569.

88. Ström L, Lindroos HB, Shirahige K, Sjögren C. Postreplicative recruitment of cohesin to double-strand breaks is required for DNA repair. *Mol Cell.* 2004;16(6): 1003–1015.

89. Ström L, Sjögren C. Chromosome segregation and double-strand break repair—a complex connection. *Curr Opin Cell Biol.* 2007;19(3): 344–349.

90. Rankin S, Dawson DS. Recent advances in cohesin biology. *F1000Res.* 2016;5: 1909.

91. Maradeo ME, Garg A, and Skibbens RV. Rfc5p regulates alternate RFC complex functions in sister chromatid pairing reactions in budding yeast. *Cell Cycle.* 2010; 9(21): 4370–4378.

Chapter 3*

Temperature-dependent regulation of rDNA condensation in *Saccharomyces cerevisiae.*

*Modified from Shen D, Skibbens RV. *Cell Cycle.* 2017 Jun 3;16(11):1118-1127

Abstract

Chromatin condensation during mitosis produces detangled and discrete DNA entities required for high fidelity sister chromatid segregation during mitosis and positions DNA away from the cleavage furrow during cytokinesis. Regional condensation during G1 also establishes a nuclear architecture through which gene transcription is regulated but remains plastic so that cells can respond to changes in nutrient levels, temperature and signaling molecules. To date, however, the potential impact of this plasticity on mitotic chromosome condensation remains unknown. Here, we report results obtained from a new condensation assay that wildtype budding yeast cells exhibit dramatic changes in rDNA conformation in response to temperature. rDNA hypercondenses in wildtype cells maintained at 37°C, compared with cells maintained at 23°C. This hypercondensation machinery can be activated during preanaphase but readily inactivated upon exposure to lower temperatures. Extended mitotic arrest at 23°C does not result in hypercondensation, negating a kinetic-based argument in which condensation that typically proceeds slowly is accelerated when cells are placed at 37°C. Neither elevated recombination nor reduced transcription appear to promote this hypercondensation. This heretofore undetected temperature-dependent hypercondensation pathway impacts current views of chromatin structure based on conditional mutant gene analyses and significantly extends our understanding of physiologic changes in chromatin architecture in response to hyperthermia.

Introduction

Chromatin condensation may have been the first dramatic cell cycle change observable to early microscopists and remains a topic both of fascination and clinical relevance. Chromatin condensation and the arrangement of chromosomes within the nuclear volume are collectively mediated by cohesin- and condensin-dependent DNA segment tetherings that occur in either cis (within a single DNA molecule) or trans (between separate DNA molecules) conformations [1, 2]. Recent evidence is consistent with the notion that cis DNA tetherings established during interphase are critical for the proper deployment of developmental transcription programs [3, 4]. Intriguingly, proper development likely also requires G1 trans tethers (here, between non-homologous chromosomes) that link together domains of either repressed or induced transcriptional activities termed TADs (Topologically Association Domains) [5].

The combination of cis and trans tethers during G1 that mediate regionalized chromatin condensation and nuclear architecture must remain plastic if cells are to respond appropriately to external cues. Numerous studies across several species document that the chromosome condensation state during interphase increases in response to heat-stress. For instance, hyperthermia induces premature chromosome condensation during S phase in CHO, HeLa and S3 cells and hypercondensation in Achlya ambisexualis hypha [6-12]. Importantly, little is known regarding the mechanisms through which these induced and premature condensation reactions occur. Moreover, the extent to which cells respond to hyperthermia during mitosis, when chromosomes are already condensed, remains largely untested. Addressing these deficiencies becomes important since physiologic changes induced by heat stress are wide-ranging and include

expression of heat shock proteins (HSPs), protein synthesis repression and altered rates of both transcription and mRNA turnover [13, 14].

Budding yeast remains a mainstay model organism from which numerous aspects of chromatin condensation have come to light. Common to most studies is the testing of temperature-dependent gene product inactivation on rDNA structure [15-27]. This is because rDNA undergoes cell cycle-specific structural changes: forming diffuse puff-like structures during G1 and condensing through multiple stages that include cluster and line formations before coalescing into discrete loop-like structures during mitosis [16, 17, 21] When either SMC (structural maintenance of chromosomes) cohesin or condensin complexes are impaired (for instance through the use of conditional alleles), mitotic cells contain puff-like rDNA loci instead of tightly condensed rDNA loops [24,26-28]. Since the rDNA locus is a highly-specialized domain comprising iterative repeats that are repressed for Homologous Recombination (HR) and under tight transcriptional regulation, parallel strategies were developed in yeast to assess changes in chromosome arm condensation [24, 29-32]. All of these studies operate under the assumption that mitotic chromatin structures in wildtype cells are refractory to the temperature shift required to inactivate conditional allele gene products. Conversely, a growing body of evidence suggests that DNA segment cis and trans tethers of interphase cells remain dynamic to respond to external cues [1-5, 33]. Here, we developed a streamlined rDNA condensation assay and report that wildtype budding yeast exhibit a mitotic chromatin hypercondensation activity that is induced at temperatures typically used to inactivate conditional alleles. Moreover, this hypercondensation activity predominantly targets the

rDNA locus, revealing a heretofore unexplored and targeted physiologic response to hyperthermia.

Results

3.1 Temperature-dependent regulation of mitotic rDNA hypercondensation

Despite technical advances that include immunodetection, GFP tagging and Fluorescence in situ hybridization (FISH), barriers to detecting changes in chromatin architecture in yeast cells include small cell and nuclear sizes and limited longitudinal chromatin compaction relative to other eukaryotic cells [16, 17, 24-26, 34, 35]. Here, we report on a streamlined procedure that provides for exquisite imaging of the yeast rDNA locus in the absence of GFP, stacked antibody complexes and hybridization of labeled nucleotide probes. To validate this procedure, we exploited a well-established observation that mutation of the cohesin subunit Mcd1/Scc1 results in condensation defects [17, 19, 24, 26, 36-38]. Log phase wildtype and *mcd1–1* mutant cells were synchronized in G1 (α factor) at 23°C and then released into 37°C (non-permissive temperature for *mcdc1–1*) fresh medium supplemented with nocodazole to arrest cells preanaphase. Cell cycle progression was confirmed by detection of DNA content using flow cytometry (Figure S1A). The resulting preanaphase wildtype cells contained predominantly loop-like rDNA structures while preanaphase *mcd1–1* mutant cells failed to condense their chromatin such that the rDNA formed predominantly puff-like structures (Fig. 1A). We quantified these differences and found that our procedure detects similar levels of condensation defects in *mcd1–1* mutant cells as those obtained using FISH and GFP-based methodologies (Fig. 1B) [17, 24, 26, 27].

During this investigation, we discovered a robust temperature-dependent effect that occurs in wildtype cells, independent of gene mutation. We modified our prior experimental strategy to further analyze this hypercondensation activity by releasing G1

arrested cells into either 23°C or 37°C medium supplemented with nocodazole (Fig. 1C). Cell cycle progression was confirmed by detection of DNA content using flow cytometry (Figure S1B). Our condensation assay revealed that preanaphase wildtype cells condense rDNA loops to form tight and discrete loops at both 23°C or 37°C. Surprisingly, however, rDNA loops were condensed but appeared significantly shorter in wildtype cells shifted to 37°C upon release from G1, compared with loops in wildtype cells maintained at 23°C (Fig. 1D). We thus quantified the loop lengths in wildtype cells at both temperatures by tracing the entire length of the loop structures. The results clearly document that rDNA loop lengths are significantly shorter (herein termed hypercondensed) in cells that progress from G1 into mitosis at 37°C (Fig. 1E).

Our condensation assay provides for detailed images of rDNA structure, but we wondered if other procedures could detect temperature-sensitive hypercondensation of rDNA. Net1 is an rDNA binding protein and represents one current standard by which rDNA structure is assessed [24, 26-28]. Wildtype cells expressing GFP-tagged Net1 were synchronized in G1, released into either 23°C or 37°C rich medium supplemented with nocodazole, and the resulting preanaphase cells assessed for rDNA loop lengths. Cell cycle progression was confirmed by detection of DNA content using flow cytometry (Figure S1C). Wildtype cells that progressed from late G1 into mitosis at 23°C exhibited significant longer rDNA loop lengths than cells released from G1 into 37°C medium (Fig. 1F, G). In combination, these results reveal that rDNA condensation is exquisitely sensitive to temperature changes in wildtype cells with elevated temperatures leading to robust hypercondensation that is easily measurable using well-established procedures.

3.2 Temperature-induced hypercondensation is not based on increased condensation rates

What is the basis for this heretofore unreported temperature-dependent effect on rDNA condensation? We speculated that the decreased loop size that occurs in wildtype cells maintained at 37°C might reflect an accelerated rate of condensation, relative to that which occurs at 23°C. If this model is correct, then longer incubations at 23°C should ultimately lead to hypercondensed rDNA. To test this prediction, cultures released from G1 were maintained in fresh medium supplemented with nocodazole for either 2.5 or 5 hours at 23° and compared with cultures instead maintained for 2.5 or 5 hours at 37°C (Fig. 2A). Cell cycle progression was confirmed by detection of DNA content using flow cytometry (Figure S1D). The results reveal that rDNA loop lengths in cells maintained in preanaphase at 23°C for 5 hours failed to approach the loop lengths of cells maintained in preanaphase at 37°C for only 2.5 hours. Moreover, rDNA loop lengths in cells maintained in preanaphase at 23°C for 2.5 hours are identical to rDNA loop lengths in cells maintained in preanaphase at 23°C for 5 hours (Fig. 2B). The same is true for loop lengths in cells maintained at 37°C, regardless of incubation time. In all cases, rDNA loop lengths were significantly shorter in cells maintained at 37°C compared with cells maintained at 23°C (Fig. 2C). Thus, changes in rDNA architecture occur independent of condensation rates.

3.3 The rDNA hypercondensation machinery is active during mitosis

In most eukaryotes, chromosome condensation is a multi-step process that requires factors (such as core histones and cohesins) that are deposited during S phase and

additional factors (such as linker histones and condensins) that associate or become activated later during the cell cycle [39, 40]. It thus became important to map the timing of this rDNA hypercondensation during the cell cycle. To test whether rDNA hypercondensation can be induced by elevated temperatures during M phase (after normal levels of condensation are already established), wildtype cells were synchronized in G1 at 23°C for 2.5 hours, then released at 23°C into fresh medium supplemented with nocodazole for 2.5 hours. Half of the resulting preanaphase cells were then shifted to 37°C for an additional hour and the other half maintained at 23°C for the same time period (Fig. 3A). Cell cycle progression was confirmed by changes in DNA content using flow cytometry (Figure S1E). As expected, rDNA in cells maintained at 23°C throughout the preanaphase arrest appeared as long loops that extend away from the DNA mass. In contrast, rDNA in cells arrested in mitosis at 23°C but then shifted to 37°C while maintaining the preanaphase arrest exhibited significantly hypercondensed rDNA loop lengths (Fig. 3B, C). Thus, cells exhibit an rDNA-directed hypercondensation activity during preanaphase that induces condensation beyond that which promotes entry into mitosis.

3.4 Temperature-induced hypercondensation is reversible and occurs independent of changes in rDNA repeat number

Budding yeast rDNA comprises approximately 150 repeats and is a hotspot for homologous recombination [41]. This raised the possibility that the apparent hypercondensation is in reality a reduction in rDNA repeats through permanent recombination-based excisions and loss from the chromosome. We thus tested whether

we could revert a hypercondensed rDNA loop back to an extended loop within a single preanaphase arrest. Wildtype cells were synchronized in G1 at 23°C, then released at 23°C into fresh medium supplemented with nocodazole. The resulting preanaphase arrested cells were then shifted to 37°C for 1 hour (which produces rDNA hypercondensation) before shifting back down to 23°C for an additional 1 hour (Fig. 4A). Cell cycle progression was confirmed by detection of DNA content using flow cytometry (Figure S1F). Similar to our earlier results, cells shifted up to 37°C during preanaphase contain hypercondensed rDNA (Fig. 4B). Importantly, when these cells were shifted down to 23°C for one hour, the rDNA recovered to a less condensed state – nearly matching the extended loop lengths of cells maintained at 23°C throughout the time course (Fig. 4B, C). Thus, rDNA hypercondensation is reversible and occurs independent of changes in the number of rDNA repeats – a revelation supported by the absence of Net1-GFP decorated excised rDNA circles under conditions that similarly produce short rDNA loops (Fig. 3C).

3.5 Temperature-induced hypercondensation occurs independent of rDNA transcriptional inhibition

rDNA transcription, ribosome biogenesis and translational outputs are all upregulated during periods of accelerated growth. This increased rDNA transcription requires a relaxed DNA conformation and RNA polymerase accessibility [23, 29, 30, 42-44]. In contrast, yeast cell rDNA transcription levels decrease to basal line during mitotis that is coordinated with rDNA condensation [45, 46]. One prediction from these findings is that wildtype cells shifted to 37°C and that contain hypercondensed rDNA would

exhibit slower growth kinetics (reduced rDNA transcription) compared with cells incubated at 23°C. To test this prediction, both S288C and W303 wildtype strains were sub-cultured over a 2 days period to ensure log phase growth before monitoring cell growth by spectroscopy. The results show that both yeast strains exhibit significantly increased growth rates at 37°C compared with 23°C (Fig. 5A, B). These findings negate the model that wildtype yeast cells exhibit hypercondensed rDNA due to slower growth at 37°C and instead are consistent with previous finding that wildtype yeast significantly increase ribosomes synthesis when shifted to 36°C from 23°C growth conditions [47]. The mechanism through which yeast cells exhibit increased growth rates that require elevated transcription from the rDNA locus, despite the hypercondensation that occurs at 37°C (Figs. 1–4), remains unknown.

3.6 Temperature-induced hypercondensation is rDNA specific

rDNA is unique in terms of architecture, binding factors, transcription regulation, and altered levels of recombination, compared with the remainder of the genome [29, 42, 43]. This raises the possibility that the temperature-dependent hypercondensation of rDNA is locus specific. To test this possibility, we obtained a chromosome arm condensation assay strain, kindly provided by Dr. Frank Uhlmann, that contains 2 lacO cassettes spaced 137 kb from each other on chromosome XII. Each LacO cassette is detected by lacR-GFP such that the inter-GFP distance allows for quantification of chromosome arm condensation [24]. To validate this procedure, we placed through mating and dissection the LacO/lacR-GFP condensation cassette into *mcd1–1* strains previously demonstrated as exhibiting condensation defects at both rDNA and

chromosome arms [17]. Log phase wildtype and *mcd1–1* arm condensation assay strains were synchronized in G1 and released into either 23°C or 37° fresh medium supplemented with nocodazole to arrest cells preanaphase (Figure S2A). The resulting pre-anaphase synchronized cells were then fixed in paraformaldehyde and the disposition of arm condensation quantified by measuring the distance between GFP loci (Figure S2B). The results reveal a significant increase in the inter-GFP distance in *mcd1–1* cells compared with wildtype cells (Figure S2C, D), confirming the efficacy of this arm condensation assay.

To test whether temperature-dependent hypercondensation extends to chromosome arm loci beyond that of rDNA, wildtype cells that harbor the arm condensation assay cassette were synchronized in G1 at 23°C and released into 23°C fresh medium supplemented with nocodazole for 2.5 hours. Half of the resulting preanaphase cells were shifted to 37°C for 1 hour while the other half was maintained at 23°C for 1 hour (Fig. 6A). Cell cycle progression and synchronization was confirmed by DNA content using flow cytometry (Figure S1G). The resulting preanaphase synchronized cells were then fixed and the distance between GFP loci quantified (Fig. 6B). The results reveal that preanaphase cells maintained at either 23°C or 37°C exhibit nearly identical inter-GFP distances (Fig. 6C, D). Thus, chromatin along the arm appears insensitive to temperature-induced hypercondensation that predominantly targets the rDNA locus.

Discussion

Chromosome condensation ensures appropriate chromosome segregation but also influences transcriptional programs and nuclear architecture [48]. Thus, it is not surprising that mutation of condensation pathways results in mitotic failure, aneuploidy and is further linked to developmental maladies such as microcephaly [49-53]. A major revelation of the current study is that yeast cells contain hypercondensation machinery that is induced specifically during mitosis in response to elevated temperatures. This newly observed phenomenon is due neither to accelerated condensation reactions (hypercondensation at 37°C cannot be balanced by longer incubation time at 23°C), nor rDNA repeat reduction through recombination (hypercondensed rDNA loop lengths re-extend quickly upon shifting to 23°C and micrographs thus far fail to detect extrachromosomal rDNA signals in Net1-GFP cells that contain hypercondensed loops). Note that the homologous recombination machinery in general is suppressed during M phase such that changes in rDNA repeat numbers typically are monitored over several generations [30, 54-56]. In contrast, we observe inducible and reversible rDNA hypercondensation within a single M-phase arrest. Intriguingly, yeast hypercondense specific DNA loci in response to nutrient starvation although the extent that these represent similar mechanisms in hypercondensation remains unknown [33].

What are the mechanisms through which rDNA hypercondensation at elevated temperature occurs? Early analyses of condensin mutants revealed reversibility in normal levels of chromosome condensation during mitosis: transient inactivation of temperature sensitive Brn1–9 condensin subunit during M phase resulted in rDNA decondensation that recondensed upon a shift back to permissive temperature. This reversibility of

normal condensation levels during mitosis depends on both condensin and cohesin, although cohesin mutants thus far do not exhibit reversibility in condensation - suggesting that cohesin promotes condensin activation [57]. These observations raise the possibility that the reversible rDNA hypercondensation documented here requires similar molecular mechanisms that include cohesin and condensin - which are critical for mitotic chromosome condensation, stabilization of rDNA architecture and transcription regulation [57, 62-65]. Condensins in addition introduce positive supercoils into chromatin, promotes complementary single strand DNA reannealing and facilitates DNA catenation resolution [66]. Cohesin-dependent tethering of DNA segments is also critical for transcription regulation, nuclear architecture and sister chromatid tethering [1]. A final mechanism of hypercondensation could involve heat shock proteins, which may act in coordination or in parallel to the recruitment of condensins and cohesins [67] (Fig. 7). The extent to which elevated temperature alters condensin, cohesin or heat shock protein deposition/activation onto rDNA remains an important goal of future research.

A second revelation of the current study is the apparent specificity of this hypercondensation activity. Using both our streamlined condensation assay and a well-established Net1-GFP strategy, we found that compaction along the longitudinal axis of rDNA is dramatically increased in response to elevated temperature. Conversely, genome-wide compaction along the chromosome arms is resistant to temperature-induced hypercondensation. In the context of cell physiology, mechanisms that selectively target rDNA are of critical interest. For instance, nutrient starvation induces rDNA hypercondensation and limits transcription factor accessibility which results in slow growth [33, 58]. On the other hand, increased cell growth kinetics correlate with elevated

rates of rDNA transcription and ribosome assembly/maturation [58, 59]. In the current study, shifting wildtype cells to an elevated temperature (23°C to 37°C) produced an increased growth rate, consistent with previous findings that transcriptional silencing at rDNA loci is decreased and rRNA levels are increased at elevated temperatures [47, 60, 61]. These observations raise a paradox: wildtype yeast at elevated temperatures exhibit both increased rDNA transcription and growth rates despite the hypercondensation of rDNA. Of the many possibilities, one model that resolves this apparent contradiction is that the shorter rDNA loop axis reflects significantly increased lateral loop extensions that accommodate elevated transcription during robust cell growth (Fig. 7). This transcriptional model is consistent with our results that exclude mechanisms of hypercondensation through accelerated condensation reactions and rDNA repeat reduction through recombination. Future efforts will be required to expose the mechanisms through which these potential longitudinal and lateral segment tetherings are regulated and document the extent to which transcriptionally active loops emerge laterally from the chromosomal axis.

The utilization of temperature-sensitive mutants remains a mainstay of yeast research. In particular, almost every condensation assay performed to date uses a temperature shift from permissive to non-permissive temperatures [16, 17, 19, 24-27]. Thus, our current study formally raises concerns regarding the extent through which defects in mutant strains (shifted to an elevated and non-permissive temperature) are predicated on comparisons to a hypercondensed rDNA locus. It thus becomes crucial to investigate the mechanism through which condensation is regulated by temperature, improve experimental strategies to better accommodate for those effects and then revisit

results from prior studies predicated on conditional alleles and analysis of the rDNA locus. Moreover, our observations are likely to be of clinical interest, given the use of hyperthermia as a cancer treatment [68]. For instance, the mechanism by which tumor cells become heat sensitive, compared with wildtype cells, is not fully understood. Our study provides a starting point through which locus-specific hypercondensation activity may promote hyperthermic resistance in wildtype cells and, in its absence, render tumor cells hyperthermically sensitive.

Materials and methods

Yeast strains and strain construction

Yeast strains and strain construction: *Saccharomyces cerevisiae* strains used in this study are listed in strain table (Table 1). GFP-tagging and deletion of genes was performed following published protocol [69].

rDNA condensation assay

Condensation assays were modified based on published FISH protocol [17]. Briefly, synchronized cells were fixed by paraformaldehyde (100 μl 36% formaldehyde per 1 ml culture) for 2 hr at 23 °C. Cells were washed with distilled water 3 times and resuspended in spheroplast buffer (1M sorbitol, 20 mM KPO4, pH7.4), then spheroplasted by adding β-mercaptoethanol (1/50 volume) and Zymolyase T100 (1/100 volume) and incubating for 1 hour at 23°C. Resulting cells were pelleted and resuspended in 1.5 pellet volume of spheroplast buffer with 0.5% Triton X-100. 10 μl of the cell suspension were added to each well on poly-L-ysine coated slides, set at room temperature for 10 min, then removed the liquid gently by pipette. 20 μl of 0.5% SDS were added to each well, and set for 10 min, room temperature, then remove the liquid gently by pipette. Air dry the slides. Cells were then dehydrated by immersing the slides in fresh 3:1 methanol:acetic acid for 5 min at room temperature. Slides were stored at 4°C until completely dry, then cells were treated with RNase (100 μg/ml) in 2XSSC buffer (0.3M NaCl, 30 mM Sodium Citrate, pH7.0), incubate 1 hour at 37°C. Slides were washed 4 times in fresh 2XSSC (2 min/per wash), then went through a series of cold (−20°C) ethanol washes (start with 70%, followed by 80%, 95% ethanol washes, 2 min/per wash), then air dry. Slides were

prewarmed to 37°C, then put into denaturing solution (70% formamide, 2X SSC) at 72°C for 2 min. Slides were immediately washed through a series of cold (−20°C) ethanol washes (start with 70%, followed by 80%, 90%, 100% ethanol washes, 1 min/per wash), then air dry. DNA mass were detected by DAPI (0.05ug/ml) staining and assayed under microscope. Cell cycle progression were confirmed by detection of DNA content using flow cytometry as described [27].

Net1-GFP condensation assay

rDNA codensation assays were performed following similar strategy as previous publications [24, 27]. Briefly, cells were arrested at preanaphase and fixed by paraformaldehyde for 10 min at 30°C. GFP signal were then assayed under microscope. Cell cycle progression were confirmed by detection of DNA content using flow cytometry as described [27].

Chromosome arm condensation assay

Chromosome arm condensation assays were performed as previous described [24]. Briefly, cells were arrested at preanaphase and fixed by paraformaldehyde for 10 min at 30 °C. Distances between GFP dots were measured by microscopy. Cell cycle progression were confirmed by detection of DNA content using flow cytometry as described [27]. To generate unbiased detection criteria of the GFP distance, cells contain a single GFP dot may reflect sister chromatids positioned vertical to the z-axial focal plane were thus excluded from analysis. In cases where GFP foci were planar to the field of view (eliminated z-axial contributions), we also excluded cells that contained 3 or 4

GFP loci, since the cohesion defect at one or both loci made it impossible to determine which GFP dot represented intra- or inter- sister chromatid loci. Thus, we focused our analysis on cells that contained 2 GFP dots resolvable within a single focal plane.

Statistical Analyses

F-Tests were used to assess the equality of 2 variances in chosen experimental groups, followed by Student's T-Tests to assess the statistical significance ($P < 0.05$).

Figures

Figure 1

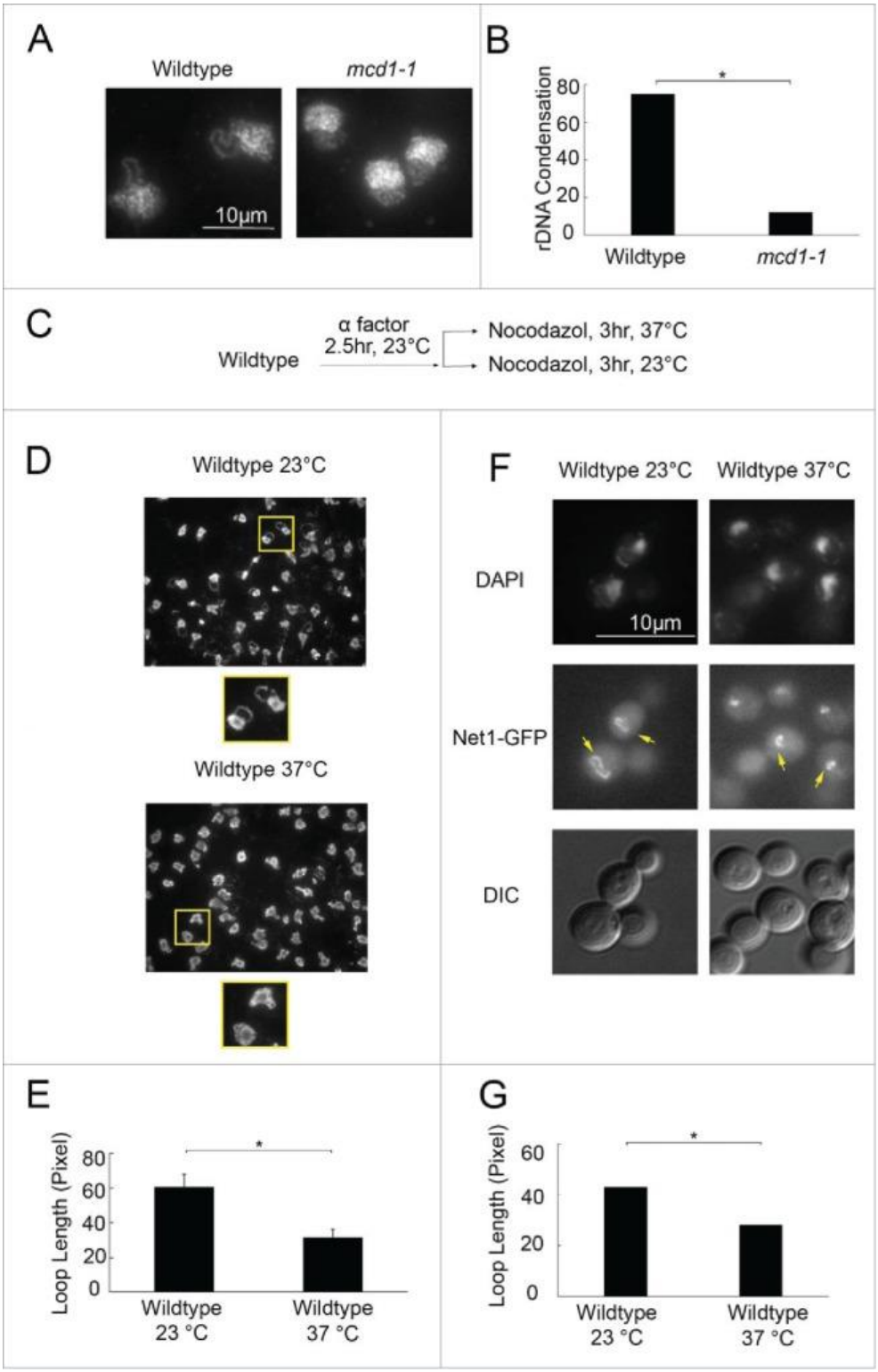

Figure 1. Temperature-dependent regulation of mitotic rDNA condensation.

A) Condensation assay validation. Micrographs of chromosomal mass and rDNA loop and puff structures detected using DAPI for wildtype (VG985) and *mcd1–1* mutant cells. B) Quantification of rDNA loops (condensation) in preanaphase wildtype and *mcdc1–1* mutant strains (N = 100 cells for each strain). C) Schematic of cell synchronization and experimental procedure performed on wildtype cells (YBS1019). D) Micrographs of chromosome masses detected using DAPI. Regions demarcated by yellow squares equally magnified below. E) Quantification and statistical analyses of rDNA loop lengths observed using our condensation assay in wildtype cells at 23°C and 37°C (3 biologic replicates with over 100 cells for each strain analyzed per replicate [N = 330 cells at 23°C and 352 cells at 37°C total]; p-value = 0.004). F) Micrographs of preanaphase wildtype cells arrested at either 23°C or 37°C. Chromosome mass detected by DAPI, rDNA architecture detected using Net1GFP and cell morphology imaged using Differential Interference Contrast (DIC) microscopy. Yellow arrows indicate rDNA loops at 23°C and diminished loops at 37°C. G) Quantification and statistical analyses of rDNA loop lengths measured using Net1-GFP in wildtype preanaphase cells arrested 23°C and then either maintained at 23°C or shifted to 37°C (N = 190 cells at 23°C and 157 cells at 37°C; P-value = 1.95E-28).

Figure 2

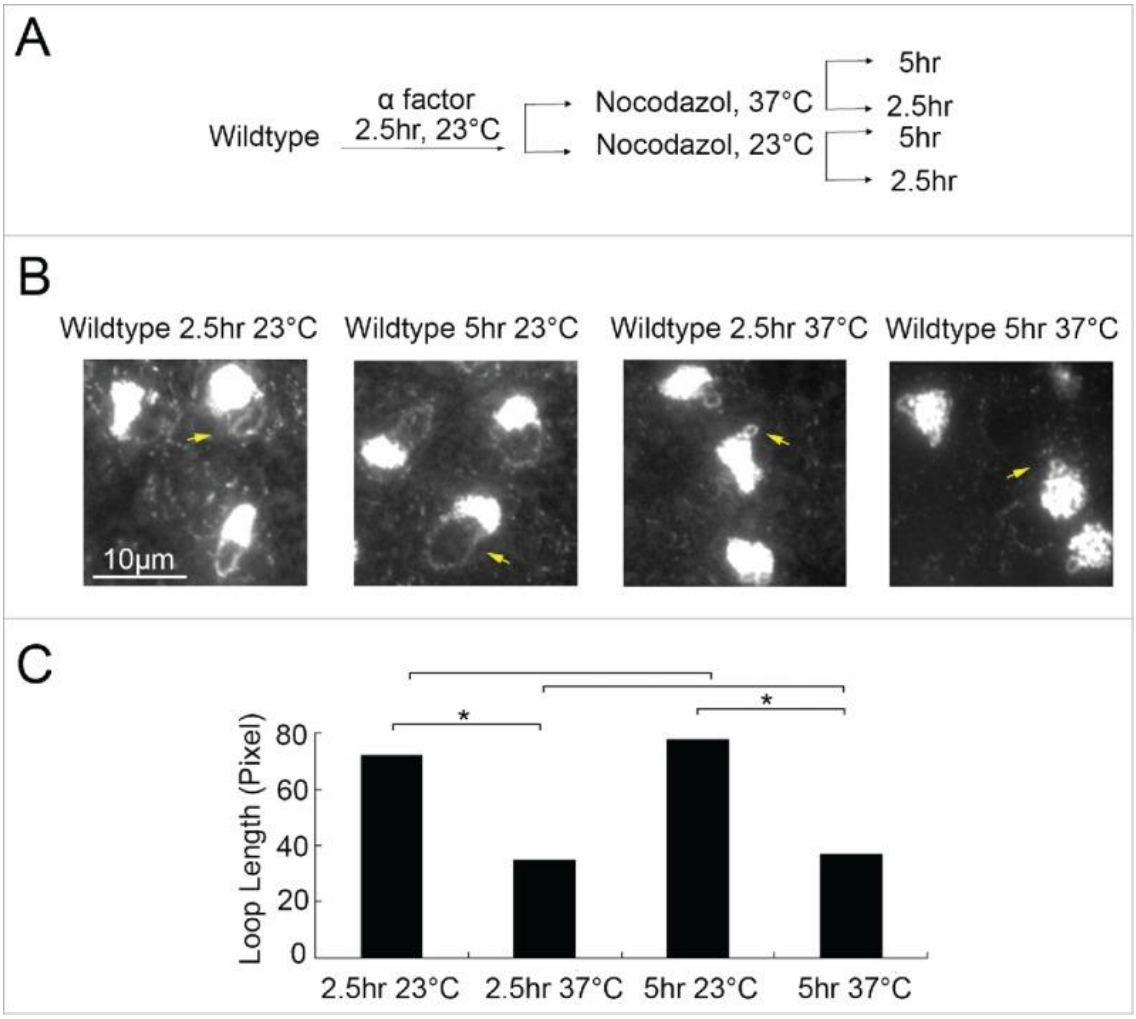

Figure 2. Temperature-induced hypercondensation is not based on increased condensation rates.

A) Schematic of synchronization and experimental procedure performed on wildtype cells (YBS1019). B) Micrographs of chromosome masses and rDNA loops detected by DAPI staining. Yellow arrows point to rDNA loops at 23°C and diminished loops at 37°C. C) Quantification and statistical analyses of rDNA loop lengths in each experimental group (N = 50 cells for each treatment, Pvalue = 0.149 for 23 °C 2.5 hr vs

5hr; P-value = 0.346 for 37 °C 2.5 hr vs 5hr; P-value = 5.54E-20 for 23 °C 2.5 hr vs 37 °C 2.5hr; P-value = 2.18E-20 for 23 °C 5 hr vs 37 °C 5hr; P-value = 5.90E-19 for 23 °C 2.5 hr vs 37 °C 5hr).

Figure 3

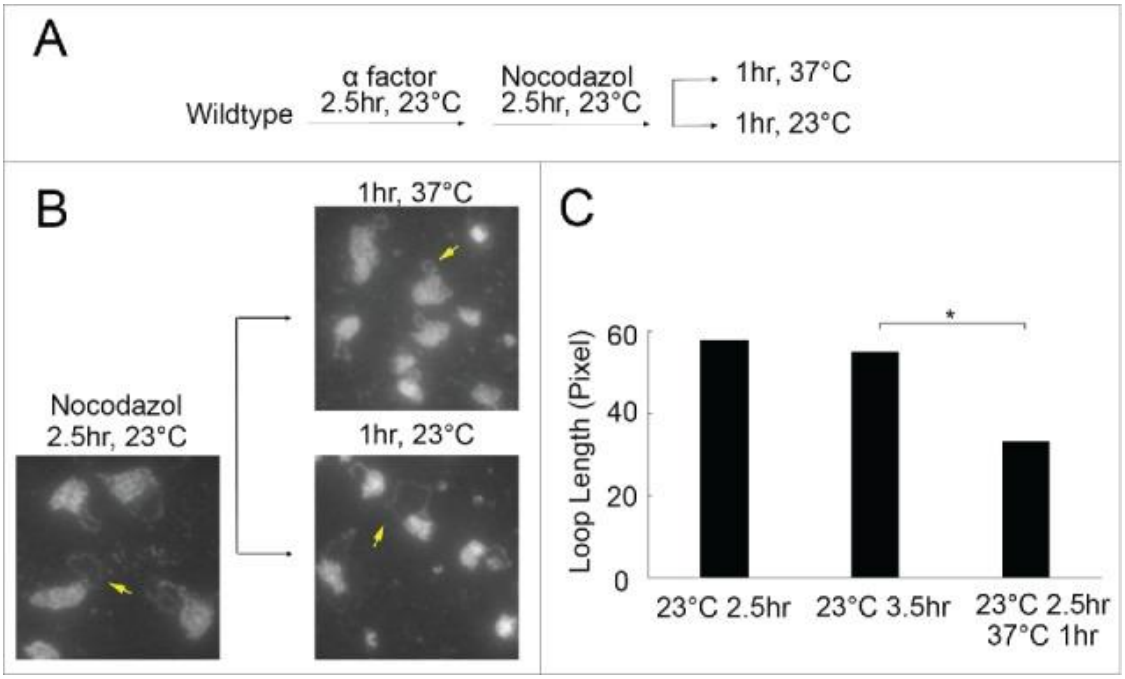

Figure 3. The rDNA hypercondensation machinery is active during mitosis.

A) Schematic of synchronization and experimental procedure performed on wildtype cells (YBS1019). B) Micrographs of chromosome masses and rDNA loops detected by DAPI staining. Yellow arrows indicate loops at 23°C and diminished loops in response to a 1 hour shift to 37°C, but not 23°C, during preanaphase arrest. C) Quantification and statistical analyses of the rDNA loop lengths in each experimental group (N = 138 cells at 23°C for 2.5 hr; N = 105 cells for 23°C for 3.5 hr; N = 115 cells for 23°C for 2.5 hrs and 37°C for 1 hr; P-value = 7.73E-17 for 23 °C 3.5 hr vs 23 °C 2.5 hr ->37 °C 1hr).

Figure 4

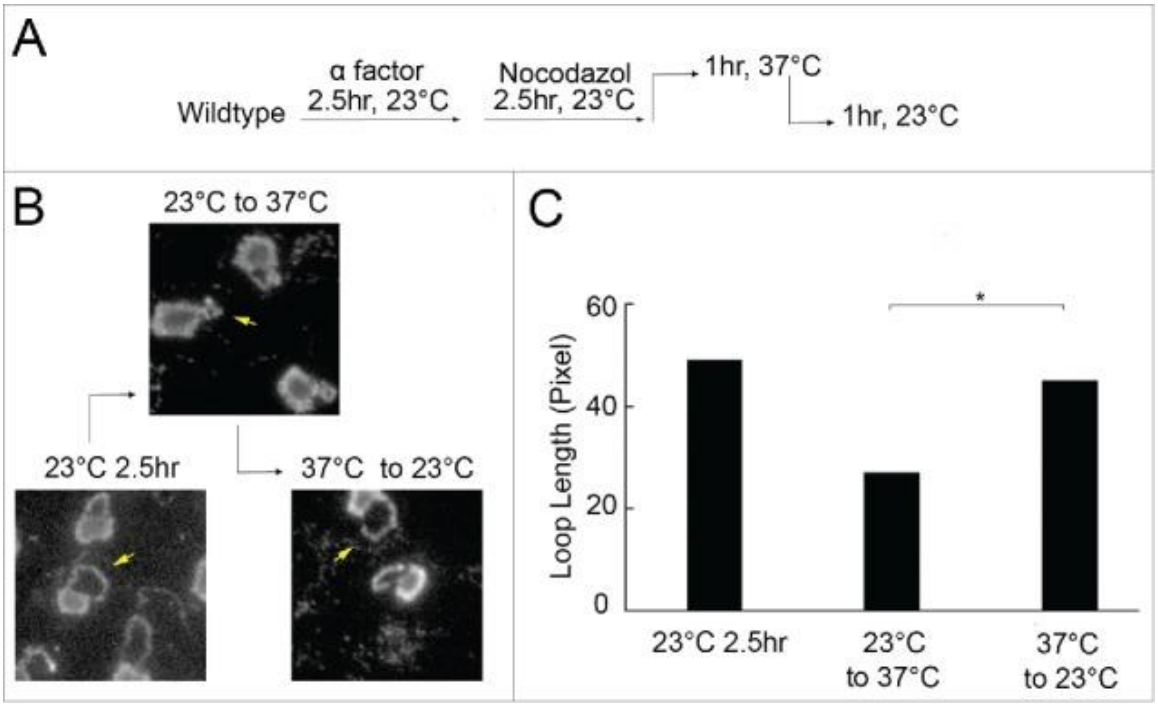

Figure 4. Temperature-induced hypercondensation occurs independent of changes in rDNA repeat number.

A) Schematic of synchronization and experimental procedure performed on wildtype cells (YBS1019). B) Micrographs of chromosome mass and changes in rDNA loop lengths throughout the experiment detected by DAPI staining. C) Quantification and statistical analyses of rDNA loop length in each experimental group (N = 130 cells at 23°C for 2.5 hr; N = 119 cells at 23°C for 2.5 hrs -> 37°C for 1 hr; N = 115 cells at 23°C for 2.5 hr -> 37°C for 1 hr -> 23°C for 1 hr; P-value = 2.53E-21 for shift from 23 °C to 37 °C vs shift from 37 °C to 23 °C).

Figure 5

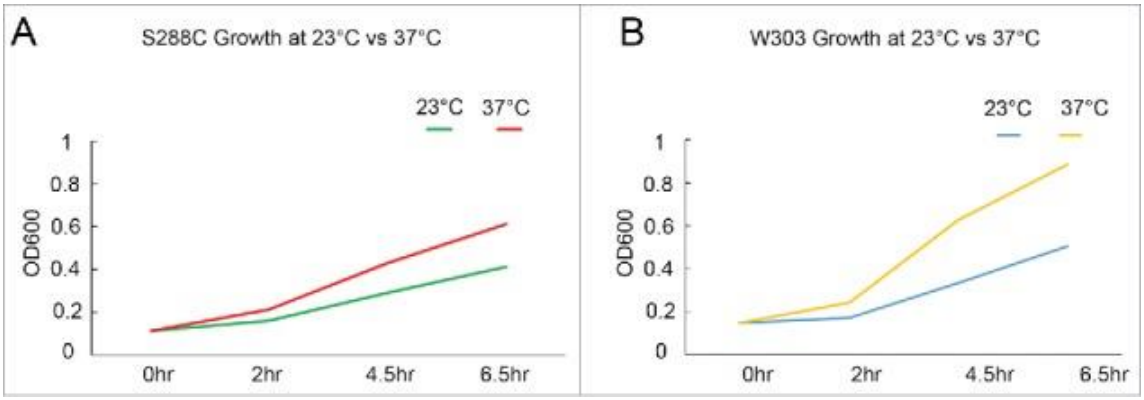

Figure 5. Temperature-induced hypercondensation occurs independent of rDNA transcription.

A) Growth curve of wildtype S288C background strain (YBS1019). B) Growth curve of wildtype W303 background strain (YBS2020).

Figure 6

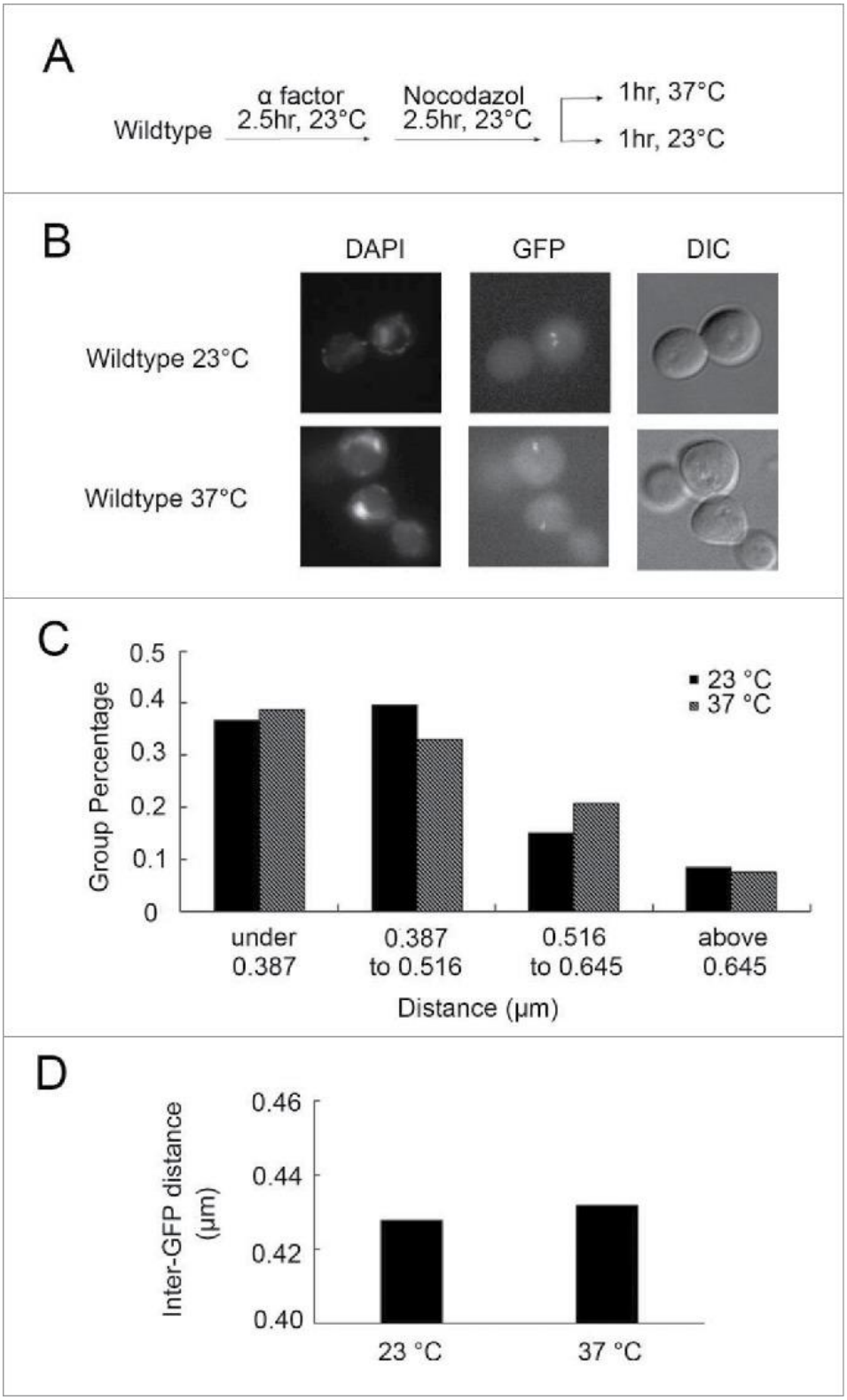
A
Wildtype
α factor
2.5hr, 23°C
Nocodazol
2.5hr, 23°C
1hr, 37°C
1hr, 23°C
B
DAPI
GFP
DIC
Wildtype 23°C
Wildtype 37°C
C
Group Percentage
0.5
0.4
0.3
0.2
0.1
0
23 °C
37 °C
under 0.387
0.387 to 0.516
0.516 to 0.645
above 0.645
Distance (μm)
D
Inter-GFP distance (μm)
0.46
0.44
0.42
0.40
23 °C
37 °C

Figure 6. Temperature-induced hypercondensation is rDNA specific.

A) Schematic of synchronization and experimental procedure performed on wildtype cells (YBS2078). B) Micrographs of DNA masses (DAPI), chromosome arm loci (GFP) and cell morphology (DIC) in preanaphase arrested cells at 23°C and 37°C. C) Quantification of the distribution of measured distances between 2 arm loci GFP dots (N = 111 cells at 23°C; N = 106 cells at 37°C). D) Quantification and statistical analyses of the GFP arm inter-loci distances in each experimental group (N = 111 cells at 23°C; N = 106 cells at 37°C; P-value = 0.812).

Figure 7

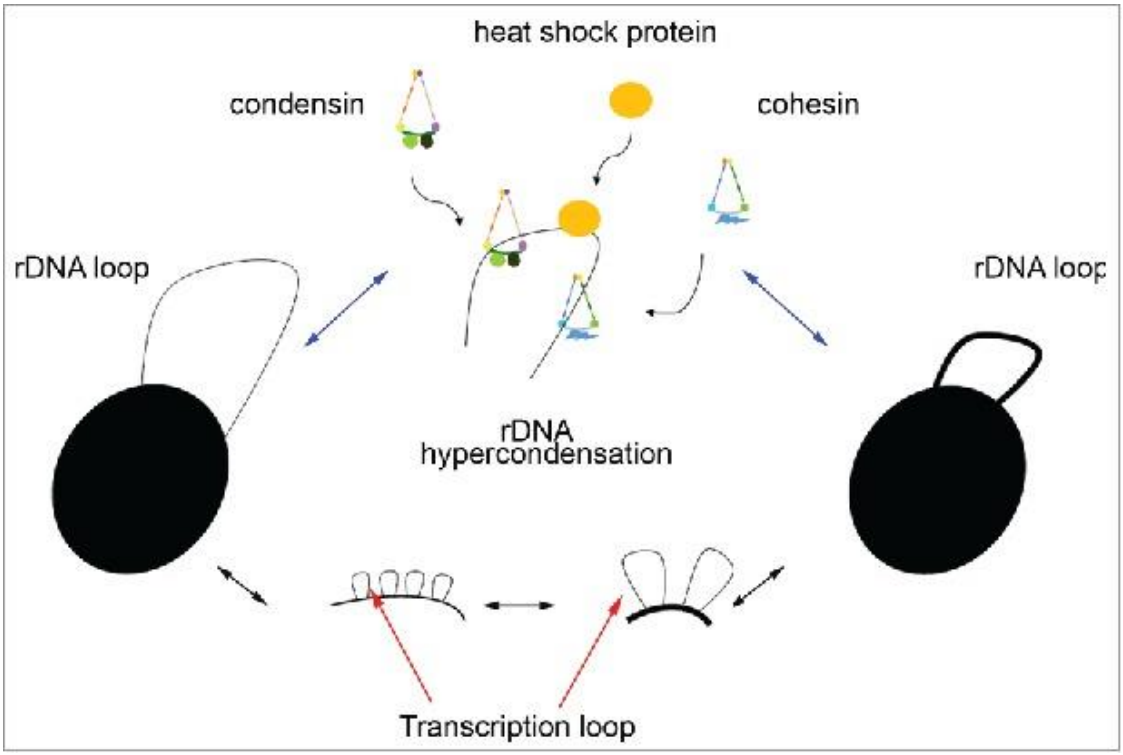

Figure 7. Model of rDNA transcription loop extension and possible mechanisms of hypercondensation.

rDNA hypercondensation occurs in cells exposed to elevated temperature, potentially through transcription-dependent increase in axial loop extension (below). Candidates required to drive mitotic hypercondensation may include temperature-dependent enhanced activation of cohesin, condensin, or heat shock proteins (either directly or through condensation inhibitor inactivation) that specifically target the rDNA loci (above).

Figure S1

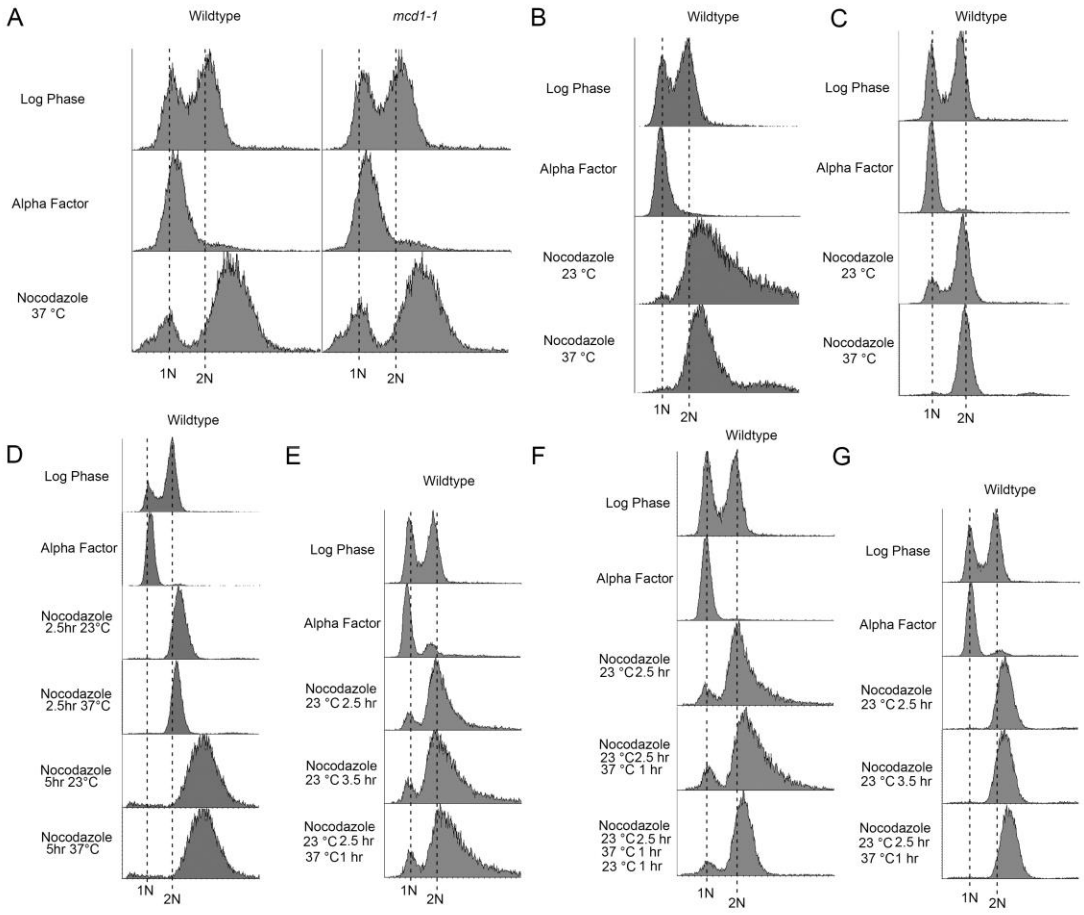

Figure S1. DNA content obtained using flow cytometry.

A) DNA content assayed for Fig. 1A. B) DNA content assayed for Fig. 1D. C) DNA content assayed for Fig. 1F. D) DNA content assayed for Fig. 2B. E) DNA content assayed for Fig. 3B. F) DNA content assayed for Fig. 4B. G) DNA content assayed for Fig. 6B.

Figure S2

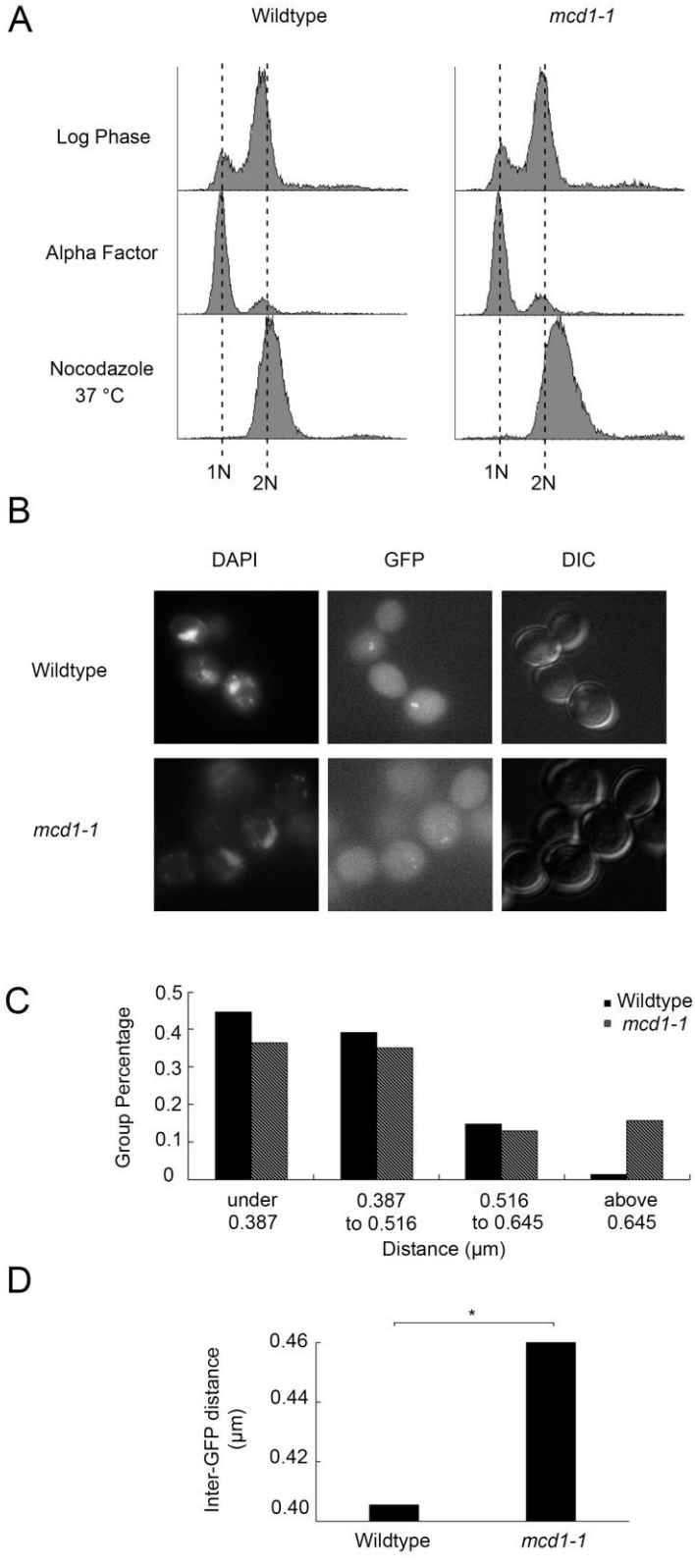
A
Wildtype
mcd1-1
Log Phase
Alpha Factor
Nocodazole
37 °C
1N
2N
1N
2N
B
DAPI
GFP
DIC
Wildtype
mcd1-1
C
Group Percentage
0.5
0.4
0.3
0.2
0.1
0
Wildtype
mcd1-1
under 0.387
0.387 to 0.516
0.516 to 0.645
above 0.645
Distance (μm)
D
*
Inter-GFP distance (μm)
0.46
0.44
0.42
0.40
Wildtype
mcd1-1

Figure S2. Validation of arm condensation assay using the condensation defective *mcd1-1* cell line.

A) DNA content assayed for wildtype cells (YBS2078) and *mcd1-1* cells (YBS3017). B) Micrographs of DNA masses (DAPI), chromosome arm loci (GFP) and cell morphology (DIC) in preanaphase arrested cells at 23°C and 37°C. C) Quantification of the distribution of measured distances between 2 arm loci GFP dots (N = 74 cells for Wildtype; N = 77 cells for mcd1-1). D) Quantification and statistical analyses of the GFP arm inter-loci distances in each experimental group (N = 74 cells for Wildtype; N = 77 cells for *mcd1-1*; P-value = 0.009).

Table 1

Yeast strains used in this study.

Strain name	**Genotype**	**Reference**
VG955	*MATa mcd1–1 trp1 leu2 bar1 gal1*	17
VG982	*MATa trp1 ura3 bar1 gal1*	17
YBS1019	*MATa; S288C*	70
YBS2020	*MATa; NET1:GFP:HIS3; w303*	For this study
YBS2078	*MATa; lacOs::YLR003c-1; lacOs::MMP1; LacI-GFP; w303*	24
YBS3017	*mcd1–1, MATa; lacOs::YLR003c-1; lacOs::MMP1; LacI-GFP; w303*	For this study

References

1. Skibbens RV. Of Rings and Rods: Regulating Cohesin Entrapment of DNA to Generate Intra- and Intermolecular Tethers. *PLoS Genet.* 2016;12(10): e1006337.

2. Jeppsson K, Kanno T, Shirahige K, Sjögren C. The maintenance of chromosome structure: positioning and functioning of SMC complexes. *Nat Rev Mol Cell Biol*. 2014;15(9):601-14.

3. Dorsett D. Cohesin: genomic insights into controlling gene transcription and development. *Curr Opin Genet Dev*. 2011;21(2): 199–206.

4. Merkenschlager M, Nora EP. CTCF and Cohesin in Genome Folding and Transcriptional. *Gene Regulation Annu Rev Genomics Hum Genet*. 2016;17: 8.1–8.27.

5. Ciabrelli F, Cavalli G. Chromatin-driven behavior of topologically associating domains. *J Mol Biol*. 2015;427(3):608-25.

6. Pekkala D, Heath B, Silver JC. Changes in chromatin and the phosphorylation of nuclear proteins during heat shock of Achlya ambisexualis. *Mol Cell Biol.* 1984;4(7):1198-205.

7. Mackey MA, Morgan WF, Dewey WC. Nuclear fragmentation and premature chromosome condensation induced by heat shock in S-phase Chinese hamster ovary cells. *Cancer Res.* 1988;48(22):6478-83.

8. Flannery AV, Hill RS. The effect of heat shock on the morphology of amphibian lampbrush chromosomes. *Exp Cell Res.* 1988;177(1):9-18.

9. Roux C, Dadoune JP. Use of the acridine orange staining on smears of human spermatozoa after heat-treatment: evaluation of the chromatin condensation. *Andrologia.* 1988;21(3):275-80.

10. Iliakis GE, Pantelias GE. Effects of hyperthermia on chromatin condensation and nucleoli disintegration as visualized by induction of premature chromosome condensation in interphase mammalian cells. *Cancer Res.* 1989;49(5):1254-60.

11. Rodriguez-Martin ML, Moreau N, Herberts C, Angelier N. Comparison between *in vivo* and *in vitro* heat-induced changes in amphibian lampbrush chromosomes. *Chromosoma.* 1991;100(2):79-86.

12. Swanson PE, Carroll SB, Zhang XF, Mackey MA. Spontaneous premature chromosome condensation, micronucleus formation, and non-apoptotic cell death in heated HeLa S3 cells. Ultrastructural observations. *Am J Pathol.* 1995;146(4):963-71.

13. Castells-Roca L, García-Martínez J, Moreno J, Herrero E, Bellí G, Pérez-Ortín JE. Heat Shock Response in Yeast Involves Changes in Both Transcription Rates and mRNA Stabilities. *PLoS ONE*. 2011;6(2): e17272.

14. Verghese J, Abrams J, Wang Y, and Kevin A. Biology of the Heat Shock Response and Protein Chaperones: Budding Yeast (*Saccharomyces cerevisiae*) as a Model System. *Microbiol Mol Biol Rev.* 2012;76(2):115-58.

15. Scherthan H, Loidl J, Schuster T, Schweizer D. Meiotic chromosome condensation and pairing in *Saccharomyces cerevisiae* studied by chromosome painting. *Chromosoma.* 1992;101(10):590-5.

16. Guacci V, Hogan E, Koshland D. Chromosome condensation and sister chromatid pairing in budding yeast. *J Cell Biol.* 1994;125(3):517-30.

17. Guacci V, Koshland D, Strunnikov A. A direct link between sister chromatid cohesion and chromosome condensation revealed through the analysis of MCD1 in *S. cerevisiae*. *Cell.* 1997;91(1):47-57.

18. Castaño IB, Brzoska PM, Sadoff BU, Chen H, Christman MF. Mitotic chromosome condensation in the rDNA requires TRF4 and DNA topoisomerase I in *Saccharomyces cerevisiae*. *Genes Dev.* 1996;10(20):2564-76.

19. Skibbens RV, Corson LB, Koshland D, Hieter P. Ctf7p is essential for sister chromatid cohesion and links mitotic chromosome structure to the DNA replication machinery. *Genes Dev.* 1999;13(3):307-19.

20. Freeman L, Aragon-Alcaide L, Strunnikov A. The condensin complex governs chromosome condensation and mitotic transmission of rDNA. *J Cell Biol.* 2000;149(4):811-24.

21. Lavoie BD, Hogan E, Koshland D. *In vivo* requirements for rDNA chromosome condensation reveal two cell-cycle-regulated pathways for mitotic chromosome folding. *Genes Dev*. 2004;18(1):76-87.

22. Sullivan M, Higuchi T, Katis VL, Uhlmann F. Cdc14 phosphatase induces rDNA condensation and resolves cohesin-independent cohesion during budding yeast anaphase. *Cell.* 2004;117(4):471-82.

23. Wang BD, Butylin P, Strunnikov A. Condensin function in mitotic nucleolar segregation is regulated by rDNA transcription. *Cell Cycle.* 2006;5(19):2260-7.

24. D'Ambrosio C, Schmidt CK, Katou Y, Kelly G, Itoh T, Shirahige K, Uhlmann F. Identification of cis-acting sites for condensin loading onto budding yeast chromosomes. *Genes Dev.* 2008;22(16):2215-27.

25. Gard S, Light W, Xiong B, Bose T, McNairn AJ, Harris B, Fleharty B, Seidel C, Brickner JH, Gerton JL. Cohesinopathy mutations disrupt the subnuclear organization of chromatin. *J Cell Biol.* 2009;187(4):455-62.

26. Lopez-Serra L, Lengronne A, Borges V, Kelly G, Uhlmann F. Budding yeast Wapl controls sister chromatid cohesion maintenance and chromosome condensation. *Curr Biol.* 2013;23(1):64-9.

27. Tong K, Robert V. Skibbens. Pds5 regulators segregate cohesion and condensation pathways in *Saccharomyces cerevisiae*. *Proc Natl Acad Sci USA*. 2015;112(22):7021-6.

28. Straight AF, Shou W, Dowd GJ, Turck CW, Deshaies RJ, Johnson AD, Moazed D. Net1, a Sir2-associated nucleolar protein required for rDNA silencing and nucleolar integrity. *Cell.* 1999;97(2):245-56.

29. Nomura M. Ribosomal RNA genes, RNA polymerases, nucleolar structures, and synthesis of rRNA in the yeast *Saccharomyces cerevisiae*. *Cold Spring Harb Symp Quant Biol.* 2001;555-65.

30. Kobayashi T, Ganley AR. Recombination regulation by transcription-induced cohesin dissociation in rDNA repeats. *Science.* 2005;309(5740):1581-4.

31. Huang J, Brito IL, Villén J, Gygi SP, Amon A, Moazed D. Inhibition of homologous recombination by a cohesin-associated clamp complex recruited to the rDNA recombination enhancer. *Genes Dev.* 2006;20(20):2887-901.

32. Wilkins BJ, Rall NA, Ostwal Y, Kruitwagen T, Hiragami-Hamada K, Winkler M, Barral Y, Fischle W, Neumann H. A cascade of histone modifications induces chromatin condensation in mitosis. *Science.* 2014;343(6166):77-80.

33. Tsang CK, Li H, Zheng XS. Nutrient starvation promotes condensin loading to maintain rDNA stability. *EMBO J.* 2007;26(2):448-58.

34. Tollervey D, Lehtonen H, Carmo-Fonseca M, Hurt EC. The small nucleolar RNP protein NOP1 (fibrillarin) is required for pre-rRNA processing in yeast. *EMBO J.*

1991;10(3):573-83.

35. Machín F, Torres-Rosell J, Jarmuz A, Aragón L. Spindle-independent condensation-mediated segregation of yeast ribosomal DNA in late anaphase. *J Cell Biol.* 2005;168(2):209-19.

36. Hartman T, Stead K, Koshland D, Guacci V. Pds5p is an essential chromosomal protein required for both sister chromatid cohesion and condensation in *Saccharomyces cerevisiae. J Cell Biol.* 2000;151(3):613-26.

37. Woodman J, Hoffman M, Dzieciatkowska M, Hansen KC, Megee PC. Phosphorylation of the Scc2 cohesin deposition complex subunit regulates chromosome condensation through cohesin integrity. *Mol Biol Cell.* 2015;26(21):3754-67

38. Orgil O, Matityahu A, Eng T, Guacci V, Koshland D, Onn I. A conserved domain in the scc3 subunit of cohesin mediates the interaction with both mcd1 and the cohesin loader complex. *PLoS Genet.* 2015;11(3):e1005036.

39. Aragon L, Martinez-Perez E, Merkenschlager M. Condensin, cohesin and the control of chromatin states. *Curr Opin Genet Dev.* 2013;23(2):204-11.

40. Hirano T. Condensin-Based Chromosome Organization from Bacteria to Vertebrates. *Cell.* 2016;164(5):847-57.

41. Nomura M. Regulation of Ribosome Biosynthesis in Escherichia coli and *Saccharomyces cerevisiae:* Diversity and Common Principles. *J Bacteriol.* 1999;181(22):6857-64.

42. Russell J, Zomerdijk JC. The RNA polymerase I transcription machinery. *Biochem Soc Symp.* 2006;(73):203-16.

43. Salminen A, Kaarniranta K. SIRT1 regulates the ribosomal DNA locus: epigenetic

candles twinkle longevity in the Christmas tree. *Biochem Biophys Res Commun.* 2009;378(1):6-9.

44. Sáez-Vásquez J, Gadal O. Genome organization and function: a view from yeast and Arabidopsis. *Mol Plant.* 2010;3(4):678-90.

45. Johzuka K, Horiuchi T. RNA polymerase I transcription obstructs condensin association with 35S rRNA coding regions and can cause contraction of long repeat in *Saccharomyces cerevisiae. Genes Cells*. 2007;12(6):759-71.

46. Clemente-Blanco A, Mayán-Santo M., Schneider DA, Machín F, Jarmuz A, Tschochner H., Aragón L. Cdc14 inhibits transcription by RNA polymerase I during anaphase. *Nature*. 2009;458(7235):219-22.

47. Warner J, Udem S. Temperature sensitive mutations affecting ribosome synthesis in *Saccharomyces cerevisiae*. *J Mol Biol.* 1972;65:243-57.

48. Cuylen S, Metz J, Hruby A, Haering CH. Entrapment of chromosomes by condensin rings prevents their breakage during cytokinesis. *Dev Cell.* 2013;27(4):469-78.

49. Martin CA, Murray JE, Carroll P, Leitch A, Mackenzie KJ, Halachev M, Fetit AE, Keith C, Bicknell LS, Fluteau A, Gautier P, Hall EA, Joss S, Soares G, Silva J, Bober MB, Duker A, Wise CA, Quigley AJ, Phadke SR; Deciphering Developmental Disorders Study, Wood AJ, Vagnarelli P, Jackson AP. Mutations in genes encoding condensin complex proteins cause microcephaly through decatenation failure at mitosis. *Genes Dev.* 2016;30(19):2158-2172.

50. Kiraly G, Simonyi AS, Turani M, Juhasz I, Nagy G, Banfalvi G. Micronucleus formation during chromatin condensation and under apoptotic conditions. *Apoptosis.* 2016;[Epub ahead of print] DOI: 10.1007/s10495-016-1316-4.

51. Zhang C, Kuang M, Li M, Feng L, Zhang K, Cheng S. SMC4, which is essentially involved in lung development, is associated with lung adenocarcinoma progression. *Sci Rep.* 2016;6:34508.

52. Kagami Y, Yoshida K. The functional role for condensin in the regulation of chromosomal organization during the cell cycle. *Cell Mol Life Sci.* 2016;73(24):4591-4598.

53. Uhlmann F. SMC complexes: from DNA to chromosomes. *Nat Rev Mol Cell Biol.* 2016;17(7):399-412.

54. Houseley J, Tollervey D. Repeat expansion in the budding yeast ribosomal DNA can occur independently of the canonical homologous recombination machinery. *Nucleic Acids Res.* 2011;39(20): 8778–8791.

55. Lees-Miller SP. DNA double strand break repair in mitosis is suppressed by phosphorylation of XRCC4. *PLoS Genet.* 2014;10(8):e1004598.

56. Mathiasen DP, Lisby M. Cell cycle regulation of homologous recombination in *Saccharomyces cerevisiae. FEMS Microbiol Rev*. 2014;38(2):172-84.

57. Lavoie BD, Hogan E, Koshland D. In vivo dissection of the chromosome condensation machinery reversibility of condensation distinguishes contributions of condensin and cohesin. *J Cell Biol.* 2002;156(5):805-15;

58. Martin RM, Cardoso MC. Chromatin condensation modulates access and binding of nuclear proteins. *FASEB J.* 2010;24(4):1066-72.

59. Moss T. At the crossroads of growth control; making ribosomal RNA. *Curr Opin Genet Dev.* 2004;14(2):210-7.

60. Bi X, Yu Q, Sandmeier JJ, Elizondo S. Regulation of transcriptional silencing in

yeast by growth temperature. *J Mol Biol.* 2004;344(4):893-905.

61. Hickman M, McCullough K, Woike A, Raducha-Grace L, Rozario T, Dula ML, Anderson E, Margalit D, Holmes SG. Isolation and characterization of conditional alleles of the yeast SIR2 gene. *J Mol Biol.* 2007;367(5):1246-57.

62. Li P, Jin H, Yu HG. Condensin suppresses recombination and regulates double-strand break processing at the repetitive ribosomal DNA array to ensure proper chromosome segregation during meiosis in budding yeast. *Mol Biol Cell.* 2014;25(19): 2934–2947.

63. Huang K, Jia J, Wu C, Yao M, Li M, Jin J, Jiang C, Cai Y, Pei D, Pan G, Yao H. Ribosomal RNA Gene Transcription Mediated by the Master Genome Regulator Protein CCCTC-binding Factor (CTCF) Is Negatively Regulated by the Condensin Complex. *J Biol Chem.* 2013;288(36): 26067–26077.

64. Lu S, Lee KK, Harris B, Xiong B, Bose T, Saraf A, Hattem G, Florens L, Seidel C, Gerton J. The cohesin acetyltransferase Eco1 coordinates rDNA replication and transcription. *EMBO Rep.*2014;15(5): 609–617.

65. Bose T, Lee KK, Lu S, Xu B, Harris B, Slaughter B, Unruh J, Garrett A, McDowell A, Box A, Li H, Peak A, Ramachandran S, Seidel C, Gerton J. Cohesin Proteins Promote Ribosomal RNA Production and Protein Translation in Yeast and Human Cells. *PLoS Genet.* 2012;8(6): e1002749.

66. Hirano T. Condensins: universal organizers of chromosomes with diverse functions. *Genes Dev.* 2012;26(15): 1659–1678.

67. Csermely P, Kajtár J, Hollósi M, Oikarinen J, Somogyi J. The 90 kDa heat shock protein (hsp90) induces the condensation of the chromatin structure. *Biochem Biophys*

Res Commun. 1994;202(3):1657-63.

68. Asita. E, Salehhuddin. H. Heat Sensitivity between Human Normal Liver (WRL-68) and Breast Cancer (MDA-MB 231) Cell lines. *International Journal of Chemical, Environmental & Biological Sciences (IJCEBS)* Volume 1, Issue 1. 2013.

69. Longtine MS, McKenzie A 3rd, Demarini DJ, Shah NG, Wach A, Brachat A, Philippsen P, Pringle JR. Additional modules for versatile and economical PCR-based gene deletion and modification in *Saccharomyces cerevisiae*.*Yeast.* 1998;14(10):953-61

70. Rudra S, Skibbens RV. Chl1 DNA Helicase Regulates Scc2 Deposition Specifically during DNA-Replication in *Saccharomyces cerevisiae. PLoS One.* 2013;8(9): e75435.

Chapter 4

A novel role for chaperones in mitotic chromatin architecture: Yeast Hps82 is critical for hyperthermic-induced rDNA hypercondensation

Abstract

Ribosomes directly control protein synthesis and are fundamental for cell growth and division. Ribosome biogenesis pathways are thus tightly regulated through nutrient sensing and stress pathways that in turn impact genome stability, aging and senescence. In the budding yeast *Saccharomyces cerevisiae*, ribosomal RNAs are transcribed from the right arm of chromosome XII, which houses ribosomal DNA (rDNA) and comprises the nucleolus. Numerous studies reveal cell cycle-dependent architectural changes in that rDNA is decondensed and forms a puff-like structure during interphase but condenses into a tight loop-like structure during mitosis. Intriguingly, a novel and additional mechanism of increased mitotic rDNA compaction was recently discovered that occurs in response to temperature stress and is rapidly reversible. The mechanism through which this hyperthermic-induced rDNA hypercondensation occurs, however, remains unknown. Here, we report that neither condensins nor cohesins play a critical role in hyperthermic-induced rDNA hypercondensation – differentiating this architecture state from normal mitotic condensation (requiring cohesins and condensins) and also from premature condensation (requiring condensins) that occurs during interphase in response to nutrient starvation. Instead, our results reveal that heat shock protein Hsp82 is critical for hyperthermic-induced rDNA hypercondensation. To our knowledge, this is the first report that chaperone proteins function during mitosis to overtly impact rDNA structure. Our findings further reveal that the high mobility group protein Hmo1 is a negative regulator of mitotic rDNA condensation, distinct from its role in promoting premature-condensation of rDNA during interphase upon nutrient starvation. These results open new avenues from which to understand stress-dependent regulation of chromatin architecture.

Introduction

Protein synthesis in all organisms takes place in the highly conserved ribonucleoprotein complex - the ribosome. Ribosome biogenesis is thus directly related to cell growth and proliferation [1]. In eukaryotes, the nuclear compartment that assembles ribosomes (including rRNA synthesis, processing and ribonucleoparticle assembly), is termed the nucleolus. rRNA arises by transcription from the rDNA locus that resides on the right arm of chromosome XII in the *Saccharomyces cerevisiae* yeast genome. This locus is approximately 1-2 Mb and consists of about 150 tandem repeats, each of which is 9.1 kb and encodes for 5S, 5.8S, 25S, and 18S rRNAs [2-4].

The canonical role for the nucleolus in rDNA transcription and ribosome biogenesis is well-established, but these represent a small subset of nucleolar functions that impact cells [5-7]. For instance, rDNA is the most highly represented gene in any eukaryote. It is also the most heavily transcribed (accounting for over 60% of the entire RNA pool) and, due to its highly repetitive structure, the most recombinogenic (and potentially mutagenic) site within the eukaryotic genome [3, 8-10]. The importance of maintaining rDNA locus stability is highlighted by the fact that DNA replication forks are programmed to stall within rDNA, precluding catastrophic head-on collision of replication and transcription complexes [11-13]. Furthermore, rDNA transcription rates and even nucleolar size are intimately coupled to changes in nutrient levels, revealing the central role of rDNA in responding to environmental cues [14-16]. rDNA also plays a key role in cellular aging and replicative lifespan in which extrachromosomal rDNA circles (ERCs) that arise through recombination deplete the remaining genome of critical regulatory factors [17, 18]. Stress responses similarly release nucleolar factors that inhibit MDM2 function and

thus promote cell cycle arrest, senescence or apoptosis through p53-dependent pathways [19]. Given that a rather surprisingly small percentage of nucleolar proteins function in ribosome biogenesis, it becomes critical to explore the regulatory mechanisms through which rDNA architecture responds to the many challenges imposed on the cell. The issue is of significant clinical importance as well because disruption of rDNA function results in neurodegeneration, tumorigenesis and severe developmental defects that include Treacher-Collins Syndrome, Blackfan Anemia, CHARGE Syndrome and several others [20-27].

rDNA structure is tightly regulated through the cell cycle. In budding yeast, rDNA forms a diffuse puff-like structure during G1 phase that coalesces into a tight loop-like structure during mitosis [28, 29]. The development of numerous strategies that include FISH, GFP-tagged rDNA binding proteins and a streamlined intercalating-dye method now provide for rapid and efficient quantification of rDNA condensation status [28-35]. These assays have focused primarily on the well-established and highly conserved roles of cohesins and condensins. Mutations in any of the cohesin/condensin subunits, or mutation of cohesion regulators such as the cohesin loader Scc2-Scc4 and cohesin acetyltransferase Eco1/Ctf7, produce profound impacts on condensation such that mitotic rDNA fails to compact and appears as diffuse puff-like structures even during mitosis [30, 32, 36-40]. In addition to appropriate condensation reactions that occur during mitosis, the rDNA locus condenses during G1 phase in response to nutrient starvation or rapamycin treatment. This premature rDNA condensation, which includes nucleolar contraction, requires *de novo* recruitment of condensin and the high mobility group protein Hmo1 [15, 16, 41]. Surprisingly, an additional rDNA state was only recently

discovered in which mitotic cells induce a hyper-condensation of rDNA in response to elevated temperature. This hyperthermic-induced rDNA hypercondensation is both rapidly induced and reversed by simple temperature shifts [35, 41]. The extent to which this hyperthermic-induced hypercondensation is predicated on cohesin or condensin dynamics, however, remains unknown. Here, we find that unlike the effects driven by nutrient starvation or rapamycin, hyperthermic-induced hypercondensation occurs in the absence of altered condensin or cohesin levels. Instead, we identify the ATPase chaperone Hsp82 as a novel regulator of rDNA hypercondensation. Our results further identify Hmo1 as a negative regulator of mitotic rDNA condensation, in opposition to its role in rDNA premature-condensation during interphase. To our knowledge, this is the first study to implicate heat shock chaperone as a regulator of rDNA chromatin structure.

Results

4.1 Cohesin deposition and/or release are not required for hyperthermic-induced rDNA hypercondensation

Wildtype cells shifted to an elevated temperature during mitosis exhibit rDNA hypercondensation [35], but the basis for this dramatic change in chromatin structure remains unknown. Cohesins play a critical role in rDNA condensation such that mutation in either cohesin subunits (MCD1, PDS5 or SCC3) or regulators (ECO1 or SCC2) all result in severe rDNA condensation defects [29, 30, 32, 36, 42-44]. These observations formally suggest that *de novo* cohesin deposition may play a critical role in hyperthermic-induced rDNA hypercondensation, in opposition to decondensed rDNA 'puffs' that occur due to cohesin mutation [29, 35]. Here, we tested this model by inactivating the Scc2, 4 heterocomplex that is required for cohesin deposition onto DNA [45, 46]. Log phase cultures of wildtype and *scc2-4* cells were synchronized in G1 at 23°C using rich medium supplemented with alpha factor, washed and then arrested in preanapase at 23°C (permissive for *scc2-4* function) by incubation for 2.5 h in medium supplemented with nocodazole. Cell cycle progression from log phase into mitosis was confirmed by flow cytometry (Figure 1A). Cells obtained following this regimen contain sister chromatid rDNA structures that are both tightly cohered and condensed into extended discrete loops [29, 30, 35, 36, 45, 46]. The resulting cultures were then shifted to 37°C (non-permissive for *scc2-4* function) for 1 h while maintaining the preanaphase arrest. As expected, rDNA in wildtype cells at 23°C appeared as long loops that often extended away from the DNA mass but then hypercondensed into very short rDNA loops after a 1-h shift to 37°C (Figure 1B) [35]. The rDNA in scc2-4 cells also condensed into long rDNA loops at

23°C. Importantly, rDNA in *scc2-4* cells also fully hypercondensed (very short loops) after a 1-h exposure to 37°C (Figure 1B). We independently confirmed that this *scc2-4* mutant strain is indeed temperature sensitive and defective in cohesin deposition onto chromatin (Shen and Skibbens, 2017). Thus, temperature-induced rDNA hypercondensation during mitosis occurs in the absence of *de novo* cohesin deposition.

Wildtype cells exhibit faster growth kinetics, despite containing hypercondensed rDNA at 37°C. To accommodate the increase in rDNA transcription required for this faster rate of cell growth, we posited that rDNA hypercondensation (axial loop shortening) might occur through cohesin dissociation to promote increased lateral looping. To test whether cohesin removal promotes shorter axial rDNA loops (observed as hypercondensation), we turned to the cohesin destabilizer Rad61/WAPL [38, 40, 47-49]. Log phase wildtype and *rad61* null cells were treated as described earlier to achieve sequential G1 and preanaphase synchronization at 23°C before shifting to 37°C for 1 h while maintaining the mitotic arrest. Similar to both wildtype and *scc2-4* mutant cells, *rad61* null cells were fully competent to condense rDNA into discrete loops at 23°C. Moreover, *rad61* null cells were fully competent to hypercondense the rDNA into very short loops upon shifting to 37°C (Figure 1B, C), revealing that rDNA hypercondensation occurs without cohesin dissociation. We noted that *rad61* null cells formed slightly shorter rDNA loops at 37°C than wildtype, consistent with previous findings that Rad61 is a negative regulator of condensation [40, 50]. In combination, these results reveal that mitotic hyperthermic-induced rDNA hypercondensation occurs independent of both cohesin deposition and release.

4.2 Condensin deposition and/or release are not required for hyperthermic-induced rDNA hypercondensation

Mitotic chromosome condensation requires condensin, in addition to cohesin, activity such that condensin mutants exhibit severe condensation defects at rDNA loci [30, 33, 34, 51, 52]. Unlike the cohesin complex, there is no known loading complex that promotes condensin deposition onto chromosome [39]. Thus, to assess whether condensin deposition is required for hyperthermic-induced rDNA hypercondensation, we directly tested for hyperthermic-induced changes in condensin binding to rDNA using chromatin immunoprecipitation (ChIP). Wildtype cells expressing HA-tagged Smc2 were synchronized in G1 at 23°C for 2.5 h, then divided and released into either 23°C or 37°C medium supplemented with nocodazole for 3 h to arrest cells in preanaphase (Figure 2A). Protein-DNA complexes were cross-linked using formaldehyde, then lysed and sonicated to shear the DNA. Chromatin complexes containing Smc2 were immunoprecipitated, cross-links reversed and condensin enrichment tested by PCR using four well-documented condensin-binding sites within rDNA [53, 54] (Figure 2B). The results reveal that Smc2 levels remain unchanged at 23°C compared to 37°C (Figure 2C), despite dramatic changes in rDNA structure. Thus, hyperthermic-induced rDNA hypercondensation occurs independent of both condensin deposition and dissociation.

4.3 Hsp82 promotes hyperthermic-induced rDNA hypercondensation

The surprising finding that neither cohesin nor condensin dynamics contribute to hyperthermic-induced rDNA hypercondensation suggested that a novel mechanism must exist by which cells regulate rDNA structure. We thus turned to heat-shock pathways

through which cells appropriately respond to elevated temperatures [55], even though no evidence to date directly implicates heat shock/chaperone factors in mitotic rDNA condensation or hyperthermic-induced hypercondensation. To generate a candidate list, we first queried the Saccharomyces Genome Database (SGD) GO term database using an iterative process in which each search contained unique combinations of any two of several terms (Response to heat; Nucleolus; Chromatin binding; Regulation of DNA metabolic process). We then cross-referenced the resulting lists to identify candidates that occur in high frequency and then selected those in which mutations are readily obtainable from a prototrophic deletion collection [56-58]. We finally prioritized 10 genes that provide the most extensive coverage of independent heat shock/chaperone pathways (Table 1).

Wildtype and all 10 heat shock protein/chaperone (HSP/C) null cells were sequentially synchronized in G1 and preanaphase as described, before shifting the resulting mitotic cells to 37°C for one additional hour while maintaining the mitotic arrest. Cell cycle progression for each strain was confirmed using flow cytometry (Figure 3A). As expected, rDNA in wildtype cells exhibited significantly hypercondensed rDNA loops after shifting to 37°C (Figure 3B). Not surprisingly, the bulk of the HSP/C candidates (*msn2, msn4, ssa1, sir2, isw1, hit1* and *fob1*) exhibited both normal mitotic rDNA condensation at 23°C and hypercondensation at 37°C (Figure 3B). Thus, rDNA hyperthermic-induced hypercondensation is a specialized and unique response that is independent of most heat shock pathways. We also found that *top1* null cells exhibited a large population (44%) of puff-like rDNA structures indicating that rDNA was decondensed regardless of temperature. Thus, *top1* was excluded from further analyses

for hyperthermic-induced hypercondensation. Regardless, our results confirm that topoisomerase I is critical for rDNA condensation at all temperatures (Figure 3B), extending prior findings that *top1* promotes condensation in *Drosophila melanogaster* and that *top1 trf4* double mutant cells exhibit rDNA condensation defects in budding yeast [59, 60].

Given the basis of our strategy, we were surprised to find an HSP/C that indeed impacts hyperthermic induced rDNA condensation. Our condensation assays revealed that *hsp82* null cells fully support normal rDNA condensation during mitosis at 23°C but failed to completely hypercondense rDNA to wildtype levels in response to 37°C incubation (Figure 3B). To both extend and quantify the extent of this rDNA hypercondensation defect, we synchronized wildtype and *hsp82* deletion cells in G1 at 23°C for 2.5 h, then released divided cultures into either 23°C or 37°C medium supplemented with nocodazole for 3 h to arrest cells in preanaphase. Cell cycle progression was confirmed using flow cytometry (Figure 3C). We then measured the axial rDNA loop length from three biological replicates in which each contains at least 100 cells. The results reveal that mitotic *hsp82* mutant cells contain significantly longer (roughly 40%) rDNA loops at 37°C than wildtype cells shifted to 37°C (Figure 3D, E). Importantly, both wildtype and *hsp82* deletion cells exhibited similarly long loops at 23°C, further highlighting the unique role for Hsp82 in specifically driving hyperthermic-induced rDNA hypercondensation. This is the first report of a heat shock chaperone functioning in rDNA condensation in general and specifically that Hsp82 promotes rDNA hypercondensation in response to thermic challenges.

4.4 Hmo1 negatively regulates mitotic rDNA condensation.

During our screen of 10 HSP/C null cells function in hyperthermic-induced rDNA hypercondensation, we observed that *hmo1* null cells contain two independent but tightly condensed rDNA rings – often appearing as rabbit ears (Figure S1A). The fact that this strain had diploidized was confirmed by Flow cytometry (Figure S1B). To our surprise, *hmo1* deletion cells from the prototrophic deletion collection contains both haploid and diploid cells and cannot consistently arrest under nocodazole treatment (Figure S1B). These observations indicate there are additional mutations in the *hmo1* deletion population from the deletion collection [56-58].

To further investigate Hmo1 function in hyperthermic-induced rDNA hypercondensation, we deleted *HMO1* in S288C wildtype background. The resulting transformants were confirmed by PCR. We then synchronized wildtype and three independent *hmo1* deletion isolates in nocodazole for 3 h at 23°C versus 37°C to arrest cells in preanaphase and then measured rDNA loop length for each strain by condensation assay. The FACS results show that *hmo1* deletion cells can be arrested in response to nocodazole treatment (Figure 4A). Wildtype cells exhibited long rDNA rings at 23°C that hypercondensed to very short hypercondensed rings at 37°C. Surprisingly, *hmo1* mutant cells contained significantly shorter loops at 23°C compared to wildtype, which further hypercondensed to wildtype level at 37°C. Thus, we term Hmo1 a novel negative regulator of mitotic rDNA condensation (Figure 4B, C). However, the fact that the *hmo1* null mutant cannot further compact the rDNA indicates the limitation of rDNA compaction dynamic is reached when rDNA is hypercondensed by activation of the Hsp82-depedent pathway at 37°C.

Discussion

The nucleolus and rDNA are exquisitely tuned to both the cell cycle and external cues. For instance, rDNA prematurely condenses during interphase in response to starvation and also condenses in a stereotypic fashion during each entry of the cell into mitosis [14, 15, 28, 29]. All of these structural changes require condensins with an additional but critical role also played by cohesins during mitotic condensation [15, 16, 29, 36-40]. Recently, we identified a novel form of hyper-condensation that occurs during mitosis in response to heat stress and thus far appears specific to the rDNA [35, 41]. The first major finding of the current study is that this hyperthermic-induced hypercondensation occurs independent of changes in binding of either condensin or cohesin to rDNA. This surprising result suggests that the last several decades of research into rDNA structure analyses remain narrowly focused and that our understanding of chromatin structure regulation remains incomplete. Toward that end, a second major finding of the current study is that the Hsp82, a member of the Hsp90 chaperone family, is critical for hyperthermic-induced hypercondensation. Attributes of this novel form of Hsp82-dependent chromatin regulation is that it is specific to mitosis, occurs after and independent of stereotypical condensation events that involve cohesin and condensin, appears specific to rDNA and is rapidly reversible. The third major finding of the current study is that Hmo1 functions in negatively regulating mitotic rDNA condensation. The fact that wildtype yeast grows faster at 37°C indicates rDNA transcription might also increase to support faster growth when rDNA is hypercondensed at higher temperature [35]. Hmo1 promotes rDNA transcription and triggers DNA bridging and looping [16, 61,

62]. Thus, both Hmo1 and Hsp82 functions together in novel regulation mechanisms of mitotic rDNA structure to balance transcription and condensation.

What is the mechanism through which Hsp82 promotes hyperthermic-induced rDNA hypercondensation? Circular dichroism spectra studies revealed that Hsp90 induces *in vitro* a more condensed state in rat liver chromatin structure [63]. Thus, Hsp82 might play a direct structural role in hypercondensing rDNA in response to heat stress. A second possibility is that Hsp82 acts upstream of hypercondensation by regulating factors that in turn directly act upon rDNA. For instance, Hsp82 exhibits synthetic growth defects with histone (H2B), histone variant (H2A.Z), histone modifiers and chromatin remodeling complexes (Dep1, Eaf1,7, Gcn5, Gis1, Hda2,3, Pho23, Rco1, Rtt109, Sap30, Set2 and Swi3) [63-65]. Such histone modification cascades (including deacetylation, phosphorylation and tail-tail interaction of adjacent histones) may provide for a condensin-independent mechanism through which rDNA hypercondenses during mitosis. Future efforts are required to resolve the issue of whether Hsp82 directly imposes rDNA structure or activates one of any number of factors to produce hyperthermic-induced hypercondensation.

Results presented here argue against a role for cohesin deposition/release in hypercondensation, but we cannot rule out a model in which post-translational modifications alter tethering activities. For instance, it is well established that condensin phosphorylation precedes condensation and that cohesin acetylation is required for sister chromatid tethering. In light of these findings, we note that *hsp82* mutants exhibit synthetic growth defects in combination with mutation of the cohesin acetyltransferase *ECO1* or the cohesin releasing factor *RAD61* (though Rad61 impacts cohesin binding

levels to chromatin, in contrast to the mechanism reported here) [64]. A recent study reports that inhibition of Hsp90 (both Hsp82 and Hsc82) causes reduction in the cohesion factor Chl1 protein level and a moderate cohesin defect; because Hsp90 family members are important to maintain protein homeostasis, the underlying mechanism of this observation remains elusive [66]. A stronger interaction exists between Hsp82 and Cdc28 in that they physically interact with each other [67]. Cdc28 is the cyclin-dependent kinase that phosphorylates condensin and triggers condensation during prophase. Based on these observations, histone, cohesin and/or condensin modifications might promote hyperthermic-induced rDNA hypercondensation in an Hsp82-dependent manner (Figure 5).

It is remarkable that a GO-term based screen in which we limited further analyses to only 10 candidates turned up two factors that regulate rDNA condensation. To our knowledge, this is the first report of HSP/C to perform in this fashion – suggesting that we are only at the very beginning of understanding HSP/C function in condensation. Toward this end, our results document that *hsp82* null mutant cells are only partially inhibited for hyperthermic-induced hypercondensation. Given that there are more than 1000 genes listed in SGD as involved in the heat shock response, we anticipate that redundant pathways exist and that many HSP/C factors are critical for chromatin regulation. Hsf1 is a transcription factor that is essential for cell viability and regulates the transcription of approximately 3.0% of the loci in the yeast genome, including Hsp82 and its cytoplasmic paralog Hsc82 [68, 69]. While Hsf1 may be an upstream regulator of Hsp82, the rapid induction and reversibility of rDNA hypercondensation suggests that equally plausible mechanisms of regulation exist (Figure 5). Toward this end, we note

that Hsp82 exhibits synthetic growth defects with many other heat shock proteins, including Hsc82, Ssa3 (hsp70 chaperone) and its own activator Hch1 [70-72]. These negative genetic interactions make them plausible candidates for promoting rDNA hypercondensation in parallel to Hsp82. While the current study focused on rDNA hypercondensation, we predict that many of these HSP/C family members will impact, in response to various stressors such as heat, starvation or in an age-dependent fashion, condensation across the genome.

Materials and methods

Yeast strains and strain construction

Saccharomyces cerevisiae strains used in this study are listed in Table 2.

rDNA condensation assay

A streamlined condensation assay is adapted from a published FISH protocol [29, 35]. Briefly, log phase cells with OD600 0.2 to 0.4 were incubated for 2.5 hr at 23 °C in rich YPD medium supplemented with alpha-factor. The resulting cells were collected, washed and then resuspended in fresh YPD supplemented with nocodazole, and incubated at 23°C for 3 hr. Cells were arrested at preanaphase and fixed by paraformaldehyde for 2hr at 23 °C. Cells were washed with distilled water and resuspended in spheroplast buffer (1M sorbitol, 20mM KPO4, pH7.4), then spheroplasted by adding beta-mercaptoethanol and Zymolyase T100 and incubating for 1 hour at 23°C. Resulting cells were added to poly-L-lysine coat slides, treated with 0.5% Triton X-100, 0.5% SDS, and dehydrated in 3:1 methanol:acetic acid. Slides were stored at 4°C until complete dry, then cells were treated with RNase in 2XSSC buffer (0.3M NaCl, 30mM Sodium Citrate, pH7.0), dehydrated and denatured under 72°C following cold ethanol wash. DNA mass were detected by DAPI staining and assayed under microscope. Cell cycle progression were confirmed by detection of DNA content using flow cytometry as described [32].

Chromatin Immunoprecipitation and ChIP primers

ChIP was performed as previously described [72], with the following modifications. Cells were cultured to log phase with OD600 1.0 to 1.2, then incubated at 23 °C in rich YPD medium supplemented with alpha-factor for 2.5 hr. The resulting cells were collected, washed and then resuspended in fresh YPD supplemented with nocodazole, and incubated at 23 °C or 37°C for 3 hr and then fixed in 1% formaldehyde for 20 mins. Cells were then harvested, spheroplasted and lysed. Cells lysates were sonicated on ice for 6 cycles of 10 seconds. The suspension was centrifuged and diluted 1:10. The diluted suspension was then centrifuged and the supernatant was collected as the chromatin solution. Smc2 enrichment was obtained by incubating chromatin solution with EZ-View Red Anti-HA affinity matrix (Sigma) overnight at 4°C. Beads were collected by centrifugation, washed and the remaining bead-bound proteins harvested using 1%SDS; 0.1 M NaHCO3. DNA-protein crosslinks were reversed in 5 M NaCl for 4 hr at 65°C. DNA precipitation from the resulting lysate was performed by overnight incubation at −20°C in 70% ethanol. Precipitates were extracted in series using 25:24:1 phenol:chloroform:isoamylalcohol and pure chloroform prior to reprecipitation of DNA overnight at −20°C in 70% ethanol. DNA was resuspended in TE buffer and analyzed by PCR using rDNA primers previously described [53, 54]. PCR products were resolved using 1% agarose gels, and histograms of pixel densities quantified in Photoshop. Smc2 enrichment was calculated as the ratio of pull down (ChIP) minus background (obtained using a Myc pull-down control) all over total chromatin minus background (obtained using a Myc pull-down control).

Statistical Analyses

F-Tests were used to assess the equality of 2 variances in chosen experimental groups, followed by Student's T-Tests to assess the statistical significance ($P < 0.05$).

Figures

Figure 1

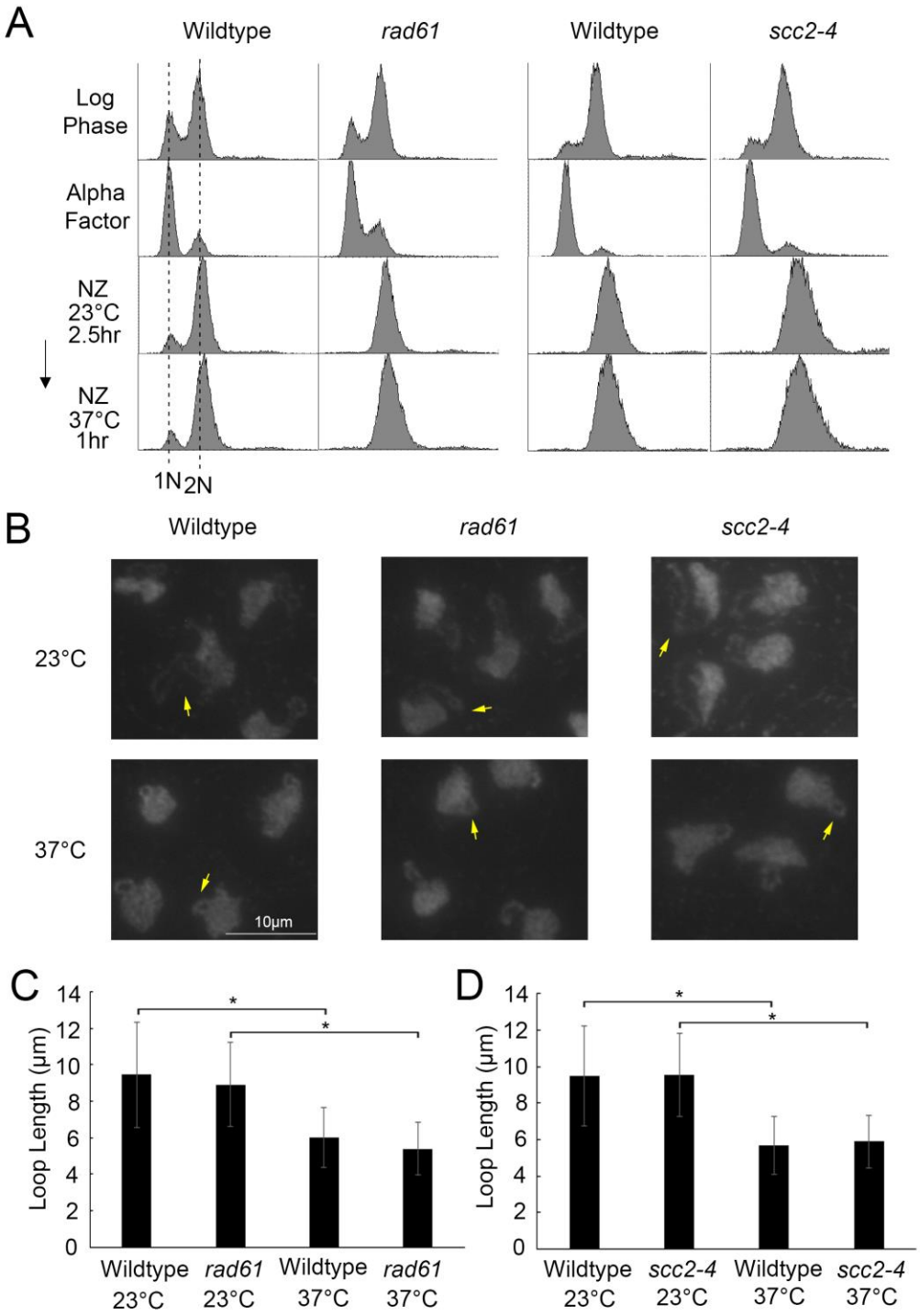

Figure 1. Cohesin deposition and/or release are not required for hyperthermic-induced rDNA hypercondensation.

A) Flow cytometer data of DNA content throughout the experiment. Cells were maintained in nocodazole for 3 hours at 23°C post-alpha factor arrest followed by an additional 1 hour at 37°C. B) Chromosomal mass and rDNA loop structures detected using DAPI. Yellow arrows indicate the rDNA loops. C) Quantification of the loop length of condensed rDNA in in wildtype (YBS1039), *rad61* null mutant (YBS2037) and *scc2-4* mutant (YMM511) cells. Data obtained from 3 biological replicates, at least 100 cells for each strain analyzed per replicate and statistical analysis performed using Student's T-test. P-Value = 0.27 indicates there is no significant differences between the average loop lengths of wildtype cells versus the *rad61* mutant cells. P-Value = 0.83 indicates there is no significant differences between the average loop lengths of wildtype cells versus the *scc2-4* mutant cells. Statistical significant differences (*) are based on $P < 0.05$.

Figure 2

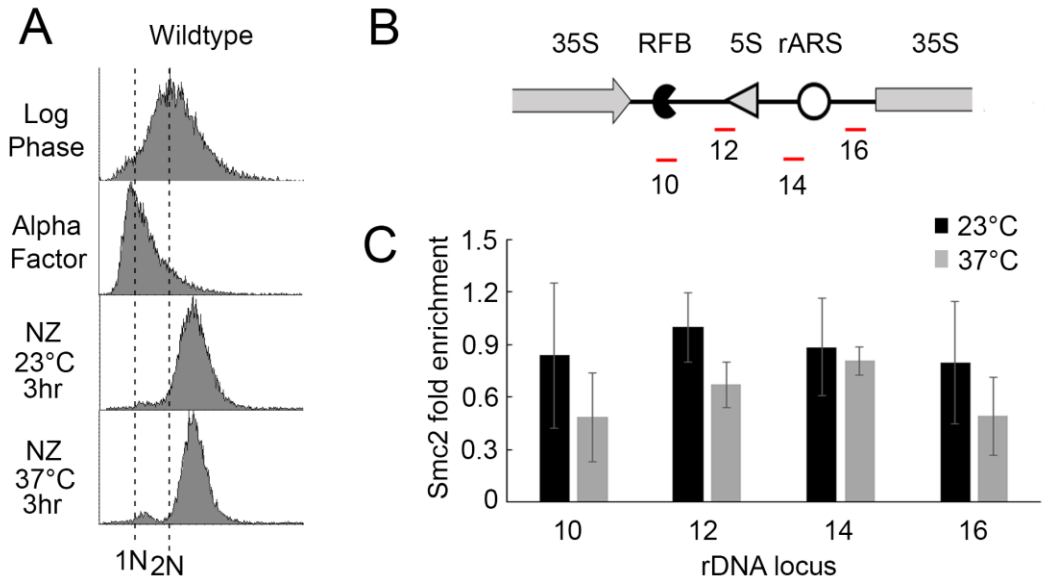

Figure 2. Condensin deposition and/or releasing are not required for hyperthermic-induced rDNA hypercondensation.

A) Flow cytometer data of DNA content throughout the experiment. Cells were maintained in nocodazole for 3 hours at 23°C or 37°C post-alpha factor arrest. B) Schematic of two rDNA repeats with the interval region and the location of four ChIP primer sets. C) Smc2 fold enrichment at four chosen rDNA loci in mitotic wildtype (YBS3036) cells at 23°C versus 37°C, Data obtained from 3 biological replicates and statistical analysis performed using Student's T-test. P-Value = 0.21, 0.12, 0.73, 0.34 for primer sets 10, 12, 14, 16 respectively indicates there is no significant differences between the average loop lengths of wildtype cells arrested at 23°C and 37°C. Statistical significant differences (*) are based on $P < 0.05$.

Figure 3

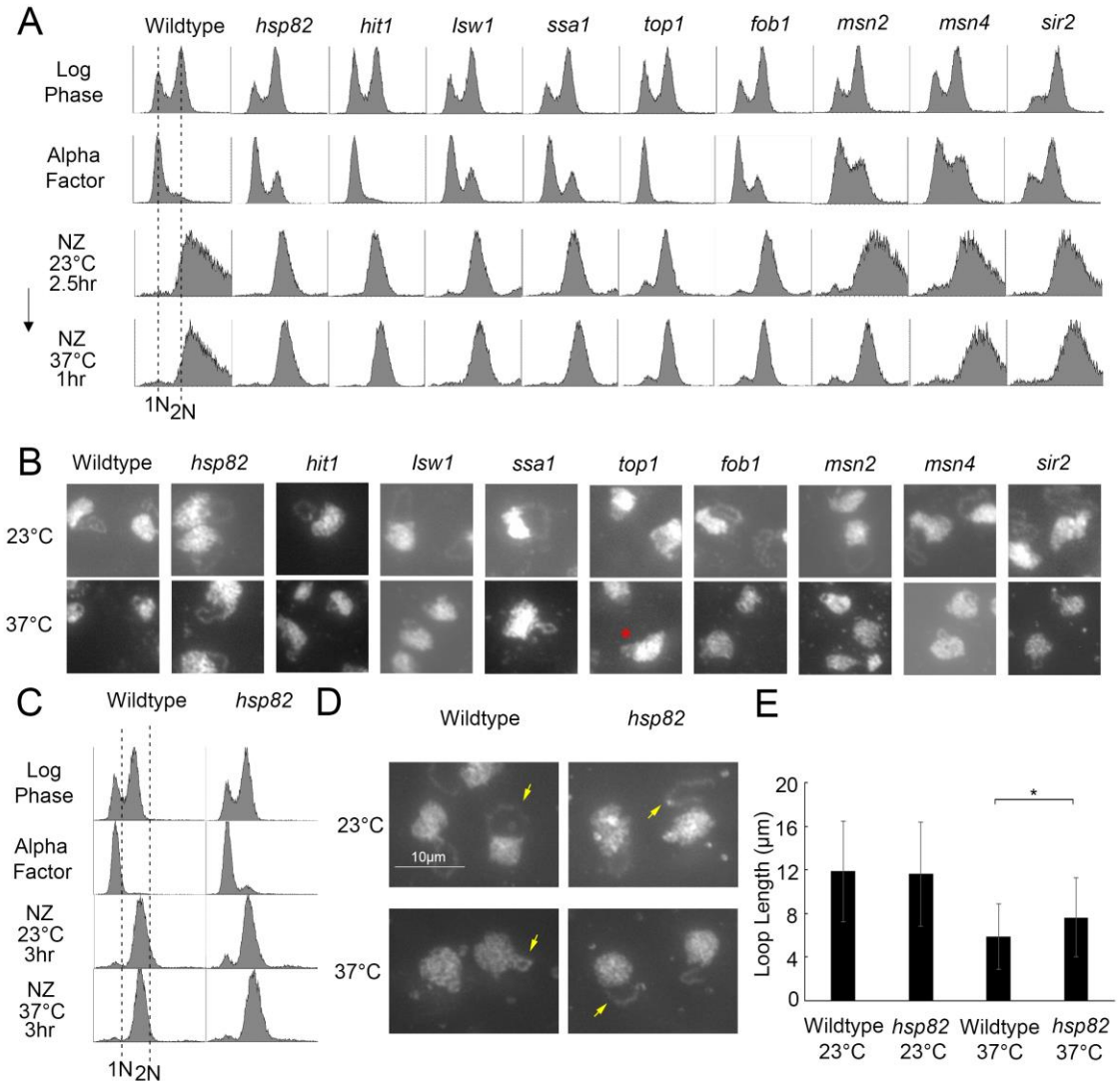

Figure 3. Hsp82 promotes hyperthermic-induced rDNA hypercondensation.

A) Flow cytometer data of DNA content for HSP/C screen. Cells were maintained in nocodazole for 3 hours at 23°C post-alpha factor arrest followed by an additional 1 hour at 37°C. B) Chromosomal mass and rDNA loop structures detected using DAPI. Red star indicates the decondensed rDNA puff observed in *top1* null mutant. C) Flow cytometer

data of DNA content for wildtype and *hsp82* synchronization. Cells were maintained in nocodazole for 3 hours at 23°C or 37°C post-alpha factor arrest. D) Quantification of the loop length of condensed rDNA in in wildtype (YBS1019) and *hsp82* null mutant (YDS203) cells. Data obtained from 3 biological replicates, at least 100 cells for each strain analyzed per replicate and statistical analysis performed using Student's T-test. P-Value = 0.0012 indicates significant differences between the average loop lengths of wildtype cells versus the *hsp82* mutant cells at 37°C. Statistical significant differences (*) are based on $P < 0.05$.

Figure 4

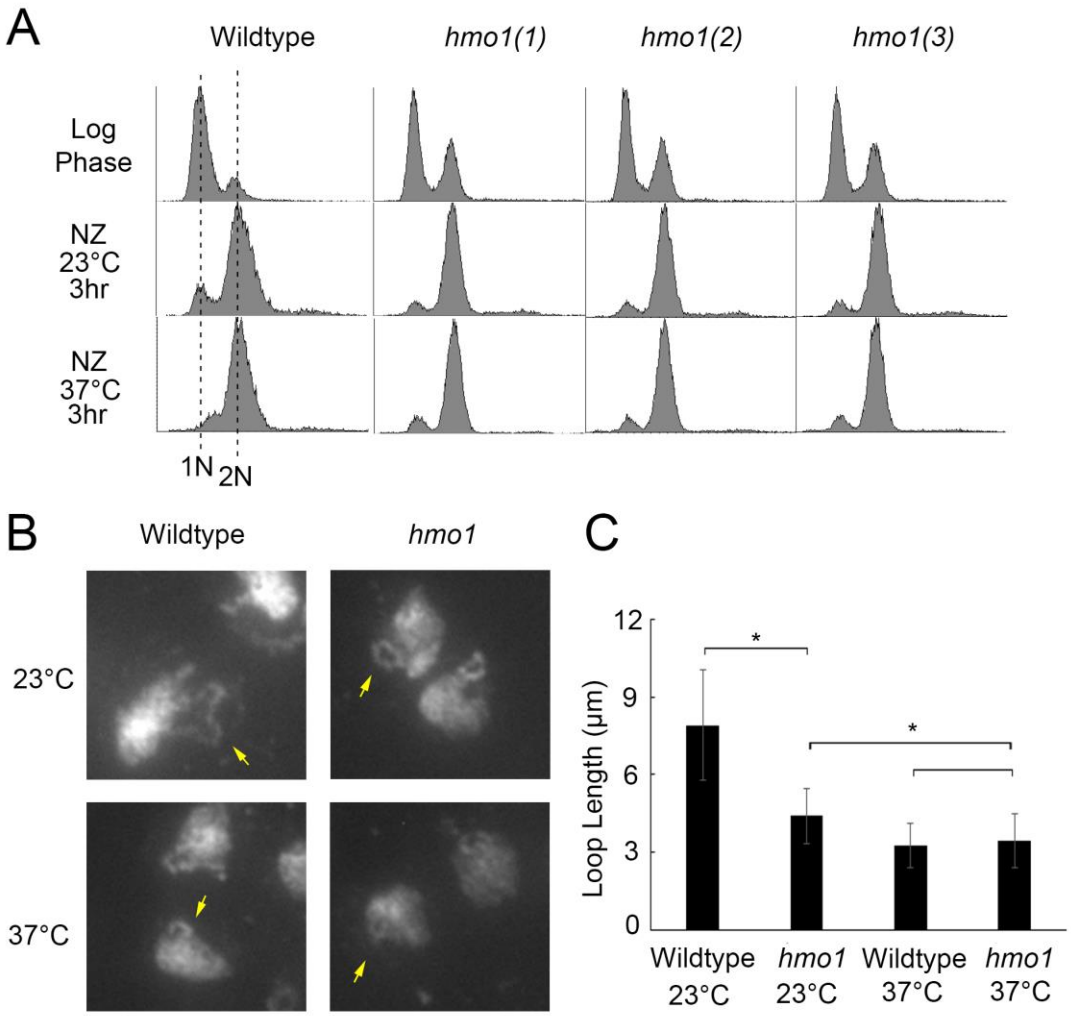

Figure 4. Hmo1 negatively regulates mitotic rDNA condensation.

A) Flow cytometer data of DNA content throughout the experiment. Log phase cultures were split to be maintained in nocodazole for 3 hours at 23°C or 37°C. B) Chromosomal mass and rDNA loop structures detected using DAPI. Yellow arrows indicate the rDNA loops. C) Quantification of the loop length of condensed rDNA in in wildtype (YBS1019) and three *hmo1* deletion mutant (YBS3047, YBS3048, YBS3049)

cells. 100 cells for wildtype strain were analyzed and we calculated the average of three independent *hmo1* deletion isolates based on measurements of 50 cells per isolates arrested at 23°C versus 37°C. Statistical analysis performed using Student's T-test. P-Value = 9.87E-31 indicates there is significant differences between the average loop lengths of wildtype cells versus the *hmo1* mutant cells arrested at 23°C. P-Value = 1.17E-15 indicates there is significant differences between the average loop lengths of *hmo1* mutant cells arrested at 23°C versus 37°C. P-Value = 0.20 indicates there is no significant differences between the average loop lengths of wildtype cells versus the *hmo1* mutant cells arrested at 37°C. Statistical significant differences (*) are based on $P < 0.05$.

Figure 5

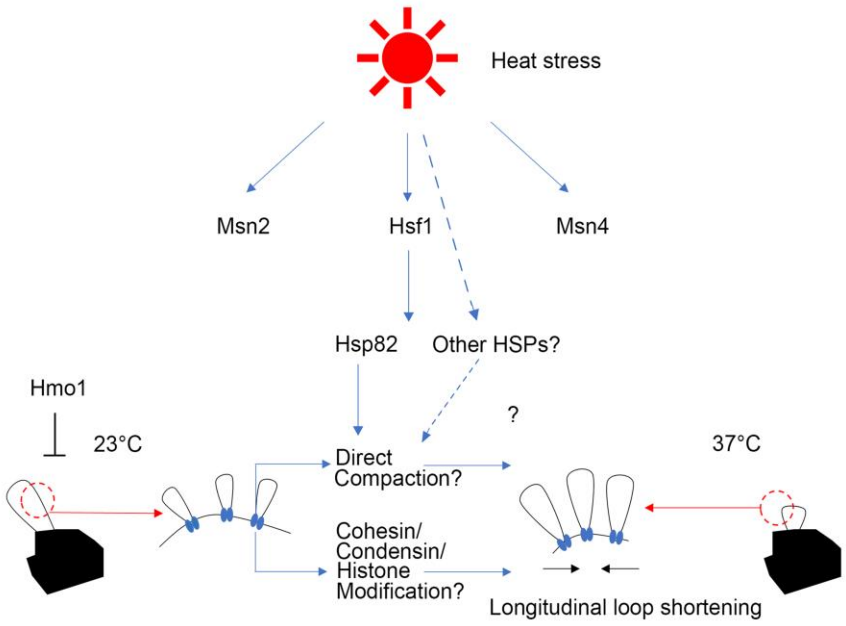

Figure 5. Possible mechanisms of Hsp82-depdent hyperthermic-induced rDNA hypercondensation. Hsp82 functions in hyperthermic-induced rDNA hypercondensation possibly through direct interaction of rDNA or indirectly through modification of cohesin, condensin or histones.

Figure S1

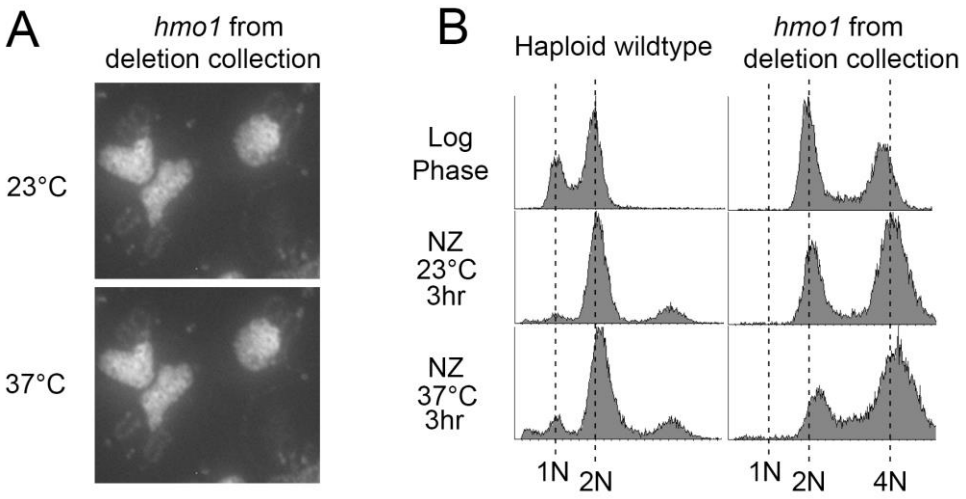

Figure S1. *hmo1* deletion strain from deletion collection is diploidized.

A) Flow cytometer data of DNA content throughout the experiment. Log phase cultures (YDS202) were split to be maintained in nocodazole for 3 hours at 23°C or 37°C. B) Chromosomal mass and rDNA loop structures detected using DAPI.

Table 1

Prioritized list of heat shock/chaperone encoding genes obtained from iterative GO terms searches and that represent a diverse set of cellular responses to elevated temperature.

Common	**Systematic**	**Descriptor**	**Reference**
FOB1	YDR110W	rDNA replication fork barrier	SGD
HIT1	YJR055W	snoRNP assembly factor	SGD
HMO1	YDR174W	High mobility group factor	SGD
HSP82	YPL240C	Hsp90 chaperone	SGD
ISW1	YBR245C	Imitation-switch chromatin remodelers	SGD
MSN2	YMR037C	Stress-responsive transcriptional activator	SGD
MSN4	YKL062W	Stress-responsive transcriptional activator	SGD
SIR2	YDL042C	NAD+ dependent histone deacetylase	SGD
SSA1	YAL005C	ATPase member of HSP70 family	SGD
TOP1	YOL006C	Topoisomerase I	SGD

Table 2

Yeast strains used in this study.

Strain name	**Genotype**	**Reference**
YBS1019	*MATa; S288C*	35
YBS1039	*MATa; w303*	35
YBS2037	*MATa; rad61::URA ; w303*	75
YMM511	*MATa; scc2-4; can1-100; w303*	76
YBS3036	*MATa; SMC2:3HA:KanMX6; w303*	77
YBS3047	*MATa; hmo1::KanMX6; isolates1*	For this study
YBS3048	*MATa; hmo1::KanMX6; isolates2*	For this study
YBS3049	*MATa; hmo1::KanMX6; isolates3*	For this study
YDS200	*MATa; fob1::KanMX6*	56-58
YDS201	*MATa; hit1::KanMX6*	56-58
YDS202	*Diploid; hmo1::KanMX6*	56-58
YDS203	*MATa; hsp82::KanMX6*	56-58

YDS204	*MATa; isw1::KanMX6*	56-58
YDS205	*MATa; msn2::KanMX6*	56-58
YDS206	*MATa; msn4::KanMX6*	56-58
YDS207	*MATa; sir2::KanMX6*	56-58
YDS208	*MATa; ssa1::KanMX6*	56-58
YDS209	*MATa; top1::KanMX6*	56-58

References

1. Kief DR and Warner JR. Coordinate control of syntheses of ribosomal ribonucleic acid and ribosomal proteins during nutritional shift-up in Saccharomyces cerevisiae. *Mol Cell Biol.* 1981;1(11):1007-15.

2. Spahn CM, Beckmann R, Eswar N, Penczek PA, Sali A, Blobel G, Frank J. Structure of the 80S ribosome from Saccharomyces cerevisiae--tRNA-ribosome and subunit-subunit interactions. *Cell.* 2001;107(3):373-86.

3. Nomura M. Ribosomal RNA genes, RNA polymerases, nucleolar structures, and synthesis of rRNA in the yeast Saccharomyces cerevisiae. *Cold Spring Harb Symp Quant Biol.* 2001;555-65.

4. Sirri V, Urcuqui-Inchima S, Roussel P, Hernandez-Verdun D. Nucleolus: the fascinating nuclear body. *Histochem Cell Biol.* 2008;129(1):13-31.

5. Tiku V, Antebi A. Nucleolar Function in Lifespan Regulation. *Trends Cell Biol.* 2018;28(8):662-672.

6. Schöfer C, Weipoltshammer K. Nucleolus and chromatin. *Histochem Cell Biol.* 2018;150(3):209-225.

7. Kobayashi T, Sasaki M. Ribosomal DNA stability is supported by many 'buffer genes'-introduction to the Yeast rDNA Stability Database. *FEMS Yeast Res*. 2017;17(1).

8. Srivastava R, Srivastava R, Ahn SH. The Epigenetic Pathways to Ribosomal DNA Silencing. *Microbiol Mol Biol Rev.* 2016;80(3):545-63.

9. Pal S, Postnikoff SD, Chavez M, Tyler JK. Impaired cohesion and homologous recombination during replicative aging in budding yeast. *Sci Adv.* 2018;4(2):eaaq0236.

10. Nomura M. Ribosomal RNA genes, RNA polymerases, nucleolar structures, and

synthesis of rRNA in the yeast Saccharomyces cerevisiae. *Cold Spring Harb Symp Quant Biol.* 2001;555-65.

11. Biswas A, Mariam J, Kombrabail M, Narayan S, Krishnamoorthy G, Anand R. Site-Specific Fluorescence Dynamics To Probe Polar Arrest by Fob1 in Replication Fork Barrier Sequences. *ACS Omega.* 2017;2(10):7389-7399.

12. Weitao T, Budd M, Campbell JL. Evidence that yeast SGS1, DNA2, SRS2, and FOB1 interact to maintain rDNA stability. *Mutat Res.* 2003;532(1-2):157-72.

13. Shyian M, Mattarocci S, Albert B, Hafner L, Lezaja A, Costanzo M, Boone C, Shore D. Budding Yeast Rif1 Controls Genome Integrity by Inhibiting rDNA Replication. *PLoS Genet.* 2016;12(11):e1006414.

14. Li H, Tsang CK, Watkins M, Bertram PG, Zheng XF. Nutrient regulates Tor1 nuclear localization and association with rDNA promoter. Nature. 2006;442(7106):1058-61.

15. Tsang CK, Li H, Zheng XS. Nutrient starvation promotes condensin loading to maintain rDNA stability. *EMBO J.* 2007;26(2):448-58.

16. Wang D, Mansisidor A, Prabhakar G, Hochwagen A. Condensin and Hmo1 Mediate a Starvation-Induced Transcriptional Position Effect within the Ribosomal DNA Array. *Cell Rep.* 2016;17(2):624.

17. Lewinska A, Miedziak B, Kulak K, Molon M, Wnuk M. Links between nucleolar activity, rDNA stability, aneuploidy and chronological aging in the yeast Saccharomyces cerevisiae. *Biogerontology.* 2014 Jun;15(3):289-316.

18. Park PU, Defossez PA, Guarente L. Effects of mutations in DNA repair genes on formation of ribosomal DNA circles and life span in Saccharomyces cerevisiae. *Mol Cell*

Biol. 1999;19(5):3848-56.

19. Turi Z, Senkyrikova M, Mistrik M, Bartek J, Moudry P. Perturbation of RNA Polymerase I transcription machinery by ablation of HEATR1 triggers the RPL5/RPL11-MDM2-p53 ribosome biogenesis stress checkpoint pathway in human cells. *Cell Cycle.* 2018;17(1):92-101.

20. Sinclair DA, Guarente L. Extrachromosomal rDNA circles--a cause of aging in yeast. *Cell.* 1997;91(7):1033-42.

21. Sinclair DA, Mills K, Guarente L. Accelerated aging and nucleolar fragmentation in yeast sgs1 mutants. *Science.* 1997;277(5330):1313-6.

22. Shcheprova Z1, Baldi S, Frei SB, Gonnet G, Barral Y. A mechanism for asymmetric segregation of age during yeast budding. *Nature.* 2008;454(7205):728-34.

23. Danilova N, Gazda HT. Ribosomopathies: how a common root can cause a tree of pathologies. *Dis Model Mech.* 2015;8(9):1013-26.

24. Udugama M, Sanij E, Voon HPJ, Son J, Hii L, Henson JD, Chan FL, Chang FTM, Liu Y, Pearson RB, Kalitsis P, Mann JR, Collas P, Hannan RD, Wong LH. Ribosomal DNA copy loss and repeat instability in ATRX-mutated cancers. *Proc Natl Acad Sci U S A.* 2018;115(18):4737-4742.

25. Wang M, Lemos B. Ribosomal DNA copy number amplification and loss in human cancers is linked to tumor genetic context, nucleolus activity, and proliferation. *PLoS Genet.* 2017;13(9):e1006994.

26. Xu B, Li H, Perry JM, Singh VP, Unruh J, Yu Z, Zakari M, McDowell W, Li L, Gerton JL. Ribosomal DNA copy number loss and sequence variation in cancer. *PLoS Genet.* 2017;13(6):e1006771.

27. Hallgren J, Pietrzak M, Rempala G, Nelson PT, Hetman M. Neurodegeneration-associated instability of ribosomal DNA. *Biochim Biophys Acta.* 2014;1842(6):860-8.

28. Guacci V, Hogan E, Koshland D. Chromosome condensation and sister chromatid pairing in budding yeast. *J Cell Biol.* 1994;125(3): 517–530.

29. Guacci V, Koshland D, Strunnikov A. A direct link between sister chromatid cohesion and chromosome condensation revealed through the analysis of MCD1 in S. cerevisiae. *Cell.* 1997;91(1): 47–57.

30. D'Ambrosio C, Schmidt CK, Katou Y, Kelly G, Itoh T, Shirahige K, et al. Identification of cis-acting sites for condensin loading onto budding yeast chromosomes. *Genes Dev.* 2008;22(16): 2215–2227.

31. Lopez-Serra L, Lengronne A, Borges V, Kelly G, Uhlmann F. Budding yeast Wapl controls sister chromatid cohesion maintenance and chromosome condensation. *Curr Biol.* 2013;23(1): 64–69.

32. Tong K, Skibbens RV. Pds5 regulators segregate cohesion and condensation pathways in Saccharomyces cerevisiae. *Proc Natl Acad Sci USA.* 2015;112(22): 7021–7026.

33. Lavoie BD, Hogan E and Koshland D. In vivo dissection of the chromosome condensation machinery reversibility of condensation distinguishes contributions of condensin and cohesin. *J Cell Biol.* 2002;156(5): 805–815.

34. Lavoie BD, Hogan E, Koshland D. In vivo requirements for rDNA chromosome condensation reveal two cell-cycle-regulated pathways for mitotic chromosome folding. *Genes Dev*. 2004;18(1): 76–87.

35. Shen D, Skibbens RV. Temperature-dependent regulation of rDNA condensation

in Saccharomyces cerevisiae. *Cell Cycle.* 2017; 1–10.

36. Skibbens RV, Corson BL, Koshland D, Hieter P. Ctf7p is essential for sister chromatid cohesion and links mitotic chromosome structure to the DNA replication machinery. *Genes Dev.* 1999;13(3): 307–319.

37. Tóth A, Ciosk R, Uhlmann F, Galova M, Schleiffer A, Nasmyth K. Yeast Cohesin complex requires a conserved protein, Eco1p(Ctf7), to establish cohesion between sister chromatids during DNA replication. *Genes Dev.* 1999;13(3): 320–333.

38. Kueng S, Hegemann B, Peters BH, Lipp JJ, Schleiffer A, Mechtler K, Peters JM. Wapl controls the dynamic association of cohesin with chromatin. *Cell.* 2006;127(5):955-67.

39. Hirano T. Condensins: universal organizers of chromosomes with diverse functions. *Genes Dev.* 2012;26(15):1659-78.

40. Lopez-Serra L, Lengronne A, Borges V, Kelly G, Uhlmann F. Budding yeast Wapl controls sister chromatid cohesion maintenance and chromosome condensation. *Curr Biol.* 2013;23(1):64-9.

41. Matos-Perdomo E, Machín F. The ribosomal DNA metaphase loop of Saccharomyces cerevisiae gets condensed upon heat stress in a Cdc14-independent TORC1-dependent manner. *Cell Cycle.* 2018;17(2):200-215.

42. Hartman T, Stead K, Koshland D, Guacci V. Pds5p is an essential chromosomal protein required for both sister chromatid cohesion and condensation in Saccharomyces cerevisiae. *J Cell Biol.* 2000;151(3):613-26.

43. Woodman J, Hoffman M, Dzieciatkowska M, Hansen KC, Megee PC. Phosphorylation of the Scc2 cohesin deposition complex subunit regulates chromosome

condensation through cohesin integrity. *Mol Biol Cell.* 2015;26(21):3754-67.

44. Orgil O, Matityahu A, Eng T, Guacci V, Koshland D, Onn I. A conserved domain in the scc3 subunit of cohesin mediates the interaction with both mcd1 and the cohesin loader complex. *PLoS Genet.* 2015;11(3):e1005036.

45. Ciosk R, Shirayama M, Shevchenko A, Tanaka T, Toth A, Shevchenko A, et al. Cohesin's binding to chromosomes depends on a separate complex consisting of Scc2 and Scc4 proteins. *Mol Cell.* 2000;5(2): 243–254.

46. Watrin E, Schleiffer A, Tanaka K, Eisenhaber F, Nasmyth K, Peters JM. Human Scc4 is required for cohesin binding to chromatin, sister-chromatid cohesion, and mitotic progression. *Curr Biol.* 2006;16(9):863-74.

47. Game JC, Birrell GW, Brown JA, Shibata T, Baccari C, Chu AM, Williamson MS, Brown JM. Use of a genome-wide approach to identify new genes that control resistance of Saccharomyces cerevisiae to ionizing radiation. *Radiat Res.* 2003;160(1):14-24.

48. Vernì F, Gandhi R, Goldberg ML, Gatti M. Genetic and molecular analysis of wings apart-like (wapl), a gene controlling heterochromatin organization in Drosophila melanogaster. *Genetics.* 2000;154(4):1693-710.

49. Sutani T, Kawaguchi T, Kanno R, Itoh T, Shirahige K. Budding yeast Wpl1(Rad61)-Pds5 complex counteracts sister chromatid cohesion-establishing reaction. *Curr Biol.* 2009;19(6):492-7.

50. Guacci V, Koshland D. Cohesin-independent segregation of sister chromatids in budding yeast. *Mol Biol Cell.* 2012;23(4):729-39.

51. Strunnikov AV, Hogan E, Koshland D. SMC2, a Saccharomyces cerevisiae gene essential for chromosome segregation and condensation, defines a subgroup within the

SMC family. *Genes Dev.* 1995;9(5):587-99.

52. Freeman L, Aragon-Alcaide L, Strunnikov A. The condensin complex governs chromosome condensation and mitotic transmission of rDNA. *J Cell Biol.* 2000;149(4):811-24.

53. Johzuka K, Horiuchi T. The cis element and factors required for condensin recruitment to chromosomes. *Mol Cell.* 2009;34(1):26-35.

54. Thattikota Y, Tollis S, Palou R, Vinet J, Tyers M, D'Amours D. Cdc48/VCP Promotes Chromosome Morphogenesis by Releasing Condensin from Self-Entrapment in Chromatin. *Mol Cell.* 2018;69(4):664-676.e5.

55. Verghese J, Abrams J, Wang Y, Morano KA. Biology of the heat shock response and protein chaperones: budding yeast (Saccharomyces cerevisiae) as a model system. *Microbiol Mol Biol Rev.* 2012;76(2):115-58.

56. Winzeler EA, Shoemaker DD, Astromoff A, Liang H, Anderson K, Andre B, Bangham R, Benito R, Boeke JD, Bussey H, et al. Functional characterization of the S. cerevisiae genome by gene deletion and parallel analysis. *Science.* 1999;285(5429):901-6.

57. Giaever G, Nislow C. The yeast deletion collection: a decade of functional genomics. *Genetics.* 2014;197(2):451-65.

58. VanderSluis B, Hess DC, Pesyna C, Krumholz EW, Syed T, Szappanos B, Nislow C, Papp B, Troyanskaya OG, Myers CL, Caudy AA. Broad metabolic sensitivity profiling of a prototrophic yeast deletion collection. *Genome Biol.* 2014;15(4):R64.

59. Castaño IB, Brzoska PM, Sadoff BU, Chen H, Christman MF. Mitotic chromosome condensation in the rDNA requires TRF4 and DNA topoisomerase I in Saccharomyces cerevisiae. *Genes Dev.* 1996;10(20):2564-76.

60. Zhang CX, Chen AD, Gettel NJ, Hsieh TS. Essential functions of DNA topoisomerase I in Drosophila melanogaster. *Dev Biol.* 2000;222(1):27-40.

61. Divakaran Murugesapillai, Micah J. McCauley, Ran Huo, Molly H. Nelson Holte, Armen Stepanyants, L. James Maher, III, Nathan E. Israeloff, and Mark C. Williams. DNA bridging and looping by HMO1 provides a mechanism for stabilizing nucleosome-free chromatin. *Nucleic Acids Res.* 2014; 42(14): 8996–9004.

62. Albert B, Colleran C, Léger-Silvestre I, Berger AB, Dez C, Normand C, Perez-Fernandez J, McStay B, Gadal O. Structure-function analysis of Hmo1 unveils an ancestral organization of HMG-Box factors involved in ribosomal DNA transcription from yeast to human. *Nucleic Acids Res.* 2013;41(22):10135-49.

63. Csermely P, Kajtár J, Hollósi M, Oikarinen J, Somogyi J. The 90 kDa heat shock protein (hsp90) induces the condensation of the chromatin structure. *Biochem Biophys Res Commun.* 1994;202(3):1657-63.

64. Millson SH, Truman AW, King V, Prodromou C, Pearl LH, Piper PW. A two-hybrid screen of the yeast proteome for Hsp90 interactors uncovers a novel Hsp90 chaperone requirement in the activity of a stress-activated mitogen-activated protein kinase, Slt2p (Mpk1p). *Eukaryot Cell.* 2005;4(5):849-60.

65. Zhao R, Davey M, Hsu YC, Kaplanek P, Tong A, Parsons AB, Krogan N, Cagney G, Mai D, Greenblatt J, Boone C, Emili A, Houry WA. Navigating the chaperone network: an integrative map of physical and genetic interactions mediated by the hsp90 chaperone. *Cell.* 2005;120(5):715-27.

66. McClellan AJ, Xia Y, Deutschbauer AM, Davis RW, Gerstein M, Frydman J. Diverse cellular functions of the Hsp90 molecular chaperone uncovered using systems

approaches. *Cell.* 2007;131(1):121-35.

67. Nidhi Khurana, Sayan Bakshi, Wahida Tabassum, Mrinal K. Bhattacharyya, Sunanda Bhattacharyya. Hsp90 Is Essential for Chl1-Mediated Chromosome Segregation and Sister Chromatid Cohesion. *mSphere.* 2018; 3(3): e00225-18.

68. Yahya G, Parisi E, Flores A, Gallego C, Aldea M. A Whi7-anchored loop controls the G1 Cdk-cyclin complex at start. *Mol Cell.* 2014 ;53(1):115-26.

69. Sakurai H, Ota A. Regulation of chaperone gene expression by heat shock transcription factor in Saccharomyces cerevisiae: importance in normal cell growth, stress resistance, and longevity. *FEBS Lett.* 2011;585(17):2744-8.

70. Zarzov P, Boucherie H, Mann C. A yeast heat shock transcription factor (Hsf1) mutant is defective in both Hsc82/Hsp82 synthesis and spindle pole body duplication. *J Cell Sci.* 1997;110 (Pt 16):1879-91.

71. Gong Y, Kakihara Y, Krogan N, Greenblatt J, Emili A, Zhang Z, Houry WA. An atlas of chaperone-protein interactions in Saccharomyces cerevisiae: implications to protein folding pathways in the cell. *Mol Syst Biol.* 2009;5:275.

72. Panaretou B, Siligardi G, Meyer P, Maloney A, Sullivan JK, Singh S, Millson SH, Clarke PA, Naaby-Hansen S, Stein R, Cramer R, Mollapour M, Workman P, Piper PW, Pearl LH, Prodromou C. Activation of the ATPase activity of hsp90 by the stress-regulated cochaperone aha1. *Mol Cell.* 2002;10(6):1307-18.

73. Marsh JA, Kalton HM, Gaber RF. Cns1 is an essential protein associated with the hsp90 chaperone complex in Saccharomyces cerevisiae that can restore cyclophilin 40-dependent functions in cpr7Delta cells. *Mol Cell Biol.* 1998;18(12):7353-9.

74. Rudra S, Skibbens RV. Sister chromatid cohesion establishment occurs in concert

with lagging strand synthesis. *Cell Cycle.* 2012;11(11): 2114–2121.

75. Tong K, Skibbens RV. Cohesin without cohesion: a novel role for Pds5 in Saccharomyces cerevisiae. *PLoS One.* 2014;9(6):e100470.

76. Maradeo ME, Garg A, and Skibbens RV. Rfc5p regulates alternate RFC complex functions in sister chromatid pairing reactions in budding yeast. *Cell Cycle*. 2010; 9(21): 4370–4378.

77. Shen D, Skibbens RV. Chl1 DNA helicase and Scc2 function in chromosome condensation through cohesin deposition. *PLoS One*. 2017 Nov 29;12(11):e0188739.

Chapter 5

Future Directions

Abstract

Hyperthermic-induced mitotic rDNA hypercondensation was first reported in 2017 [1]. It revealed the great plasticity that condensed rDNA retains during mitosis and also a novel regulatory pathway that specifically impacts the rDNA locus in response to external stimuli. In this chapter, I discuss future plans regarding the newly discovered finding that heat shock chaperone Hsp82 functions in regulating rDNA structure under heat stress.

Introduction

rDNA hypercondenses under moderate heat stress in a reversible manner. We have identified the chaperone protein Hsp82 as a novel regulator of hyperthermic-induced mitotic rDNA hypercondensation. The mechanism through which Hsp82 regulates rDNA hypercondensation remains elusive. Moreover, we know little regarding the balance through which cells increase growth rate at higher temperatures (indicating increased ribosome biogenesis and rDNA transcription) versus rDNA hypercondensation. We are also interested in the possible outcomes of this hyperthermic-induced rDNA hypercondensation. Addressing the following questions will help us move forward in understanding this site-specific, stress sensitive regulation of mitotic chromosome architecture:

1. What is the underlying mechanism through which Hsp82 regulates rDNA hypercondensation? Does Hsp82 bind DNA to compact rDNA directly, or does Hsp82 act indirectly through other compaction components?

2. Are there parallel mechanisms that facilitate hyperthermic-induced rDNA hypercondensation in conjugation with Hsp82?

3. How does rDNA balance hypercondensation with transcription?

4. How does this hyperthermic-induced rDNA hypercondensation benefit yeast?

Below, I discuss each question separately. Answering these questions in the near future will extend our understanding of rDNA metabolism and extend our current big picture of mitotic chromosome structural regulation.

5.1 Exploring Hsp82 function in regulating hyperthermic-induced rDNA hypercondensation.

5.1.1 Does Hsp82 directly induce rDNA hypercondensation?

Hsp82 might promote rDNA hypercondensation in a direct manner. Circular dichroism spectra *in vitro* studies revealed that Hsp90 chaperone induces a more condensed state in rat liver chromatin structure [2]. Given that the yeast Hsp82 is the homolog of Hsp90, Hsp82 might also play a direct role in compacting rDNA. To test this hypothesis, we can perform ChIP to directly test Hsp82 binding to rDNA at 23°C versus 37°C. We can also use fluorescently tagged Hsp82 to check in real time for Hsp82 enrichment and dynamics on rDNA loci in respond to heat stress. If Hsp82 is enriched at rDNA loci at higher temperature, we can further test *in vitro* whether purified Hsp82 can directly compact rDNA.

5.1.2 Does Hsp82 indirectly induce rDNA hypercondensation through other condensation components?

As opposed to directly interacting with rDNA, Hsp82 might function indirectly through regulating other condensation components to hypercompact rDNA. Interestingly, Hsp82 physically interacts with the cyclin-dependent kinase Cdc28 [3]. Cdc28 phosphorylates and activates condensins to promote condensation during prophase. Although hyperthermic-induced rDNA hypercondensation is not based on altered condensin levels, we cannot exclude the possibility that post-translational modification of condensin is involved in rDNA hypercondensation [1, 4]. To test the hypothesis that Hsp82 might facilitate Cdc28-dependent condensin phosphorylation to induce rDNA hypercondensation at elevated temperature, we would generate Hsp82 mutants that are defective in interacting with Cdc28 and then perform condensation assays to test if the mutant fails to hypercondense rDNA at elevated temperature. We can also perform mass spectrometry to test for condensin phosphorylation in wildtype and *hsp82* deletion cells at 23°C versus 37°C. In combination, these experiments would determine whether Hsp82 indirectly promotes hyperthermic-induced rDNA hypercondensation through a Cdc28-dependent mechanism that might include condensin hyperphosphorylation.

5.2 Exploring other factors that function in hyperthermic-induced rDNA hypercondensation.

We observed an intermediate defect in rDNA hypercondensation in the *hsp82* deletion strain, suggesting that parallel mechanisms facilitate hyperthermic-induced rDNA hypercondensation. As the first step to identify these factors, we would focus on genes that exhibit synthetic lethality with *HSP82* deletion. This list can be generated using SGD to identify Hsp82 interactome. Form this list, we can cross-reference

candidates to GO terms described in Chapter 4 that contain the following terms: Response to heat; Nucleolus; Chromatin binding; and Regulation of DNA metabolic process. We would perform condensation assays on the resulting candidates at 23°C versus 37°C to screen for mutants that exhibit rDNA hypercondensation defects at higher temperature.

An alternative mechanism to identify parallel rDNA hypercondensation factors is based on the heat shock transcription factor Hsf1. In budding yeast, there are three major transcription factors, Hsf1, Msn2 and Msn4, that act upstream of numerous other factors in response to elevated temperature [5, 6]. We have already tested Msn2 and Msn4 in our previous screen and found no effect [1]. Thus, we can exclude downstream factors that are activated by Msn2 and Msn4. Interestingly, Hsf1 activates Hsp82, making Hsf1 and its downstream effectors an appealing candidate pool for novel factors that function in hyperthermic-induced rDNA hypercondensation [7] (Figure 1). We can test for rDNA hypercondensation defects using an *hsf1* conditional mutant that is inactivated at 37°C. If the mutant exhibits a more severe hypercondensation defect than *hsp82* alone, then we would further narrow down our screen to factors that are targets of Hsf1 activities. If *hsf1* and *hsp82* mutants exhibit similar hypercondensation defects, then the parallel factor is acting through additional unknown mechanisms. Excluding Hsf1, Msn2 and Msn4 pathways will thus help limit the remaining pool of candidates.

5.3 Exploring the balance of rDNA hypercondensation and transcription.

5.3.1 How does this hyperthermic-induced rDNA hypercondensation impact rDNA transcription?

The impact of hyperthermic-induced rDNA hypercondensation on rDNA transcription remains elusive. During our investigation of rDNA hypercondensation, we observed a faster growth rate of wildtype yeast cells at 37°C compared to 23°C. Accelerated growth is normally coupled to upregulated rDNA transcription, ribosome biogenesis and translational outputs [8, 9]. This increased rDNA transcription requires a relaxed rDNA conformation and RNA polymerase accessibility – requirements that appear at odds with our observations that rDNA is more condensed at 37°C compared to 23°C. On the other hand, rDNA is highly recombinogenic such that hypercondensation may protect cells form heat-induced homologous recombination. Thus, we posit that cells must achieve a balance between transcription, recombination and hypercondensation.

To directly test rDNA transcription in its hypercondensed state at 37°C, we can perform RT-qPCR on rDNA transcripts of 18S, 5.8S, 5S and 25S rRNA. One possibility is that rDNA transcription is inhibited at 37°C, and this result would be consistent with previous findings that condensation normally restricts transcription factor accessibility and antagonizes transcription [10, 11]. In contrast, if we observe upregulated transcription levels at 37°C, the hypercondensed rDNA loci might indicate a more complex structure that contracts longitudinally to allow for shorter axial looping of transcribed rDNA. Addressing this is complex due to the large number of rDNA repeats. Only a small number of repeats may be highly transcribed to elevate transcription levels, while the majority of rDNA is hypercondensed. Resolving this structure might require microscopy techniques, such as super-resolution microscopy and electron microscopy (5.3.2).

5.3.2 How is rDNA organized and transcribed when hypercondensed?

Can we observe rDNA structure directly? Our streamlined condensation assay provides a largely extended and exquisite view of rDNA loops, with the average loop length of around 10 microns. Recent advances in super-resolution microscopy have achieved single molecule and single DNA fluorescence imaging [12]. Additionally, electron microscopy has long been utilized to observe yeast rDNA, providing detailed images of transcript-associated rDNA strands [13, 14]. We can generate a protocol that allows us to apply our streamlined condensation assay to microscopy sample preparation for super-resolution microscopy as well as electron microscope to directly view chromatin compaction and transcription in detail. Thus, we will be able to observe rDNA transcription status by measuring transcript-associated repeats and hypercondensed repeats distribution along rDNA loci. For instance, some rDNA repeats may be highly transcribed to support faster growth, and the remaining sites are hypercondensed to inhibit homologous recombination at elevated temperature. By using updated microscopy techniques, we will get a better understanding about the balance of rDNA transcription, recombination and hypercondensation.

5.4 Exploring the role of hyperthermic-induced rDNA hypercondensation in budding yeast.

How does hyperthermic-induced rDNA hypercondensation impact life in yeast? Interestingly, accumulation of extrachromosomal rDNA circles (ERCs) is one major cause of aging in yeast mother cells, while moderate heat stress results in extended life span in yeast [15, 16]. Taken together with our observation that rDNA is hypercondensed at elevated temperature, we hypothesize that upon moderate heat stress, rDNA is

hypercondensed in an Hsp82-dependent manner that protects rDNA stability and decreases ERC generation over the short-term during mitosis.

To test this hypothesis, we can compare the survival curves of wildtype and *hsp82* deletion cells at 23°C versus 37°C to see if *hsp82* mutant cells lose the ability to extend lifespan at 37°C. We can also perform Southern blots to test for ERC accumulation at 23°C versus 37°C in both wildtype and *hsp82* deletion strains. If moderate heat stress represses ERC accumulation in wildtype cells and then deletion of Hsp82 restores high ERC and reduces longevity, we can conclude that Hsp82-dependent rDNA hypercondensation that inhibits ERC formation is one mechanism for yeast life span extension at elevated temperature.

Figures

Figure 1

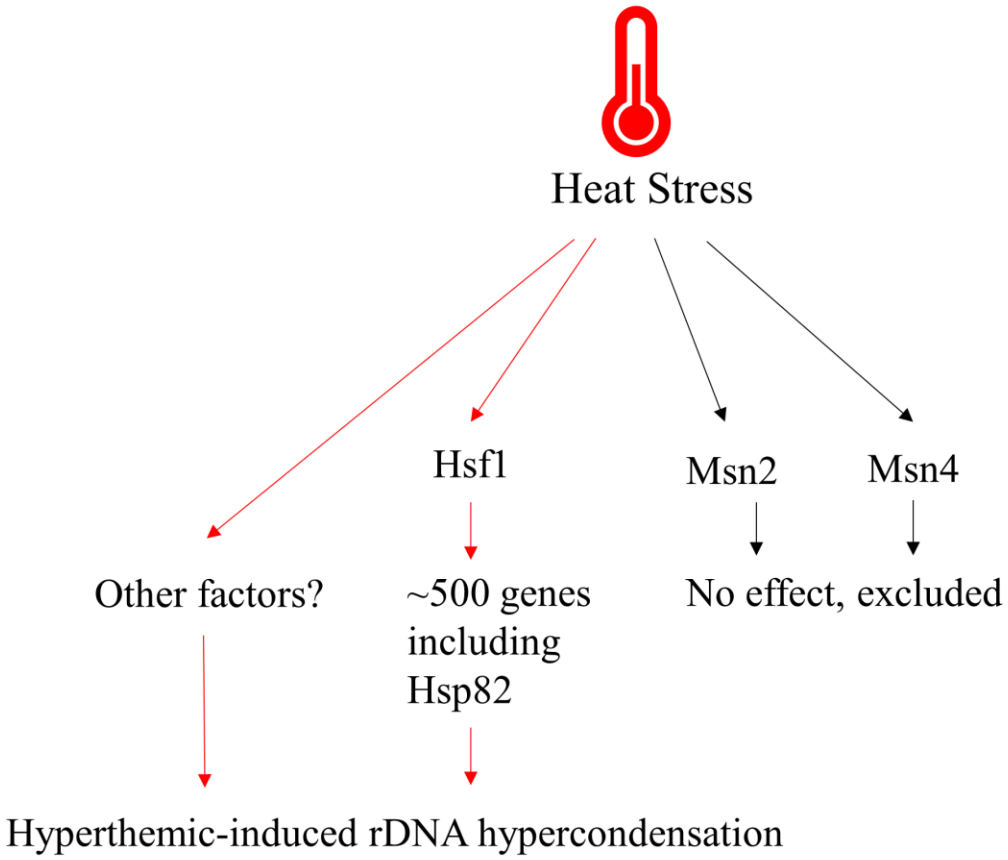

Figure 1. Schematic shows that heat stress activates Hsf1, Msn2 and Msn4 (shown in solid red and black arrow), together with other unknown mechanisms (shown in dashed red arrow). Both Msn2 and Msn4 are not involved in hyperthermic-induced rDNA hypercondensation (black arrow, Shen 2017), thus, we will focus our screen on Hsf1 and its downstream effectors, and other unknown mechanisms that get activated by heat.

References

1. Shen D, Skibbens RV. Temperature-dependent regulation of rDNA condensation in *Saccharomyces cerevisiae. Cell Cycle.* 2017; 1–10.

2. Csermely P, Kajtár J, Hollósi M, Oikarinen J, Somogyi J. The 90 kDa heat shock protein (hsp90) induces the condensation of the chromatin structure. *Biochem Biophys Res Commun.* 1994;202(3):1657-63.

3. Yahya G, Parisi E, Flores A, Gallego C, Aldea M. A Whi7-anchored loop controls the G1 Cdk-cyclin complex at start. *Mol Cell.* 2014 ;53(1):115-26.

4. Matos-Perdomo E, Machín F. The ribosomal DNA metaphase loop of *Saccharomyces cerevisiae* gets condensed upon heat stress in a Cdc14-independent TORC1-dependent manner. *Cell Cycle.* 2018;17(2):200-215.

5. Verghese J, Abrams J, Wang Y, Morano KA. Biology of the heat shock response and protein chaperones: budding yeast (*Saccharomyces cerevisiae*) as a model system. *Microbiol Mol Biol Rev.* 2012;76(2):115-58.

6. Sakurai H, Ota A. Regulation of chaperone gene expression by heat shock transcription factor in *Saccharomyces cerevisiae*: importance in normal cell growth, stress resistance, and longevity. *FEBS Lett.* 2011;585(17):2744-8.

7. Zarzov P, Boucherie H, Mann C. A yeast heat shock transcription factor (Hsf1) mutant is defective in both Hsc82/Hsp82 synthesis and spindle pole body duplication. *J Cell Sci.* 1997;110 (Pt 16):1879-91.

8. Nomura M. Ribosomal RNA genes, RNA polymerases, nucleolar structures, and synthesis of rRNA in the yeast *Saccharomyces cerevisiae*. *Cold Spring Harb Symp Quant Biol.* 2001;555-65.

9. Russell J, Zomerdijk JC. The RNA polymerase I transcription machinery. *Biochem Soc Symp.* 2006;(73):203-16.

10. Martin RM, Cardoso MC. Chromatin condensation modulates access and binding of nuclear proteins. *FASEB J.* 2010;24(4):1066-72.

11. Tsang CK, Li H, Zheng XS. Nutrient starvation promotes condensin loading to maintain rDNA stability. *EMBO J.* 2007;26(2):448-58.

12. Pyle JR, Chen J. Photobleaching of YOYO-1 in super-resolution single DNA fluorescence imaging. *Beilstein J Nanotechnol.* 2017;8:2296-2306.

13. Saffer LD, Miller OL Jr. Electron microscopic study of *Saccharomyces cerevisiae* rDNA chromatin replication. *Mol Cell Biol.* 1986;6(4):1148-57.

14. Dammann R, Lucchini R, Koller T, Sogo JM. Chromatin structures and transcription of rDNA in yeast *Saccharomyces cerevisiae*. *Nucleic Acids Res*. 1993;21(10):2331-8.

15. Shama S, Lai CY, Antoniazzi JM, Jiang JC, Jazwinski SM. Heat stress-induced life span extension in yeast. *Exp Cell Res.* 1998;245(2):379-88.

16. Swieciło A, Krawiec Z, Wawryn J, Bartosz G, Biliński T. Effect of stress on the life span of the yeast *Saccharomyces cerevisiae*. *Acta Biochim Pol.* 2000;47(2):355-64.

Donglai Shen
+1 4846326525
dos212@lehigh.edu

Education

Bachelor of science, majoring in Biotechnology
China Pharmaceutical University.
From 09/13/2008 to 07/01/2012

Ph.D.
Lehigh university
From 08/20/2012 to 11/19/2018

Fellowships

Marjorie Nemes Fellowships
From 08/27/2017 to 12/31/2017

College of Arts and Sciences Graduate Fellowship
From 01/01/2018 to 07/31/2018

Teaching Positions

Biochemistry Lab
From 08/20/2012 to 12/20/2012

Bio Core I: Cell & Molecular
From 01/20/2013 to 05/10/2013

Bio Core II: Genetics
From 08/20/2013 to 12/20/2013

Bio Core I: Cell & Molecular Lab
From 01/20/2014 to 05/10/2014

Biostatistics
From 01/20/2016 to 05/10/2016

Bioscience in the 21st Century
From 08/20/2016 to 12/20/2016

Publications

Shen D, Skibbens RV. (2017) Temperature-dependent regulation of rDNA condensation in *Saccharomyces cerevisiae*. Cell Cycle. 20: 1-10.

Shen D, Skibbens RV. (2017) Chl1 DNA helicase and Scc2 function in chromosome condensation through cohesin deposition. PLoS One. 12(11):e0188739.

Meetings

Cold spring harbor laboratory course on Yeast Genetics & Genomics
From 07/22/2014 to 08/11/2014

The American Society for Cell Biology/ International Federation for Cell Biology Meeting
From 12/06/2014 to 12/10/2014

Cold spring harbor laboratory meeting The Cell Cycle (Presenter)
From 05/17/2016 to 05/21/2016

The American Society for Cell Biology/ International Federation for Cell Biology Meeting (Presenter)
From 12/02/2017 to 12/06/2017